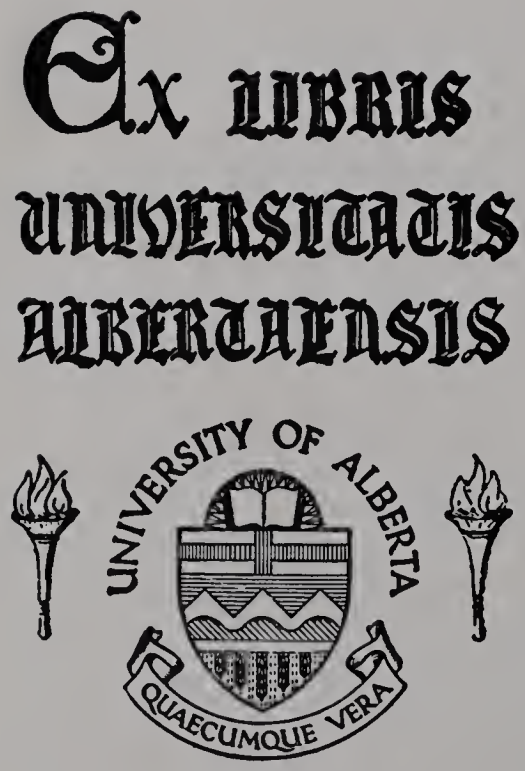

University of Alberta
Printing Department

THE UNIVERSITY OF ALBERTA

STRUCTURAL ANALYSIS OF PART OF THE BRAZEAU RANGE ANTICLINE, NEAR NORDEGG, ALBERTA

A THESIS

SUBMITTED TO THE FACULTY OF GRADUATE STUDIES

IN PARTIAL FULFILMENT OF THE REQUIREMENTS FOR THE DEGREE

MASTER OF SCIENCE

DEPARTMENT OF GEOLOGY

by

DAVID MILNE CRUDEN, B.A.

EDMONTON, ALBERTA

MAY, 1966

UNIVERSITY OF ALBERTA

FACULTY OF GRADUATE STUDIES

The undersigned certify that they have read and recommend to the Faculty of Graduate Studies for acceptance a thesis entitled "Structural Analysis of Part of the Brazeau Range Anticline, Near Nordegg, Alberta", submitted by David Milne Cruden, B.A. in partial fulfilment of the requirements for the degree of Master of Science.

ABSTRACT

A geologic map of part of the Brazeau Range Anticline in the Rocky Mountain Foothills near Nordegg, Alberta has been made on the scale of 4 inches to 1 mile. The results of the mapping are presented as structure contour maps of the tops of the Alexo, Palliser and Banff Formations.

In the preparation of the structure contour maps a new method for determining the generatrix of a cylindrical fold based on a generalization of the normal distribution onto a sphere has been used. This method allows a surface to be subdivided into domains which have been cylindrically folded. Orientations of the bedding surface are then extrapolated down the generatrix of the fold from exposed areas of the surface to give information on covered areas of the surface within the same domain.

A kinematic analysis of the northern half of the Brazeau Range suggested the Range is a northwesterly plunging anticline formed by the northeastward movement of strata up the Brazeau Range Fault - a splay of the Brazeau Thrust. The structures observed in the thesis area conform with this analysis. In the dynamic analysis, the form of the thrust faults which develop in the plane strain of a perfectly plastic body moving across a perfectly rough surface has been calculated. These resemble the thrust faults which developed in the Foothills Belt of Central Alberta.

ACKNOWLEDGEMENTS

Dr. J. R. McGregor was patient in explaining the background of the spherical normal distribution to the writer. He also read earlier drafts of the statistical material and checked the calculations. Dr. K. R. Smillie discussed the analysis of the precision parameter data and gave assistance in the early stages of programming the calculation of the fold axes. Thanks are due to Mr. V. Yanda of the Department of Agricultural Economics for help with the programming. The writer was also helped by Mr. G. Jackson and Mr. D. Simpson of the Department of Computing Science. Dr. J. Haddow criticized an earlier version of the model study and provided references. The writer is grateful to members of the Department of Geology and to Dr. M.R. Stauffer of the Department of Geological Sciences, University of Saskatchewan, for discussions on various subjects. To his supervisor, Dr. H.A.K. Charlesworth, he owes thanks for providing support, encouragement and critical inspiration.

A grant from the Shell Canada Limited, to cover field expenses is acknowledged. During the writing of this thesis, the author was a Graduate Teaching Assistant in the Department of Geology.

TABLE OF CONTENTS

LIST OF ILLUSTRATIONS

INTRODUCTION

In this thesis an attempt is made to trace the steps involved in the structural analysis of a small, well-exposed area of sedimentary rocks where the structure is probably the result of only one episode of deformation. The analysis is in three parts, geometric, kinematic and dynamic.

The geometric analysis determined the orientation of the bedding planes to the exclusion of other surfaces and lineations (such as slickensides and joints) of possible structural significance. The results are given as contour maps on parts of three stratigraphic surfaces. These surfaces have been subdivided into domains - portions of the surface statistically determined to be cylindrically folded.

The kinematic and dynamic analyses are based on the assumption that the geometry of the surfaces, the movements that placed the surfaces in their present position, and the stress field that caused the movements all have the same symmetry. This assumption leads to difficulties, for the geometric analysis reveals a large number of small domains in the structure.

A kinematic analysis has been put forward but rather than attempt the trivial solution of the dynamic analysis, the thesis begins work on a more general approach aimed at discovering not only the orientation of the principal stresses but also their size and history. There is a brief discussion of the mathematical models that have been proposed for deformation of the type shown in the Brazeau Range, and the analysis of a new model based on the assumption that the rocks involved in the deformation behaved as a perfectly plastic body moving across a perfectly rough, horizontal surface towards a stable area has been started. The analysis shows that the type of fault which would develop under these circumstances closely resembles faulting observed in the Foothills region.

The eventual outcome of the analyses of mathematical models will be predictions about the form and location of bedding surfaces and faults. If these are to be compared with field evidence the limits of accuracy of mapping and extrapolation into covered areas should be known. The thesis begins the investigation of these limits.

Summary of Previous Work

Early geological work in the Nordegg area is described in detail by Sanderson (1958) and Pitcher (1958). The first work carried out by the Geological Survey of Canada in the area involved the mapping of the Mesozoic coals of the Nordegg and Bighorn basins. Systematic mapping of the thesis area by the G.S.C. began in 1940. The map areas along the Brazeau Range were first mapped on the scale of 2 inches to 1 mile, and then revised on the scale of 1 inch to 1 mile. The revised maps of the thesis area are Nordegg (Douglas, 1956), Chungo Creek (Douglas, 1958) and Alexo and Saunders (Erdman, 1950). The thesis area also includes the extreme southwest corner of the Harlech map area which the G.S.C. has yet to map.

In 1958, the Alberta Society of Petroleum Geologists held their eighth annual field congress in the Nordegg area. The guidebook contains a 4 inches to 1 mile map compiled from published and unpublished mapping of about 1,000 square miles centred on Nordegg townsite. With a section and notes by A.N. Thomas, it gives a general picture of the area. Shaw (1963) contained a section through the area. An index map of the area showing G.S.C. mapping forms Fig. 1.

Location and Accessibility

The area mapped for this thesis includes the southeast end of Shunda Mountain, the whole of Coliseum Mountain and continues southeastwards along the Brazeau Range to take in part of the unnamed hills which overlook Shunda Gap from the southeast. The westerly limit follows the old forestry trunk road northwestwards from Nordegg to the turnoff for Shunda (Baldy) lookout. The trace of the Brazeau Thrust (Douglas, 1958) forms the eastern boundary to the area.

Highway 11, which crosses the area, joins the Banff-Jasper highway 25 miles to the west. Eastwards, Highway 11 leads to Rocky Mountain House (57 miles away) and Red Deer. The North-South Forestry Trunk Road crosses Highway 11 two miles west of Nordegg and connects it to the Jasper-Edmonton Highway to the north and the old Banff-Calgary Highway to the south.

Within the area, the Forestry road turning north from Highway 11 at the Beaver Pools in Shunda Gap gives access to the southeast end of Coliseum Mountain. The only other road open to vehicles is the trail to the lookout on the top of Shunda Mountain. There is a pack trail up the southwest side of Coliseum Mountain to the old lookout.

The area lies within the Rocky Mountain Forest Reserve. It is therefore covered by 4 inches to 1 mile aerial photographs and planimetrically corrected 4 inches to 1 mile uncontoured maps of the tree cover (Forestry Access Maps). A contoured map of the Nordegg area is published on the scale of 1 inch to 1 mile; 1:50,000 contour maps of the surrounding areas are published.

Stratigraphy

Introduction

The stratigraphy of the thesis area is summarized in Table 1 and in a geological map of the northern half of the Brazeau Range (Fig. 9). Further detail is available in the publications by Erdman (1950) and Douglas (1956, 1958).

TABLE I. Stratigraphic succession in the thesis area.

ERA	PERIOD OR EPOCH	GROUP OR FORMATION	LITHOLOGY	THICKNESS
MESOZOIC	LOWER CRETACEOUS	LUSCAR	Sandstone, shale, coal.	900'
		CADOMIN	Conglomerate, sandstone.	25'
		NIKANASSIN	Sandstone, shale.	400'
	JURASSIC	FERNIE	Conglomerate, mudstone, chert, sandstone.	500'
		DISCONFORMITY		
PALAEOZOIC	MISSISSIPPIAN	RUNDLE MOUNT HEAD & TURNER VALLEY	Vuggy, massive bedded dolomite (undifferentiated).	300'
		SHUNDA	Limestone, shale, anhydrite, dolomite breccia.	200'
		PEKISKO	Limestone	120'
		BANFF	Argillaceous limestone, shale.	550'
	DEVONIAN	EXSHAW	Shale.	5'
		PALLISER	Limestone, dolomite	800'
		ALEXO	Sandstone, siltstone, dolomite	200'

GEOMETRIC ANALYSIS

Determination of the Orientation of Surfaces

The area was mapped on 4 inch to 1 mile aerial photos. Detail easily correlated with the photos made transfer to the Forestry Access Maps accurate and simple. Spot heights have been determined by the Topographical Survey on the peaks of Coliseum and Shunda Mountains and step outs from these were made by the writer in 1964 by Brunton compass and in 1965 by altimeter.

The writer concentrated on determining with a definable precision the attitude of a number of surfaces throughout the map area. Practically all exposures (or stations) close to the Alexo-Palliser, Devonian-Mississippian and Banff-Pekisko boundaries were visited. Wherever possible the orientation of the surface was established. The ideal size and spacing of the stations is governed by the rate of variation of the orientation of the surface. In areas, such as fold hinges, where the surface changes orientation rapidly, more stations are required to determine the surface than on the limbs. The size of stations on fold hinges are also reduced, for the statistics used to analyse the stations assume that the errors in measurement are randomly distributed about a mean direction (with a certain probability density function), so that the mean orientation of the surface should not change significantly within the station.

It is possible to distinguish three sources of uncertainty in the mapping of a particular exposure of a folded surface, uncertainty about the topographic position of the exposure, uncertainty about the stratigraphic position of the exposure and uncertainty about the orientation of the surface within the exposure. Only the last of these will be discussed because the first source can be reduced to negligible proportions by sufficiently sophisticated survey methods, and the importance of the second is at a minimum in the mapping of well-exposed, well-defined boundaries.

The importance of the third source is indicated in Mertie's work (1947). This source does not include uncertainty as to whether the exposed surface is a sample of the covered surface or has been affected by processes such as hill creep. The existence of hill creep can be demonstrated only by comparison with exposed undisturbed rocks and these can be used to determine the representative orientation of the surface. Where hill creep cannot be demonstrated a decision about a particular exposure is a decision about a likely value for the surface at this point. Such decisions belong to a dynamic analysis not to a geometric one.

It is natural to assume that errors involved in measuring the orientation of a surface are normally distributed. However, if the data are to be treated by the usual graphical techniques they are displayed as directed lines radiating from the centre of a sphere of finite radius. Whereas Gauss developed the normal distribution on a surface whose topology could be ignored, in this case the errors involved, often several degrees, require the topology of the sphere be taken into account. Fisher (1953) has suggested how this might be done. Suppose the distribution of possible observations be on the surface of a unit sphere. He proposed that the distribution of elementary errors over this surface had a frequency density proportional to $e^{K\cos\theta}$ where θ is the angular displacement from the estimated mean. The density is a maximum at $\theta = 0$ (if K is positive). If $K = 0$ the density is uniform over the sphere. If K is large and positive the distribution is confined to a small area in the neighbourhood of the maximum (i.e. θ is small). Fisher's proposal seems natural, for if θ is small,

$$\cos\theta \doteq \left(1 - \frac{\theta^2}{2}\right)$$

and the frequency density becomes

$$A e^{-\frac{K\theta^2}{2}}$$

which is a 2-dimensional, normal distribution with K the analog of the inverse of the variance, a consequence of minimizing the effects of the topology. Integration of the function over the sphere gives a normalizing constant, $c = \frac{K}{4\pi \sinh K}$ and a probability density function, P (θ),

$$P(\theta) = \frac{K}{4\pi \sinh K} e^{K\cos\theta}$$

Paleomagnetic data have been found to fit this distribution and Muecke (1965) has suggested, though not tested, that multiple readings of apparently parallel joints in rocks are distributed in this manner. To test whether this distribution can be used to deal with replications of bedding planes from the same domain, 61 dip and strike measurements were made on an outcrop of Palliser limestone on the southeast end of Coliseum Mountain.

The null hypothesis that these 61 measurements did not significantly differ in distribution from Fisher's distribution could then be examined at the 5 per cent significance level. The procedure is set out (for paleomagnetic data) in Watson and Irving (1957). A computer calculation (see Appendix 4) of the mean bedding plane revealed a dip of 12° to 212° with precision parameter, K = 833. The poles to the bedding planes were plotted on a stereographic projection and rotated to bring the mean to the centre of the projection (Turner and Weiss, 1963, p. 67).

Two test of the hypothesis were then applied. The first tests whether the data are significantly divergent from axial symmetry about the calculated mean direction, the second whether the data are significantly divergent in distribution from the probability density function, P (θ)

In the first test the distribution of poles on the projection was divided into octants and the significance of the results tested against chi-square with 5 degrees of freedom (Lindley & Miller, 1953). The hypothesis (that the data are a sample

from a population with a Fisher distribution) is rejected at the 5% level of significance, if, on the assumption that the hypothesis is true, the probability is less than 1 in 20 of exceeding the observed value of chi-square by chance.

	0°-45°	45°-90°	90°-135°	135°-180°	180°-225°	225°-270°	270°-315°	315°-360°
fo	7	9	9	6	10	11	6	3
fe	7.6	7.6	7.6	7.6	7.6	7.6	7.6	7.6

$\sum(f_o-f_e)^2/f_e$	χ^2_5	Significance
6.55	11.07	None

where fo is the observed frequency and fe is the frequency predicted by a Fisher distribution.

Watson and Irving (1957) showed that the expected frequency, fe, of readings between the angular distances θ_1, θ_2 from the mean (where θ, is less than θ_2) is for large K,

$$fe = N\,(\exp(-K(1-\cos\theta_1)) - \exp(-K(1-\cos\theta_2))),$$

where N is the total number of readings. The hypothesis is again tested against chi-square.

	0-1°	1-2°	2-3°	3-4°	4+°
fo	5	16	19	13	8
fe	5.7	18.6	16.6	12.1	8.0

$\sum(f_o-f_e)^2/f_e$	χ^2_1	Significance
1.21	3.84	None

There is again no reason to reject the hypothesis, so the distribution of the bedding planes in both tests does not significantly depart from Fisher's distribution. It is worthwhile noting that these tests can be more accurately performed by doing the arithmetic rather than by the graphical method from Turner and Weiss. The process is tedious by hand but is suited to computer techniques.

Watson and Irving (1957) derived several relations which are helpful in estimating in advance the number of bedding-plane measurements required at a particular station, assuming the measurements follow Fisher's distribution. In this survey,

stations were set up with one of two objectives in mind.

(1) Suppose that it is required to determine the orientation of bedding at a particular station to within α° of the estimated mean. Then, after Watson and Irving (1957, p. 291) for large K

$$\alpha_{95} = 140^{\circ} (KN)^{-\frac{1}{2}}$$

where N is the number of readings, and

α_{95} is the radius of the 95% cone of confidence.

Fig. 2 is a graph of α_{95} against N for different values of K,

for K = 1000 N = 3

K = 500 N = 6

K = 100 N = 31, for $\alpha_{95} = 2\ 1/2^{\circ}$

Thus, as long as K is known, N can be determined. A preliminary analysis showed that K estimates usually fell between 200 and 700. Ten readings were thus usually adequate to reduce α_{95} to $2\ 1/2^{\circ}$. A fuller discussion is given in Appendix 1.

(2) It seems to have been the practice (see e.g. Bielenstein, 1964) in some previously published studies of fractures in rocks to consider two groups of S planes distinct if their 95% cones of confidence do not intersect. Agterberg (1964) pointed out that the optimal procedure in two dimensions is to use Student's t-test. This sets up the hypothesis that both samples are drawn from the same population and tests it against tables of the distribution of the variance of the estimated mean of small samples. If $\bar{X}$ is the difference in the estimated means, X_1, X_2 of the two samples, with sizes N_1, N_2, the hypothesis is rejected if

$$|\bar{x}| > \hat{s} \cdot t (N_1 + N_2 - 2) \left(\frac{N_1 + N_2}{N_1 N_2} \right)^{\frac{1}{2}}$$

where t is the value of the ti distribution (Lindley & Miller, 1953, Table 3) with $(N_1 + N_2 - 2)$ degrees of freedom, and $\hat{s}$ is the estimated variance of the

the population. This may be contrasted with an analogy of "Bielenstein's" procedure which would be

$$|\bar{x}| > \hat{s}_1 t'(N_1-1)^{-\frac{1}{2}} + \hat{s}_2 t''(N_2-1)^{-\frac{1}{2}}$$

t' is the value of t with N_1 - 1 degrees of freedom,

t" is the value of t with N_2 - 1 degrees of freedom.

In three dimensions, Watson (1956a) has shown that an approximate F test of the hypothesis can be derived from an analysis of variance analogy. The hypothesis is rejected if

$$(N-2)\left(\frac{R_1+R_2-R}{N-R_1-R_2}\right) > F_{2,2(N-2)}$$

If a sample, size N_1, is composed of readings with normals which have direction cosines (l_{i1}, m_{i1}, n_{i1}) then

$$R_1^2 = \left(\sum_{i=1}^{i=N_1} l_{i1}\right)^2 + \left(\sum m_{i1}\right)^2 + \left(\sum n_{i1}\right)^2$$

$N = N_1 + N_2$,

R is the length of the resultant vector of the vectors with lengths of R_1 and R_2,

F is tabulated in Lindley and Miller (1953) Table 7.

The test assumes that the samples of sizes, N_1, N_2, are drawn from populations with the same K. It can be shown

$$(N-2)\left(\frac{R_1+R-R}{N-R_1-R_2}\right) \rightarrow 2(\hat{K}-1)(N_1-1)(1-\cos x$$

for two populations where $N_1 = N_2$, $R_1 = R_2$, $R = 2R_1 \cos x/2$, $\hat{K} = \frac{R_1}{N_1 - R_1}$

and the estimated population means are x° apart.

Thus if K = 500, $x = 2^\circ$, then N_1 12. A computer program (described in

Appendix 4) has been written to calculate R_1, R_2 and R. This is a sensitive method of measuring small angular unconformities. The technique is presented in Appendix 3.

To summarize, no more than 10 readings are usually required at a station to determine the orientation of a surface at that station to within 2 1/2 degrees, and about 12 are required to distinguish it from another station whose mean differs by more than 2 degrees.

Determination of Fold Geometry

Folds are usually described by specifying their axes and the orientation of their axial planes. This thesis, however, presents the data as structure contour maps on parts of three surfaces, the base of the Palliser, the base of the Banff and the base of the Pekisko. It will be shown that to construct the contour diagram the folded surface must be divided into cylindrical portions and the axes of these portions calculated. From these axes, the axial traces and hence the axial plane of the main fold can be constructed. There is no loss of information involved in this mode of presentation. In fact, the contour diagram presents considerably more information than the conventional method of description. For instance it contains sufficient information to enable the drawing of cross sections of the folded surface in any direction.

Construction of structure contour maps

The contour maps on the three surfaces have been constructed almost independently of one another; very little of the information used to construct one map has been used in the construction of any of the other maps. This restriction causes more extrapolation into covered areas or areas of poor exposure but it avoids the effects of the restrictive assumptions made in the downward and upward projection of information.

Oertel (1962) has given a qualitative demonstration of the importance of symmetry axes in extrapolating data. It is useful to demonstrate this technique more formally. Suppose part of a fold can be shown to be cylindrical (and it seems a general assumption that any fold may be divided into cylindrical portions, see, for example, Turner and Weiss, (1963, p. 163)). Consider a small part of the generatrix (or fold axis) of that surface at a height, P. The locus of all points, P_1, lying on the contour line x feet below P is such that the horizontal distance separating P from P_1 parallel to the trend of the fold axis is $x \cot \alpha$ where the plunge of the axis is α. This construction has the advantage that it concentrates uncertainty about the form of the surface in uncertainty about the position of the contour line, the end result of the construction (Fig. 3)

Calculation of the Generatrix

Fleuty in a review paper (1964) pointed out that "the concept of the calculated fold axis is fundamental to much modern structural analysis". Techniques of calculating the axes of cylindrical folds have received a good deal of attention but no recent additions have been made to the two common graphical techniques, using pi and beta diagrams, for nearly forty years. However dissatisfaction with these techniques, particularly the beta intersection technique, had been growing.

Ramsay (1964) pointed out that beta diagrams have the disadvantages that the number of beta axis determinations increases very rapidly with the number of observations until graphically the data becomes unwieldy; errors in data lead to spurious beta axes; and that the diagrams do not yield as much information about the shape of folds as pi diagrams.

Muecke (1965) has shown how the first disadvantage can be overcome using a computer program. If (l_1, m_1, n_1) (l_2, m_2, n_2) are the direction cosines of the

outward directed normals to 2 bedding planes then

$$l_3 = \frac{m_1 n_2 - m_2 n_1}{M}$$

$$m_3 = \frac{l_2 n_1 - l_1 n_2}{M}$$

$$n_3 = \frac{l_1 m_2 - m_1 l_2}{M}$$

$$M = \left((m_1 n_2 - m_2 n_1)^2 + (l_2 n_1 - l_1 n_2)^2 + (l_1 m_2 - l_2 m_1)^2 \right)^{\frac{1}{2}}$$

(l_3, m_3, n_3) are the direction cosines of the line of intersection.

To find the mean, he assumed that the distribution of the beta intersection determinations is a Fisher distribution round the mean direction. He also used this distribution to set up a test of whether the fold is cylindrical, using the precision parameter and implicitly suggesting the use of Watson's tables for random K (1956b). Unfortunately this elegant solution fails since it can be shown that the intersection does not have a Fisher distribution (Appendix 2). The actual form of the distribution of the intersections seems extremely complex and it is not likely that further work will give any convenient statistical tests (MacGregor, 1963). Ramsay's second and third objections still stand however, and impair, the usefulness of the beta intersection technique.

The pi diagram also has its disadvantages; there is no clear criterion for deciding the "best fit" axis; drawing the best fit great circle by eye, as is usual, leads to inconsistency and error, for equal distances on the projection do not represent equal angular distances on the sphere; there are finite errors in plotting readings and constructing the diagrams - the maximum likely error in plotting a reading is probably about 2 degrees.

The contouring of pi diagrams is discussed at some length in Appendix 5 but even supposing the problems associated with contouring pi diagrams had been solved by the method proposed there, two disadvantages of the method remain. Both these disadvantages and the contouring problem can be overcome if the generatrix is calculated mathematically. It is also desirable to test whether the fold is cylindrical. If the fold is not cylindrical the direction of the axis calculated as described below is meaningless. To perform this test, the effects due to uncertainty about the position of the pole must be separated from those due to uncertainty about the fit of the poles themselves to a cylindrical surface. This requires a prior estimate of the variance of the individual readings, obtained by taking sufficient bedding plane readings from the population of bedding plane readings at each station to give an adequate estimate of the variance of the population.

Suppose then that p stations (or outcrops) on the fold have been sampled and that the i^{th} of these p samples contains N_i readings and has a resultant with direction cosines (l_i, m_i n_i) of length R_i. Then, providing that the samples are drawn from populations having Fisher distributions, following Watson (1960) it can be shown by an analysis of variance analogy that the estimate of the direction of the fold axis is the eigen vector corresponding to the least eigen value of the matrix V,

$$V = \begin{vmatrix} \sum R_i l_i^2 & \sum R_i l_i m_i & \sum R_i l_i n_i \\ \sum R_i l_i m_i & \sum R_i m_i^2 & \sum R_i n_i m_i \\ \sum R_i l_i n_i & \sum R_i n_i m_i & \sum R_i n_i^2 \end{vmatrix}$$

providing that the precision parameters of the p populations ar e the same and subject to a number of approximations. These assume that K is large and that all the N_i are large. The effect of departures from these assumptions is difficult to unravel and Watson does not discuss this.

$$\Delta_k = \begin{vmatrix} & & & \\ & & & \\ & & & \end{vmatrix}$$

A test of coplanarity is given by

$$\frac{\sum N_i \cdot (\text{least eigen value of } V)}{\sum (N_i - R_i)} \approx \chi^2_{p-2}$$

The principal radii θ_1, θ_2 of the cone of confidence about the axis are given by

$$\theta_1 = \sin^{-1}\left(\frac{\sum N_i - R_i}{\sum N_i} \cdot \frac{\chi^2_2}{A_{max} - A_{min}} \right)^{\frac{1}{2}}$$

$$\theta_2 = \sin^{-1}\left(\frac{\sum N_i - R_i}{\sum N_i} \cdot \frac{\chi^2_2}{A_{int} - A_{min}} \right)^{\frac{1}{2}}$$

where A_{max}, A_{int}, A_{min} are the maximum, intermediate and minimum latent roots of V. Watson (1960) goes on to show that for unequal K, W should be computed.

$$W = \begin{vmatrix} \sum \frac{R_i(N_i-1)}{(N_i-R_i)} 1,i^2 & \sum \frac{R_i(N_i-1)}{(N_i-R_i)} m,1 \sum \frac{R_i(N_i-1)}{(N_i-R_i)} 1,n \\ \sum \frac{R_i(N_i-1)}{N_i-R_i} m,1 \sum \frac{R_i(N_i-1)}{(N_i-R_i)} & m,i^2 \sum \frac{R_i(N_i-1)}{(N_i-R_i)} n,m \\ \sum \frac{R_i(N_i-1)}{N_i-R_i} n,1 \sum \frac{R_i(N_i-1)}{N_i-R_i} & n,m \sum \frac{R_i(N_i-1)}{(N_i-R_i)} n, \end{vmatrix}$$

The test of coplanarity is

$$A_{min} \approx \chi^2_{p-2}$$

The direction of the normal to the best fit circle is the eigen vector of the least eigen value. Confidence limits about this direction are given by

$$\theta_1 = \sin^{-1}\left(\frac{\chi^2_2}{A_{max} - A_{min}} \right)^{\frac{1}{2}}$$

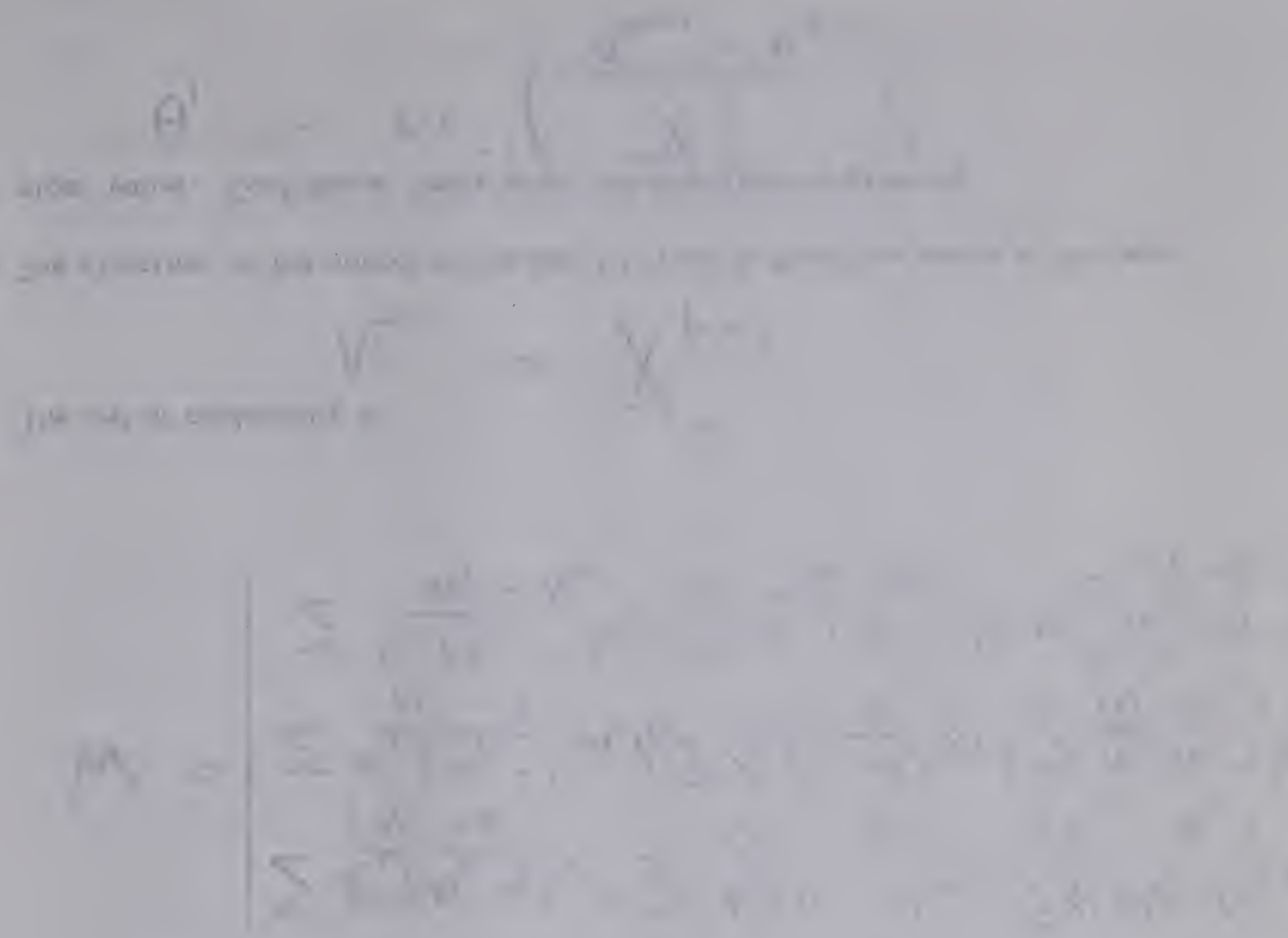

$$\theta_2 = \sin^{-1}\left(\frac{\chi^2_2}{A_{int.} - A_{min}} \right)^{\frac{1}{2}}$$

where the A are the corresponding eigen values of W.

Notice that in W the station averages are weighted not only by their length but by their precision parameters. (The best estimate of K_i is

$$\hat{K}_i = \frac{N_i - 1}{N_i - R_i}$$ for the i^{th} population)

Outstanding problems with the general use of W to calculate B axes lie in the unexplored effects of Watson's approximations and the unverifiable character of the results. The calculations are to problem; an IBM 7040 computer can be persuaded to compute an average size W in about half a minute.

How large should N_i be before the approximations Watson uses are valid? Watson (1960) considers an example with N_i as low as 9. In a later paper (1965) he treated data where N_i has the value 1 and K for the populations is known. If N_i is 1, V takes the form, U

$$U = \begin{vmatrix} \sum l_i^2 & \sum l_i m_i & \sum l_i n_i \\ \sum l_i m_i & \sum m_i^2 & \sum m_i n_i \\ \sum l_i n_i & \sum m_i n_i & \sum n_i^2 \end{vmatrix}$$

This is the matrix Scheidegger (1965) derived by a different method using a different statistical distribution. He used it to solve an analogous problem--"the determination of the 'best' axis from each of a series of axes (the normals to the bedding planes or the long axes of sand grains)".

In Watson's analysis, the test for coplanarity is

$$K \left(\text{minimum eigen value of } U \right) \approx \chi^2_{p-2}$$

The results of this test, he commented, have no sound probability basis but are useful in describing the distribution. Somewhat arbitrarily the least permissible value of N_i in this study has been set at 10.

How may the fit of great circle be tested? Creer (1962) argued that the fit of the best great circle is satisfactory (at the 5% level?) if the great circle passes through the 5% error circles around the mean directions of the p populations. This is not however a sufficient condition. The probability that the true means at p stations simultaneously lie inside the 5% error circles around their estimated means is $(0.95)^P$ (less than 0.95). So that the radii of the circles to be used in the check is properly smaller than the 5% circles. But, since the distribution of probability around the true mean varies with the precision parameters of the population, this whole approach is a little oversimplified. The eventual solution of the problem of finding an independent check may lie in methods of the type suggested by Selby (1965).

Discussion of procedure

Because Watson's method gives an objective test of the domain of a cylindrical fold, the matrix, W, has been used to calculate the generatrix of cylindrically folded portions. A computer program to perform these calculations is given in Appendix 4.

After three neighbouring stations which lie on the same cylindrical fold have been found, neighbouring stations were added to the domain until the addition of any further station gave insignificant results. In this way nearly all stations within the thesis area were assigned to a domain.

Some stations fit in two or more adjacent domains, but in general, surfaces have been divided into discrete domains by the analysis. The positioning of the

boundaries of domains is rather arbitrary. Obviously they lie somewhere between the last station within the domain and the first outside it, but where is difficult to say. Conventionally they were placed at the halfway mark.

It is possible that dividing the surfaces into domains is an artificial process much like the statistician's display of a continuous variate as a histogram--a computational convenience. It may have the effect of concentrating changes in shape of the fold along the margins of the domains in an unrealistic manner. Although the analysis reveals a fold axis single-valued throughout the domain, it is possible that the axis varies systematically but insignificantly across the domain. The analysis takes no account of the relative positions of the stations in space. This effect might be examined by dividing large domains into a number of subdomains and calculating the axes.

Since the analysis takes no account of the relative positions of the stations these might be expected to provide some additional information about the shape of the fold. This information can be used in two ways. (1) If the axis is designated by the most probable value given by the analysis, then the information can be used to construct the contours and thus the shape of part of the fold. (2) There is no reason to assume, however, that when the new information is considered the probable value of the fold axis is still the same. It might be supposed, for instance, that a value of the fold axis should be chosen that keeps the contour lines as smooth as possible as this is the most "natural" shape for a contour line. In practice the procedure adopted compromises between these two extremes. Contours have been constructed by displaying the limits the calculated fold axis places on them and then drawing contour lines to pass within these limits subject to the condition that the fold axis is single valued.

In detail, the program outputs a most likely value for the fold axis together with the lengths and directions of the semi-axes of the elliptical cone of confidence about the axis. Then it has been shown that the next lowest contour line is xcota feet away (p.) down the trend of the fold axis. Nearly all the fold axes encountered dip gently. This has the effect of producing an ellipse of confidence whose projection down the fold axis has negligible thickness. It can be approximated by a straight line. The contour line must then pass between two points x cot(a-a'), x cot(a+a') from the point of projection down the trend of the fold axis where a' is the angle the major semi axis of the ellipse of confidence subtends at the apex of the cone. If the value of x is certain (see p.) then the only effect of x is to increase the area of uncertainty as its value increases, a natural consequence of increasing distance from the point of projection.

Suppose the compromise leads to a value a" for the plunge of the fold axis. Then the contour line 250 feet below the constructed contour line is (250 cota" + x cota" feet), (250 cota" + x cot(a-a')), (250 cota" + x cot(a+a')) from the point of projection. The limits on the lines are displayed on the contour diagram of the top of the Alexo formation. On the other diagrams these limits have been omitted for drafting convenience.

As there is little exposure north east of the trace of the highest splay of the Brazeau Range fault there was little point in extending contours across it. On the map of the top of the Palliser this has made the contouring on the Palliser below the thrust plane easier to appreciate. There is of course no discontinuity in the contours at the trace of a fault plane. The discontinuity exists only where the contour line and the trace of the fault plane are at the same height.

KINEMATIC ANALYSIS

The Northern Part of the Brazeau Range

To make a reasonable kinematic analysis, the rest of the major structure of which the thesis area is part must be considered. Material for this has been taken from Douglas (1956, 1958) and Erdman (1950).

The thesis area lies within the Brazeau thrust sheet, towards the northwest end of the Brazeau Range. The Lower Mesozoic and the Palaeozoic strata that make up the Range have been brought to the surface along the Brazeau Range fault, a splay of the Brazeau thrust. These strata are folded into the Brazeau Range anticline. On the Chungo Creek sheet (Douglas, 1958) the anticline plunges northwestwards and disappears ten miles northwest of Shunda Gap. A southeast limit to the anticline can be seen near the head of Lundine Creek on the margins of the Alexo and Saunders map areas. "Further to the southeast the Brazeau Range anticline plunges below the surface as a wide plate with no definite axial trace." (Erdman, 1950, p. 23). The total length of the anticline is twenty-four miles.

Between Shunda Creek and the North Saskatchewan River the strike of the axial surface of the anticline is approximately 135 degrees. North of Shunda Gap the strike changes gradually. Where the anticline dies out on the Chungo Creek sheet the strike is about 100 degrees.

The Brazeau Range anticline is a multiple-plunging structure. There are two major culminations north of the North Saskatchewan River, one three miles northwest of the river where the top of the Palliser is at a height of 7,500 feet, and the other the culmination on Coliseum Mountain mapped in this thesis, where the top of the Palliser is at 6,100 feet.

The strata lying between the Brazeau Range fault and the Brazeau thrust itself are folded into the Swale Creek syncline. North of the more southerly culmination in the Brazeau Range anticline, strata on the northeast limb of the anticline rest on successively older strata in the southwest limb of the syncline: Luscar strata, for instance, rest on Brazeau just north of the culmination, and on Blackstone where the Range dies out in the extreme northwest.

A kinematic analysis of the northern half of the Brazeau Range should explain the general northwesterly plunge of the Brazeau Range anticline and the arcuate strike of its axial surface. Fig. 10 is a simplified model explaining how the plunge of the anticline and the arcuate strike follow from the initial assumption that there is a decrease in transport northwestwards along the Brazeau Range fault. The interpretation of folding in the model (after Gwinn, 1964) has already been put forward by Douglas (1950) and Hume (1957). Though details of the theory have been criticized by Scott (1954) and Fox (1959) their criticisms were not aimed at the "thin-skinned" interpretation of Foothills tectonics so much as at Douglas' choice of several, minor zones of decollement. While there is still some dispute over possible decollement zones within the sedimentary column, the uncoupling of the basement from the overlying deformation is confirmed by seismic evidence and there now seems little doubt, that at (or just above) the contact of the PreCambrian basement complex with the overlying sediments there is a major zone of decollement under much of the Foothills and Eastern Ranges of the Rocky Mountains.

The Thesis Area

One and a half miles southeast of Shunda Gap, the Palliser is exposed in the valleys of the streams that flow northeast to join Shunda Creek. The contour map on the Palliser top (Fig. 7) shows it is folded into two anticlines---the equivalent of the Brazeau Range anticline and a smaller anticline northeast of this. The intervening syncline is almost isoclinal towards its apex, the limbs dipping towards one another at 80 degrees in the extreme southeast of the thesis area (Fig. 7).

It is possible to trace Palliser continuously through the same two anticlines and tight syncline on the hillside looking into Shunda Gap from the southeast. The syncline in the Palliser is isoclinal, both limbs dipping to the southwest at about 65 degrees. In the overlying Banff strata, the syncline is less tight with uninverted dips from 30 to 40 degrees in the limbs, evidence of structural disharmony.

The next exposures to the northeast are in the cuts along the railway line in Shunda Gap. The syncline and anticline northeast of the Brazeau Range anticline are no longer clearly identifiable. The section shows a series of fault slices of overturned strata, the top of the Palliser and most of the Banff Formation are thrust in contact with Mount Head and Fernie rocks which themselves lie in thrust contact with Cadomin and Luscar.

A thrust has been inserted between the northeast dipping Palliser on the northeast limb of the Brazeau Range anticline and the overturned southwest dipping Palliser, even though there is no space problem on the line of section. The map of the Palliser top (Fig. 7) shows this fault is necessary both to the southeast and northwest of the Gap.

Douglas' (1956) Section CD which here lies almost along the railway

line, inserted an anticlinal hinge below the fault, implying that the fault had locally migrated to the back limb of the Brazeau Range anticline. A look at the contour map on the top of the Alexo (Fig. 6) shows that this may have oversimplified the problem. On the southeast side of Shunda Gap the fold plunges in a direction slightly north of northwest, on the northeast side the crest of the fold in the Alexo is not exposed but appears offset considerably to the northeast with the fold axis dipping into the Gap. Strike lines drawn on the fault trace indicate that the fault plane has probably changed attitude rapidly across the Gap from a gentle dip to slightly west of south to a steeper dip to slightly south of west. This sharp change shows up in the domains constructed on the contour map: southeast of the Gap the domains share two stations, and the change of dip and strike is gradual, whereas these domains share no stations with the domain to the north of the Gap. The minor fault appears to displace the Brazeau Range anticline and is probably later than the initiation of the fold.

No further discussion of the railway section is necessary till the Luscar exposure is reached. This seems to be overturned from the altitude of 2 examples of truncated cross bedding and it is probable that the Cadomin conglomerate above it belongs to the same thrust slice. Careful measurement shows that there is room in the thrust slice above the Cadomin only for most of the Fernie, so the Nikanassin is cut out of the section. The Cadomin and Luscar slice is then part of the overturned northeast limb of the minor anticline. The Palliser and Banff slice comes from the southwest limb (also overturned) of this anticline and there is sufficient room for the syncline, almost plunged out, above the fault. On the northwest side of the Gap the syncline has disappeared.

Douglas mapped the highest minor thrust as dying out in the Palliser a mile northwest of the railway line. In this thesis it is interpreted as running between the overturned and upright strata on the northeast flank of Coliseum Mountain till it dies out under the minor culmination shown on the contour map of the top of the Palliser.

Observation suggests that there is no room problem in the Banff strata where Douglas maps a lower thrust fault nor are there signs of the trace of such a fault. But along the northeast side of Coliseum Mountain the strata between the top of the Pekisko and the base of the Fernie are almost invariably disturbed and in a number of sections there is a definite room problem. This lower thrust fault moves Palliser and Banff strata onto Mount Head and Fernie strata in the railway section and probably terminates against the highest minor fault.

Both minor faulting and minor folding within the thesis area seem to give similar results kinematically, they transfer some of the horizontal portion of the total transport along the Brazeau Range fault to the vertical portion. This is more easily seen in the case of the faults. The splaying of the Brazeau Range fault distributes total movement along it over a number of minor faults. As these lie above the main thrust they have a steeper dip to the west than the main thrust and a greater proportion of the total movement on them is vertical (assuming that the movement on these faults is dominantly dip-slip).

The argument in the case of the minor folding is less clear since the alternative style of deformation is not as exactly specified. However by comparison with the section to the southeast where there are no minor structures on the northeast limb of the main anticline, we can argue that the effect of the minor fold is to reduce the "apparent shortening" (or horizontal transport) on the Brazeau Range Fault. We

may also note the sequence northwestwards along strike of no minor structures, minor folding and then splaying of the Brazeau Range fault and argue that the minor faulting is a more intense expression of the same kind of deformation that caused minor folding.

The result of the minor faulting and folding is the local reversal of the plunge of the Brazeau Range anticline. The contour map on the top of the Palliser shows that this surface is carried up on the minor faults to reach a culmination slightly southeast of the peak of Coliseum Mountain before the dying out of two of the splays of the fault cause it to resume its downward plunge. The contour map on the top of the Banff shows a culmination further to the northwest. The northwesterly displacement of the culmination is probably due to the smaller curvature of the Banff surface--it is a greater distance from the fault plane than the Palliser surface.

The change of fold profile along strike is also worth noting. The top of the Banff is almost vertical in the northeast limb of the Brazeau Range anticline above the highest splay of the Brazeau Range fault. When this dies out the northeast limb of the anticline slackens dip and the hinge of the fold migrates five hundred feet down the northeast limb from near the crest. This should be explained.

It has already been argued that the initiation of folding was prior to the initiation of minor faulting. The character of the folding might be expected to localize the minor faulting. This argument has already been used to show that minor faulting evolved from minor folding. Unfortunately the thrust splays show no signs of disappearing into minor folds at their northwesterly ends and to preserve the hypothesis a "conventionalist twist" (Popper, 1957) has to be introduced. Once minor faulting has taken place it will be assumed that it spreads faster than minor folding and eventually moves into areas where minor folding has yet to be initiated and so relieves the necessity for minor folding. As the major fold has been presumed in the kine-

matic analysis to have been produced by "up and over" movement along the Brazeau Range fault, it is likely that movement along a minor fault will cause some modification by "drag" of the profile of the major fold. Drag causes a hinge to develop above the fault plane and explains the migration of the hinge down the northeast limb to just above the Coliseum Fault. There remains the problem of why minor faulting and folding developed where they did. There are at least two plausible solutions to this problem.

The geological map of the northern half of the Brazeau Range shows that the northward decrease in transport on the Brazeau Range fault is apparently reversed in Shunda Gap. On both sides of the Gap the Luscar strata lie on Brazeau strata, in the Gap itself they lie on Wapiabi strata. Douglas' (1958) map suggests that there is a local doming of the axis of the (Swale Creek) syncline. Such a doming would force doming of the structures above and behind it and cause some horizontal movement to be transferred to vertical movement.

Alternatively, the sharp change in strike of the fold across the Gap might be taken as evidence that there is a sudden increase in resistance to horizontal movement along the Brazeau Range fault and this causes an increase in the vertical portion of total transport. Such an increase might be due to changes in the properties of the horizon of decollement. The section drawn by Shaw (1963) (which presumably makes use of Imperial Oil's unpublished geophysical data) shows that the Brazeau Range is the most northeasterly thrust slice in the Disturbed Belt of Central Alberta with a horizon of decollement below the top of the Cambrian. The Devonian and Cambrian strata under the Stolberg anticline, for instance, to the northeast are believed to be undisturbed. This change of horizon of decollement might be due to a change in the properties of the horizon in which this decollement takes place --

perhaps a facies change from shale to limestone. This kind of facies change on a larger scale might reasonably account for the northwestward plunge of the whole Range.

In summary the assumptions the kinematic analysis makes are listed as they were developed.

1) The analysis requires a "thin-skinned" model for the tectonics of the Disturbed Belt.

2) Movement on the Brazeau Range fault dies away northwestwards with the Brazeau Range anticline. The decrease in movement may be due to a change in the mechanical properties of the layer of decollement.

3) The sequence of events within the area was probably -- major faulting and folding initiated more or less contemporaneously (the folding is caused by movement up the fault). Then minor folding 'followed closely by minor faulting'. The formation of minor folds probably ended before any of the other forms of deformation, though the major folds continued to be modified by movement on minor and major faults.

The dynamic analysis begins the testing of these assumptions. They imply much about the mechanical properties of materials which behaved in this way. A solution to the dynamic analysis would consist of finding a material with properties consistent with present knowledge of the behaviour of rocks under stress and finding a stress field history consistent with present knowledge of a likely stress history which would cause such movements as have been postulated. This would be a fairly rigorous test of the kinematic analysis.

DYNAMIC ANALYSIS

Shaw (1963) has compiled a useful bibliography of the rather scanty literature on Foothills tectonics up to 1961. It is enough to show that geologists are occupied with a model of a rock mass slipping towards the northeast over a rough basement. This kind of model immediately suggests experiments with a sand box, a box filled with layers of sand, one end of which is a movable plunger which is advanced to force the material northeastwards.

Link (1949) uses the results of sand box experiments to "confirm" his results for a cross section of a typical Foothills structure--his Alpha structure.

The sand box is an unsatisfactory piece of apparatus. Haddow (1965) pointed out that the form of the "fault" surfaces developing in the sand, assuming the sand behaves as a perfectly plastic body (Ode, 1960) is strongly dependent on the shape and frictional properties of the surface of the plunger. In particular if the plunger is smooth and planar, the contact of the plunger with the base of the sand box is a singular point in a plastic slip line field. This field has at least one simple solution, a fault plane at 45° to the horizontal originating at the singular point and reaching the free surface of the sand. This solution strongly resembles Link's illustrated models, but since there is no equivalent of the plunger in the Rocky Mountain orogeny it hardly confirms Link's interpretations.

A more reasonable approach was that of Hafner (1951) who attempted to explain some of Hubbert's (1951) results with sand box experiments using the theory of elasticity. Hafner (p.383) visualized the following set of events in the failure of a rock body under a stress field.

A condition of stress is produced. As long as the shearing stress is everywhere below the elastic limit of the material, the stress field can be determined.

With further increase of the stresses, the yield strength is exceeded at some point and faulting occurs. The positon of this point can be determined from the initial conditions. Around the point there is a drastic reduction of stress, while further away the stress field remains substantially unchanged. The fault thus provides local relief in the most intensely stressed portion of the body. The further build-up of the stress field is presumed to go on until renewed faulting eventually takes place at some distance from the first fracture where the stress relief was negligible. So the new fracture still conforms quite closely to the old stress field.

The opinions set forth in Hafner's paper have prompted the use of his Fig. 6 to give a qualitative explanation of the stress field in the Rockies at the time of the orogeny (Charlesworth 1959, Fig. 4). Fig. 6b shows that failure takes place first in the top left hand corner of the block. If the effect of the failure is local, faulting resumes at other localities on the same "thrust fault surface" (Fig. 6b) outside the range of the local stress relief. There seems no reason why this process should stop till the block is actually split along this trajectory. The stress this block can sustain is then simply the sliding friction on the fault plane. Stresses greater than this amount cause movements of the block and Hubbert in the immediately preceding paper has shown that commonly experienced movements are caused by negligible increases in the stresses. There is then, no reason why the stress in the region of the fault should again approach the value causing initial failure in the rock nor will stresses capable of causing failure be transmitted into the stable mass to the right so the situation which Hafner illustrates in Fig. 6b is improbable. At $x = -4$ the rock mass has failed, at $x = -12$ the already fractured rock mass is supporting a stress three times its strength. If c (Fig. 6b) is reduced to a more likely value, the boundary between the stable and the unstable fields approaches the horizontal and the thrust

planes lose their curvature. So much of the original close resemblance to the structural cross sections of the Rockies is lost. As Hafner himself concludes ...."the examples are only rigorously correct if the stress is everywhere below the strength of the material."

Attempting to use elasticity theory to analyze the behaviour of the rock mass has several disadvantages. At the root of these is the inability of the theory to deal with bodies in which finite displacement takes place under stresses above the elastic limit.

Above the elastic limit of the substance some aspects of the body's behaviour might be reasonably expected to be approximated by a perfectly plastic body. The model to be examined will be a perfectly plastic body undergoing plane strain. It is slipping across a perfectly rough horizontal surface towards a rigid area. Much of the analysis follows Jaeger (1962, pp. 146-149)

The initial object of the analysis is to determine the form of potential surfaces of faulting in the moving mass. Ode (1960) pointed out that in plasticity analysis, faults can be interpreted as surfaces of velocity discontinuity along which movement has taken place for some time.

1) The principal axes of rate of strain and of stress deviation are the same.

2) The substance is uncompressible,

$$e_1 + e_2 + e_3 = 0$$

where the e_i are the principal strains.

3) Elastic strains are negligible in comparison with the plastic strains.

4) The principal stress deviations are proportional to the principal rates of strain.

That is

$$S_1 = 2\phi\dot{e}_1 \quad , \quad S_2 = 2\phi\dot{e}_2 \quad , \quad S_3 = 2\phi\dot{e}_3$$

where the S_i are the principal components of the stress deviation at some fixed point, the e_i are the principal rates of strain at the point, ϕ is a constant.

The above are Jaeger's (Jaeger, 1962) § 29 (3). He shows that they lead to:

$$S_x = 2\phi\dot{e}_x \,, \quad S_y = 2\phi\dot{e}_y \,, \quad S_z = 2\phi\dot{e}_z$$

$$S_{yz} = \phi\dot{\gamma}_{yz} \,, \quad S_{zx} = \phi\dot{\gamma}_{zx} \,, \quad S_{xy} = \phi\dot{\gamma}_{xy}$$

Jaeger § 29 (4).

In plane perfectly plastic strain the z direction is conventionally chosen as the direction of zero motion.

$$e_z = 0$$

from Jaeger § 29 (4) $S_z = 0$

As the stress deviator in this direction is zero, the z direction must be a direction of principal stress.

By Jaeger § 27 (4) $\sigma_3 = \frac{\sigma_1 + \sigma_2}{2}$ σ_1, σ_2 are the principal stresses in the xy plane.

Besides the assumptions involved in the concept of perfect plasticity some yield condition must be assumed before the analysis can proceed. This yield condition holds at every point within the region in which the body is behaving perfectly platically. The most common choice of yield condition is that due to Von Mises:-

J_2 = a constant,

$J_2 = (S_1^2 + S_2^2 + S_3^2)$, J_2 is the second invariant of the stress deviator tensor,

$= \frac{\sigma_o^2}{3}$ by Jaeger § 27 (24)

where σ_o is the yield stress in uniaxial tension (or compression).

By Jaeger § 27 (25) and § 27 (4), in plane perfectly plastic strain,

$$\sigma_1 - \sigma_2 = 2k \qquad (1)$$

where $k = \sigma_o \cdot 3^{-\frac{1}{2}}$

Since the maximum value of the shear stress is

$$\frac{1}{2}\left(\left(\sigma_x - \sigma_y\right)^2 + 4T_{xy}^2\right)^{\frac{1}{2}} \qquad (2)$$

with the conventions of sign and definitions given by Jaeger (1962), pp. 3-4)

(1) becomes (3)

$$\left(\sigma_x - \sigma_y\right)^2 + 4T_{xy} = 4k^2$$

There are two other equations in $\sigma_x, \sigma_y, T_{xy}$

$$\frac{\partial \sigma_x}{\partial x} + \frac{\partial T_{xy}}{\partial y} + \rho X = 0 \qquad (4)$$

$$\frac{\partial \sigma_y}{\partial y} + \frac{\partial T_{xy}}{\partial y} + \rho Y = 0 \qquad (5)$$

X, Y are the body forces per unit volume in the x, y directions, ρ is the density of the body. (4) and (5) are the equivalents in plain strain of Jaeger's § 34 (1) and (2) (Jaeger, 1962). Jaeger derives these equations. They are equivalent to the assumption that the velocities U, V in the x, y directions at a point in the plane do not change with time--in other words, the system of stresses is in equilibrium.

Since it is only intended to consider gravity here

$$Y = O, \quad X = -g$$

If (4), (5) are partially differentiated with respect to y, x (6), (7), result:

$$\frac{\partial^2 T_{xy}}{\partial y^2} + \frac{\partial^2 \sigma_x}{\partial x \partial y} = 0 \qquad (6)$$

$$\frac{\partial^2 T_{xy}}{\partial x^2} + \frac{\partial^2 \sigma_y}{\partial x \partial y} = 0 \qquad (7)$$

(8) results by subtraction and using (3)

$$\frac{\partial^2 T_{xy}}{\partial x^2} - \frac{\partial^2 T_{xy}}{\partial y^2} = \frac{\partial^2 (\sigma_1 - \sigma_y)}{\partial x \partial y} = \pm 2 \frac{\partial^2 (k^2 - T_{xy}^2)^{\frac{1}{2}}}{\partial x \partial y} \quad (8)$$

(8) is a 2nd order partial differential equation in T_{xy}. Normally its solution presents considerable difficulty but in this case a plausible simplifying assumption can be made. Choosing x, y axes so that the perfectly rough surface is given by $y = -a$, the maximum shearing stress will be developed along this surface--as it has been already assumed that this surface is one on which slip is taking place. Then from the discussion of Jaeger § 27 (25),

$$|T_{xy}| = k$$

a boundary condition independent of x. This suggests that T_{xy} may be a function of y only. If this is the case,

(8) then gives (9)

$$\frac{\partial^2 T_{xy}}{\partial y^2} = 0 \quad (9)$$

$T_{xy} = Ay + B$, as $y = O$ is the earth's surface

$B = O$ since the atmosphere cannot withstand a shearing stress.

Substituting the boundary conditions,

$T_{xy} = k$ when $y = -a$, if the material is slipping to the right across the rough surface,

$$T_{xy} = -\frac{ky}{a} \quad (10)$$

σ_x, σ_y can be found by substitution in (4) and (5)

$$\sigma_x = \frac{k}{a} x + f(y) + C \quad (11)$$

$$\sigma_y = \rho g y + g(x) + c \qquad (12)$$

where f(y), g(y) are functions of x, y to be determined and c is a constant. Substituting (11) and (12) in (3)

$$\pm 2k\left(1 - \frac{y^2}{a^2}\right)^{\frac{1}{2}} = \frac{k}{a}x + f(y) - \rho g y - g(x) \qquad (13)$$

By comparing coefficients of x, y,

$$f(y) = \rho g y \pm 2k\left(1 - y^2/a^2\right)^{\frac{1}{2}} \qquad (14)$$

$$g(x) = \frac{k}{a}x \qquad (15)$$

Substituting (14) and (15) in (11) and (12)

$$\sigma_x = \frac{k}{a}x + \rho g y \pm 2k\left(1 - \frac{y^2}{a^2}\right)^{\frac{1}{2}} + c \qquad (16)$$

$$\sigma_y = \rho g y + \frac{k}{a}x + c \qquad (17)$$

$$\sigma_x - \sigma_y = \pm 2k\left(1 - \frac{y^2}{a^2}\right)^{\frac{1}{2}} \qquad (18)$$

In this analysis the negative root is chosen in (18). This choice will be justified when the velocity field is examined.

Having derived the stresses, the next step is to derive the relationship between these and the trajectories of maximum shear stress. These will coincide with the directions of maximum shear strain and (according to Jaeger 1962, p. 144) be

the locus of points at which the relative movement between neighbouring parallel points is a maximum. They are the "faults" or slip-lines whose form was to be derived.

The trajectories of maximum shearing stress bisect the principal axes of stress. The equations connecting the stresses across an element inclined at α to the principal axes with the principal stresses are (Jaeger, pp. 6-7)

$$\sigma_x = \frac{\sigma_1 + \sigma_2}{2} + \frac{\sigma_1 - \sigma_2}{2} \cos 2\alpha \qquad (19)$$

$$\sigma_y = \frac{\sigma_1 + \sigma_2}{2} - \frac{\sigma_1 - \sigma_2}{2} \cos 2\alpha \qquad (20)$$

$$T_{xy} = \frac{\sigma_1 + \sigma_2}{2} \sin 2\alpha \qquad (21)$$

The trajectories of maximum shearing stress will be inclined at $\beta, \beta + \frac{1}{2}\pi$ to the x axis where $\beta = \alpha + \pi/4$ (Jaeger, Fig. 52).

Replacing α by $\beta - \pi/4$, $\sigma_1 \frac{+\sigma_2}{2}$ by σ_n and $\sigma_1 \frac{-}{2} \sigma_2$ by k (from (1)), (22), (23), (24) result.

$$\sigma_x = \sigma_n + k \sin 2\beta \qquad (22)$$

$$\sigma_y = \sigma_n - k \sin 2\beta \qquad (23)$$

$$T_{xy} = -k \cos 2\beta \qquad (24)$$

$\tan \beta$ is the gradient of one slip line system, then from (22-24)

$$= \frac{1 - \cos 2\beta}{\sin 2\beta} = \frac{2(k + T_{xy})}{\sigma_x + \sigma_y} \qquad (25)$$

the other slip line system is orthogonal to this, its gradient

$$-\cot\beta = \frac{-(\sigma_x - \sigma_y)}{2(k + \tau_{xy})} \qquad (26)$$

So the stresses may now be substituted into (25) or (26) to derive the differential equations of the systems of slip lines. Using (26)

$$\frac{dy}{dx} = \frac{\left(1 - \frac{y^2}{a^2}\right)^{\frac{1}{2}}}{\left(1 - \frac{y}{a}\right)} \qquad (27)$$

Using the substitution, $y = a\cos\theta$ the integral becomes

$$x = -a\int(1 - \cos\theta)\,d\theta$$

and hence $y = a\cos\theta,\ x = -a(\theta - \sin\theta) + D$ (28)

(where D is a constant) is the solution.

(28) are the parametric equations of a family of cycloids. From (27), $\frac{dy}{dx}$ is always positive, so only the portions where y increases with x may be taken.

The other slip line system is orthogonal to these, it has parametric equations

$$y = a\cos\theta,\ x = a(\theta + \sin\theta) + E \qquad (29)$$

E is a constant.

A velocity distribution compatible with the stress, (16) - (18), must now be chosen.

The components of the stress deviator are by (16) - (18)

$$s_x = -s_y = -k\left(1 - \frac{y^2}{a^2}\right)^{\frac{1}{2}} \qquad (30)$$

since $\sigma_x - \sigma_h = s_x,\ \sigma_h - \sigma_y = s_y,\ \frac{\sigma_y + \sigma_x}{2} = \sigma_h$

These are connected to the velocities at (x, y) by

$$s_x = 2\phi\dot{\epsilon}_x,\ s_y = 2\phi\dot{\epsilon}_y,\ s_{xy} = \phi\dot{\gamma}_{xy} \quad \text{(Jaeger § 29 (4)}$$

where $\dot{\epsilon}_x$, $\dot{\epsilon}_y$ are the rates of extension in the x, y directions and $\dot{\gamma}_{xy}$ is the rate of shear.

A velocity distribution compatible with compression in the x direction is required. Since $k\left(1 - \frac{y^2}{a^2}\right)^{\frac{1}{2}}$ is always positive, by (30), the negative root must be chosen in (16) - (18). From (31)

$$S_x = -k\left(1 - \frac{y^2}{a^2}\right)^{\frac{1}{2}} = 2P\dot{\epsilon}_x = 2P\frac{\partial u}{\partial x} \quad (32)$$

$$S_y = k\left(1 - \frac{y^2}{a^2}\right)^{\frac{1}{2}} = 2P\dot{\epsilon}_y = 2P\frac{\partial v}{\partial y} \quad (33)$$

$$T_{xy} = -\frac{k}{a}y = P\dot{\gamma}_{xy} = P\left(\frac{\partial v}{\partial x} + \frac{\partial u}{\partial y}\right) \quad (34)$$

where U, V are the velocities in the x, y directions.

P is an unknown function involving the strain rate. The choice of P will give some freedom to the choice of velocity distribution. There is one boundary condition--at $y = -a$, $V = 0$.

$$V = \frac{yV_0}{a} + V_0 \quad (35)$$

where V_0 is the upward velocity of the free surface, satisfies this condition if we choose

$$P = \frac{k\left(a^2 - y^2\right)^{\frac{1}{2}}}{2V_0} \quad (36)$$

Substituting (36) in (32)

$$u = -\frac{2V_0}{a}x + f(y)$$

(34) determines f(y)

$$f'(y) = \frac{2V_0 y}{a\left(a^2 - y^2\right)^{\frac{1}{2}}}$$

$$f(y) = -2V_0\left(1 - \frac{y^2}{a^2}\right) + F$$

F is a constant.

$$U = -2V_0\left(\frac{x}{a} + \left(1 - \frac{y^2}{a^2}\right)^{\frac{1}{2}}\right) + F \qquad (37)$$

The only other analysis of this type is the geological literature which could be found (Varnes, 1962), ended with the calculation of the slip line fields, and did not go on to consider the effects of finite displacements along slip lines.

Fig. II illustrates the form of the slip line field calculated in this model and represents diagrammatically the distribution of stresses on horizontal and vertical sections through the body.

The "thrust fault" in the slip line field bears a close resemblance to a typical Foothills thrust--it rises very gradually out of the zone of decollement and then steepens more rapidly towards the surface. This superficial resemblance is obviously a preliminary requirement. At some time in the future the form of a typical Foothills thrust should be compared statistically to the form of the ideal slip line and of any other models that may have been proposed by then.

Hill (1950) showed that the calculations involved (Chapter VI-7) in determining the velocity field around the velocity discontinuity are not so much theoretically formidable as arthmetically tedious.

REFERENCES

Agterberg, F.P., 1964; The Method of Statistical Structural Analysis applied to the Crystalline Basement of the Dolomites in Northern Italy, Geol. Mijnb. 43e Jaar. pp. 222-235.

Bielenstein, H.U., 1964; The Miette Formation, Jasper, Alberta, Unpublished M.Sc. thesis, University of Alberta.

Bokman, J., 1963; Post Mississippian Unconformity in Western Canadian Basin, Amer. Assoc. Petrol. Geol., Mem. 2, pp. 252-263.

Brady, W.B., 1958; Mississippian Strata of the Central Foothills and Eastern Ranges of the Nordegg Area, Alberta, A.S.P.G. 8th Guidebook, pp. 51-63.

Charlesworth, H.A.K., 1959; Some Suggestions on the Structural Development of the Rocky Mountains in Canada, Journ. Alberta Soc. Petrol. Geol., V.7, pp. 249-256.

Creer, K.M., 1962; A Statistical Enquiry into the Partial Remagnetization of Folded Old Red Sandstone Rocks, J. Geophys. Research, Vol. 67, pp. 1899-1906.

Douglas, R.J.W., 1950; Callum Creek, Langford Creek and Gap map-areas, Alberta, Geol. Surv. Canada, Mem. 255.

_____ 1956; Nordegg, Alberta, Geol. Surv. Canada, Paper 55-34.

_____ 1958; Chungo Creek Map Area, Alberta, Geol. Surv. Canada, Paper 58-3.

Fisher, R.A., 1953; Dispersion on a Sphere, Proc. Royal Soc., Ser. A, Vol. 217, pp. 295-305.

Fleuty, M.J., 1964; The Description of Folds, Proc. Geol Ass., Lond., Vol. 75, pp. 461-492.

Flinn, D., 1958; On Tests of Significance of Preferred Orientation in Three Dimensional Fabric Diagrams, Jour. Geol., Vol. 66, pp. 526-539.

Fox, F.G., 1959; Structure and Accumulation of Hydrocarbons in the Southern Foothills, Alberta, Canada, Amer. Assoc. Petrol. Geol., Vol. 43, pp. 993-1025.

Erdman, O.A., 1950; Alexo and Saunders Map Area, Geol. Surv. Canada, Mem. 254, 100 p.

Gwinn, V.E., 1964; Thin Skinned Tectonics in the Plateau and Northwest Valley and Ridge Provinces of the Central Appalachians, Bull. Geol. Soc. Amer., Vol. 75, pp. 863-900.

Haddow, J., 1965; Personal communication, Department of Mechanical Engineering, University of Alberta.

Hume, G.S., 1957; Fault Structures in the Foothills and Eastern Rocky Mountains of Southern Alberta, Bull. Geol. Soc. Amer., Vol. 58, pp. 395-412.

Hafner, W., 1951; Stress Distributions and Faulting, Bull. Geol. Soc. Amer., Vol. 62, pp. 373-398.

Hill, R., 1950; Plasticity, Oxford, 356 p.

Hubbert, M.K., 1951; Mechanical Basis for Certain Familiar Geologic Structues, Bull. Geol. Soc. Amer., Vol. 62, pp. 355-372.

Jaeger, J.C., 1962; Elasticity, Fracture and Flow, Methuen, London, 208 p.

Lindley, D.V., and Miller, J.C.P., 1953; Cambridge Elementary Statistical Tables, Cambridge, 35 p.

Link, T.A., 1949; Interpretations of Foothills Structues, Alberta, Canada, Amer. Assoc. Petrol. Geol., Vol. 33, pp. 1475-1501.

Mertie, J.B., 1947; The Delineation of Parallel Folds, Bull. Geol. Soc. Amer., Vol. 58, pp. 779-802.

Muecke, G., 1965; Fracture Analysis in the Canadian Rocky Mountain, Unpublished M.Sc. thesis, University of Alberta.

Noble, D.C., and Eberly, S.W., 1964; A digital computer procedure for preparing beta diagrams, Amer. Jour. Sci., Vol. 262, pp. 1124-1129.

Ode, H., 1960; Faulting as a Velocity Discontinuity in Plastic Deformation, Bull. Geol. Soc. Amer., Mem. 79, pp. 293-323.

Oertel, G., 1962; Extrapolation in Geologic Fabrics, Bull. Geol. Soc. Amer., Vol. 73, pp. 325-342.

Pitcher, G.G., 1958; Review of Oil Exploration in Nordegg Area, Alberta Soc. Petrol. Geol. 8th Guidebook, pp. 11-17.

Popper, K.R., 1957; The Philosophy of Science: A Personal Report, in British Philosophy in the Mid-Century, George Allen & Unwin, London, 396 p.

Ramsay, J.G., 1964 The uses and limitations of beta-diagrams and pi-diagrams in the geometrical analysis of folds, Quart. Jour. Geol. Soc., Lond., Vol. 120, pp. 435-454.

Sanderson, J.O.G. 1958; Early History of Geological Investigation of the Nordegg Area, Alberta Soc. Petrol. Geol. 8th Guidebook, pp. 1-4.

Scheidegger, A.E., 1965; On the statistics of the orientation of bedding planes, grain axes and similar sedimentological data, U.S. Geol. Surv. Prof. Paper 525-C, pp. 164-167.

Scott, J.C., 1954; Folded Faults in the Foothills of Alberta, Amer. Assoc. Petrol. Geol., Rutherford Memorial Volume, pp. 309-341.

Selby, B., 1964; Girdle distributions on a sphere, Biometrika 51, pp. 381-392.

Shaw, E.W., 1963; Canadian Rockies--Orientation in Time and Space, Amer. Assoc. Petrol. Geol., Mem. 2, pp. 231-242.

Spivak, J., 1949; Jurassic Sections in the Foothills of Alberta and Northeastern British Columbia, Amer. Assoc. Petrol. Geol., Vol. 33, pp. 533-546.

Strand, T.,1944; A Method of Counting out Petrofabric Diagrams, Nordsk. Geol. Tidskr., Vol. 24, pp. 112-114.

Turner, F.J., and Wiess, L.E., 1963; Structural Analysis of Metamorphic Tectonites, New York, 545 p.

Varnes, D.J., 1962; Analysis of Plastic Deformation according to Von Mises' Theory with Application to the South Silverton Area, San Juan County, Colorado, U.S. Geol. Surv. Prof. Paper 378-B, 48 p.

Watson, G.S., 1956a; Analysis of Dispersion on a Sphere: Mon. Not. Roy. Astron. Soc., Geophysical Supplement, Vol. 7, pp. 153-159.

_____ 1956b; A Test for Randomness of Directions, Mon. Not. Roy. Astron. Soc., Geophysical Supplement, Vol. 7, p. 160.

_____ 1960; Further Significance Tests on a Sphere, Biometrika, Vol. 47, pp. 87-91.

_____ 1965; Equational Distributions on a Sphere, Biometrika, Vol. 52, pp. 193-203.

Watson, G.S. and Irving, E., 1957; Statistical Methods in Rock Magnetism, Mon. Not. Roy. Astron. Soc., Geophysical Supplement, Vol. 7, pp. 289-300.

APPENDIX 1

THE ANALYSIS OF THE PRECISION PARAMETER, K

It has been suggested (on p. 9) that it would be convenient to have some means of estimating the precision parameter, K, at a particular outcrop before visiting it. With this in mind K values for 108 outcrops where samples of ten or more readings had been taken were analyzed. (The restriction on the sample size follows from the statistical assumption that the error in the determination of the independent variable should be negligible). A plot of part of the data suggested the mean dip and the lithology were important in determining K at a particular outcrop.

To test this suggestion Dr. K. W. Smillie proposed that for each lithology an attempt be made to fit the same function to the K values plotted against dip which could be transformed to a straight line, and then examine the straight lines to determine whether they were coincident. The first step was designed to show how the value of K depended on the dip and the second to test whether the lithology had any significant effect.

A preliminary plot suggested the functions

$$X_2 = AX_1^B \quad (1) \qquad X_2 = K$$

$$X_2 = A + \frac{B}{X_1} \quad (2) \qquad X_1 = \text{Dip}$$

$$X_2 = A + B\log_{10}X_1 \quad (3) \qquad A, B \text{ are constants}$$

might be suitable. These transform to

where

(1) $X_5 = A^1 + B^1X_4$ $\qquad X_5 = \log_{10}X_2$ $\qquad A^1, B^1$ are constants

(2) $X_2 = A^1 + B^1X_3$ $\qquad X_4 = \log_{10}X_1$

(3) $X_2 = A^1 + B^1X_4$ $\qquad X_3 = \frac{1}{X_1}$

a)

b)

c)

Dr. Smillie's multiple regression program (1965, Chapter 6) was used to test the the fit of these functions to the data. The results are set out in the Table 1:2. The results of fitting the first function to each of the five lithologies were analyzed by the technique set out in Hald (1952), pp. 579-584. The calculations involved are lengthy and only the results will be quoted here. The data for the calculations are set according to Hald's Table 18:19 with his notation in Table 1:1.

While the slopes of the regressions did not significantly differ, the statistics showed at the 1% significance level that the regression lines did not coincide. It appears then that the lithology of the strata has a significant effect on the value of K as does the dip.

Suppose that for each lithology, the number of samples of bedding planes of this lithology is N_1 and $\log_{10}$ (mean dip) of these samples takes values x_i ($i=1,.,N_1$) and $\log_{10}$ K takes values y_i ($i=1,\ldots,N_1$) then, Hald's notation is that

$$\overline{x_{1.}} = \sum_{i=1}^{i=N_1} x_i \qquad \overline{\overline{x}} = \frac{\overline{x_{1.}}}{N_1}$$

$$\overline{y_{1.}} = \sum_{i=1}^{i=N_1} x_i \qquad \overline{\overline{y}} = \frac{\overline{y_{1.}}}{N_1}$$

$$b_1 = B^1$$

$$SPD_{x_1y_1} = \sum_{i=1}^{i=N_1} (x_i - \overline{x})(y_i - \overline{y})$$

$$SSD_{x_1} = \sum_{i=1}^{i=N_1} (x_i - \overline{x})^2 \qquad SSD_{y_1} = \sum_{1}^{N_1} (y_i - \overline{y})^2$$

$$SSD_{y_1|x_1} = SSD_x - \frac{SPD^2_{x_1y_1}}{SSD_{x_1}}$$

$$f = N-2$$

$$S_{11} = SSD_{Y_1|X_1} / f$$

In Table 1:2

R^2 is the correlation coefficient

F is the critical F value

TABLE I:1

Lithology	$\bar{X}_i$	$\bar{Y}_i$	SSD_{x_i}	$SPD_{x_i y_i}$	b_i	SSD_{y_i/x_i}	f	s_{ii}^2	N_i
Fernie	5.365	12.857	0.994	-2.040	-2.049	0.522	3	0.1741	5
Mount Head & Turner Valley	9.911	23.644	1.558	-0.248	-0.537	0.263	7	0.0376	9
Pekisko	36.754	70.156	3.914	-1.888	-0.480	1.653	24	0.0375	26
Banff	18.926	35.888	0.908	-0.653	-0.717	1.057	11	0.0961	13
Palliser	77.105	148.327	5.646	-4.406	-0.794	3.489	53	0.0658	55

TABLE I:2

Lithology	R^2	F		A^1	B^1
Fernie	88.89	24.00**	1	4.771	-2.049
	47.55	2.72	2		
	60.69	4.63*	3		
Mount Head & Turner Valley	33.54	3.53*	1	3.219	-0.537
	17.88	1.23	2		
	25.61	2.41	3		
Pekisko	35.31	13.10**	1	3.377	-0.480
	31.33	10.95**	2		
	34.85	12.84**	3		
Banff	30.65	4.86*	1	3.804	-0.717
	10.82	1.13	2		
	17.38	2.31	3		
Palliser	50.07	53.15**	1	3.810	-0.794
	29.62	22.31**	2		
	31.16	23.98**	3		

** significant at the 1% level
* significant at the 10% level

TABLE 1:3 DATA USED IN ANALYSIS OF K

EXPOSURE NUMBER	DIP OF BEDDING	DIRECTION OF DIP	PRECISION PARAMETER	SAMPLE SIZE
Lithology, Palliser-limestone, dolomite				
068*	59.3	058.6	0093.5	16
071	10 .6	234.4	0524.9	16
210	16.4	046.9	3301.4	11
254	44.8	053.6	0193.1	10
260	21.5	176.1	0670.0	10
285	10.7	215.8	0586.6	10
291	46.9	027.2	0 247.9	10
301	45.9	040.8	0498.6	10
302	81.1	215.2	0219.0	10
303	75.4	037.4	0137.1	10
304	76.8	229.8	0189.0	10
310	60.9	045.2	0274.6	10
311	69.0	221.6	0137.6	10
312	49.1	047.4	0209.5	10
314	44.5	221.6	0122.5	10
315	65.6	045.4	0858.8	10
316*	68.5	217.6	0171.4	10
317*	61.2	213.6	0341.4	10
318	59.3	039.6	0129.5	10
319	37.7	216.9	0141.9	10
320	61.4	036.3	0393.4	10
321	44.6	037.4	0385.6	10
323	64.9	026.1	0047.3	10
330	06.9	186.6	0826.4	10
331	10.2	239.1	0700.1	10
339	14.4	205.7	0644.3	10
340	13.0	211.5	0973.1	10
341	14.3	215.1	1840.9	10
342	21.7	217.9	1409.1	10

TABLE 1:3 continued

EXPOSURE NUMBER	DIP OF BEDDING	DIRECTION OF DIP	PRECISION PARAMETER	SAMPLE SIZE
344	85.1	221.1	0532.2	10
344	15.5	216.0	0405.1	10
345	50.9	225.5	0109.0	10
345	11.8	206.4	1857.9	10
346	12.3	206.1	0960.4	10
346	16.9	047.7	0468.1	10
347	43.6	043.3	0486.7	10
347	10.0	211.9	0589.8	10
349	11.3	212.1	0784.5	10
350	12.6	218.0	1408.4	11
351	17.6	223.2	0521.9	10
352	18.6	217.7	0565.6	10
356	10.0	233.3	0755.1	11
359	71.6	026.1	0309.7	10
360	65.1	032.1	0303.0	10
364	20.5	034.6	0234.9	10
374	26.3	019.7	1082.3	10
375	25.8	021.8	0407.5	10
376	11.6	009.7	1131.8	10
378	18.1	029.1	1237.0	10
381	18.8	005.9	0480.8	10
382	14.9	026.7	0825.5	10
383	23.1	020.8	1104.1	10
388	09.5	225.6	1461.3	11
390	81.7	027.9	0137.2	10
391	30.6	022.6	0258.9	10
401	23.1	184.3	0249.4	10
402	14.6	190.3	0659.9	10
404	07.7	185.7	2450.2	10
405	18.1	207.2	0576.0	10

TABLE 1:3 continued

EXPOSURE NUMBER	DIP OF BEDDING	DIRECTION OF DIP	PRECISION PARAMETER	SAMPLE SIZE
Lithology, Banff-argillaceous limestone, shale				
066 *	58.2	214.8	0229.3	10
110	77.9	038.4	0392.6	11
111	78.4	036.1	0423.9	10
124	30.6	055.8	0562.3	12
274	15.4	214.6	1203.8	10
276	14.0	216.9	0594.2	10
277	23.1	209.1	0935.8	10
278	24.6	209.7	1860.9	10
296	70.4	021.5	0111.6	10
300	43.3	058.3	0259.0	10
332	21.3	222.1	0252.4	10
333	13.9	212.1	0606.3	10
407	19.1	203.8	0726.3	10
408	21.6	205.0	2060.9	10
Lithology, Pekisko-limestone				
042	15.2	027.5	0236.3	67
046	08.4	010.2	0686.4	10
101	07.4	020.6	1555.3	15
104*	86.5	214.4	0159.9	27
107	15.4	018.2	1017.7	16
115	18.6	299.0	1363.3	11
116	16.1	212.2	0804.2	12
120	76.6	037.5	0370.2	15
121	74.3	039.4	0599.5	16
123	79.5	043.7	0561.9	20
262	22.0	188.2	0331.0	10
267	10.2	231.7	0926.3	14

TABLE 1:3 continued

EXPOSURE NUMBER	DIP OF BEDDING	DIRECTION OF DIP	PRECISION PARAMETER	SAMPLE SIZE
269	10.4	234.3	1258.7	12
271	15.2	206.3	1654.9	10
273	32.8	208.8	0544.7	10
279	22.3	200.5	0657.3	10
289	54.8	035.7	0248.9	10
299	71.8	047.9	0163.8	10
308	70.3	048.0	0209.7	10
335	08.9	206.7	0748.1	10
336	13.8	198.7	0872.4	10
337	10.8	198.9	172.7	10
338	08.5	215.9	483.4	10
363	78.0	036.3	248.1	10
365	83.9	029.0	297.2	10
387	73.5	018.5	421.1	10
307	81.7	043.8	124.6	10
Lithology, Turner Valley, Mount Head - vuggy, massive bedded dolomite				
003	08.6	038.5	216.1	14
004	05.0	035.3	569.1	11
008	08.2	030.4	467.4	14
027	21.1	006.5	241.7	19
057	07.1	051.7	1033.6	12
060	12.6	003.5	613.7	11
118	23.4	039.3	189.5	15
170*	67.8	207.3	2411.5	12
255*	77.7	213.9	504.0	10
256*	77.8	212.5	1129.7	10
258	16.4	208.1	460.8	12
261	24.8	188.7	395.2	10

TABLE1:3 continued

EXPOSURE NUMBER	DIP OF BEDDING	DIRECTION OF DIP	PRECISION PARAMETER	SAMPLE SIZE
263	84.8	222.0	209.3	10
286	61.8	204.6	123.9	10
344*	85.1	221.1	523.2	10
366*	66.6	208.5	176.7	10
Lithology, Fernie-Conglomerate, mudstone, chert, sandstone				
049	04.2	062.2	1919.6	10
050	04.6	313.4	1247.0	10
077	09.2	242.4	2364.1	17
169*	54.2	194.8	680.8	17
255*	74.8	217.8	278.6	10
256*	74.8	217.8	278.6	10
259	18.8	216.4	212.2	16
263*	81.3	223.3	2689.7	10
288	68.0	207.3	6.3	10
298*	88.5	227.9	424.7	10
305*	86.2	043.5	462.8	10
343*	83.3	222.4	1402.6	10

* overturned

ADDITIONAL REFERENCES

Hald, A., 1952, Statistical Theory with Engineering Applications, J. Wiley & Sons Inc., New York, 783 p.

Smillie, K.W., 1965, Multiple Regression, Publication No. 1, Department of Computing Science, University of Alberta, Edmonton.

APPENDIX 2

TO SHOW THAT THE PROBABILITY OF THE INTERSECTION OF TWO PLANES THE NORMALS TO WHICH HAVE FISHER DISTRIBUTIONS DOES NOT ITSELF ALWAYS HAVE A FISHER DISTRIBUTION.

It is sufficient to cite a particular case in which the normals do not have a Fisher distribution.

Consider two coincident planes. Then the intersection of the planes is equally likely to lie in any direction within the two planes. If the normals to the planes have Fisher probability distributions, this probability will be distributed with axial symmetry around the normals. The probability of the intersection of the planes lies in a band symmetrical about the planes and with a maximum density in the planes. This distribution is illustrated in Ramsay (1964) Figs. 3-5.

While the distribution of the probability of the intersection thus has axial symmetry about the normal to the planes this coincides with a minimum likelihood of the intersection. The distribution of the intersection is, therefore, not a Fisher distribution.

APPENDIX 3

THE MISSISSIPPIAN-JURASSIC UNCONFORMITY NEAR NORDEGG, ALBERTA

INTRODUCTION

In the Rocky Mountain Foothills of central Alberta, the essentially concordant contact between the Mississippian Mount Head and Jurassic Fernie Formations is exposed near Nordegg in a low cut on the south side of Highway 11, quarter of a mile east of the bridge over the abandoned railway line in Shunda Gap. This exposure, in which the beds are slightly overturned, was examined to determine the angular relationship between the two formations.

DETERMINING ANGULAR RELATIONS BETWEEN SUB-PARALLEL SURFACES

Determining the angular relations between two planar structures is difficult if, as in the case of bedding in the Mount Head and Fernie Formations at the above road cut, the structures are almost parallel. Under these conditions it is difficult to decide whether an observed difference in orientation is significant, or whether it results from scatter caused by a combination of, say, instrument error, observer error, and the departure of the bedding planes from perfect planarity. The problem of how to recognise significant differences can be approached by putting forward a plausible hypothesis about the distribution of this scatter. The hypothesis is that repeated measurements of a planar structure within a domain (a rock body that is homogeneous with respect to the planar structure being studied) have a distribution about the estimated mean of the measurements which is given by the Fisher (1953) probability density function, $P(\theta)$,

$$P(\theta) = Be^{K\cos\theta},$$

where

B is a constant,

θ is the angle between a given measurement and the estimated mean, and

K is the precision parameter, the precision parameter is the three-dimensional analogue of the inverse of the variance, such that the lower the dispersion of a sample of measurements the higher its precision parameter.

Three domains elsewhere in the Nordegg area were investigated with a view to testing the validity of the hypothesis. In each the distribution of the 60 to 70 measurements of bedding does not differ significantly from a Fisher distribution. It is therefore assumed that any number of randomly collected measurements of a planar structure in any domain have a Fisher distribution.

If the two samples to be compared have Fisher distributions it is possible to set up an approximate F-test based on an analysis of variance analogy. This is the test of the null hypothesis that the two samples come from a population with the same mean, i.e. that their orientations do not differ significantly. The hypothesis is conventionally rejected if there is less than once chance in twenty of its being true. The rejection of the null hypothesis implies that the two samples come from populations with different means and hence that their orientations are significantly different. According to Watson (1956), for samples with Fisher distributions and equal K values, the hypothesis is rejected if

$$\frac{(N-2)(R_1+R_2-R)}{(N-R_1-R_2)} > F_{2,\,2(N-2)}$$

where

$$R_1^2 = \left(\sum_1^{N_1} l_{1i}\right)^2 + \left(\sum_1^{N_1} m_{1i}\right)^2 + \left(\sum_1^{N_1} n_{1i}\right)^2$$

and

$$R_2^2 = \left(\sum_1^{N_2} l_{2i}\right)^2 + \left(\sum_1^{N_2} m_{2i}\right)^2 + \left(\sum_1^{N_2} n_{2i}\right)^2$$

(l_{1i}, m_{1i}, n_{1i}) and (l_{2i}, m_{2i}, n_{2i}) being the direction cosines of the normals to the planar structure (upward directed in the case of bedding) to the i^{th} measurement in samples 1 and 2 respectively,

and $N = N_1 + N_2$,

N_1 and N_2 being the numbers of measurements in samples 1 and 2 respectively,

$$R^2 = \left(\sum_1^{N_1} l_{1i} + \sum_1^{N_2} l_{2i}\right)^2 + \left(\sum_1^{N_1} m_{1i} + \sum_1^{N_2} m_{2i}\right)^2 + \left(\sum_1^{N_1} n_{1i} + \sum_1^{N_2} n_{2i}\right)^2$$

and $F_{2,2(N-2)}$ is tabulated in Lindley and Miller (1953, p.8).

The estimated precision parameters $\hat{K}_1$, and $\hat{K}_2$, $\left(\hat{K}_1 = \frac{N_1 - 1}{N_1 - R_1}\right)$ of any two samples to be compared are unlikely to be equal, which suggests that the F-test described above will usually be inapplicable. However these estimates are subject to large errors (Watson 1956, p. 154) and Watson and Irving (1957, p. 292) have suggested an approximate test of the hypothesis that the estimated precision parameters of the two samples are estimates of the same precision parameter K_1, $(=K_2)$. They commented that "values of $\hat{K}_1/\hat{K}_2$ far from unity strongly suggest $K_1 \neq K_2$." K_1, K_2 are the precision parameters of the populations from which the samples were taken. The effect of departures from the hypothesis on the validity of the F-test has not been examined.

A Fortran IV computer program to calculate the value of the statistic

$$\frac{(N-2)(R_1 + R_2 - R)}{(N - R_1 - R_2)}$$

(here called the coplanarity statistic)

from an input of strikes and dips of the planar structure is available. If this value is greater than the corresponding F value, the null hypothesis may be rejected at the conventional level of significance.

The angular discordance θ between the two samples can be determined from

$$\cos\theta = l_1 l_2 + m_1 m_2 + n_1 n_2$$

where (l_1, m_1, n_1) and (l_2, m_2, n_2) are the direction cosines of the estimated means of the two samples of the planar structure (upward directed in the case of bedding), given in the case of sample 1 by

$$l_1 = \frac{\sum l_{1i}}{R}, \quad m_1 = \frac{\sum m_{1i}}{R}, \quad n_1 = \frac{\sum n_{1i}}{R}$$

A Fortran IV program has been designed to calculate estimated means of samples (Muecke, 1965).

THE UNCONFORMITY IN THE SHUNDA GAP ROAD CUT

It can be verified by substitution in the test that for domains with precision parameters of 500, 10 measurements are required in each sample to distinguish estimated means two degrees apart. Previous experience had shown that the precision parameters of the samples would likely be between 200 and 700, so 10 measurements of bedding were taken on either side of the contact in the Shunda Gap road cut. The bedding planes on which these measurements were made are those closest to (within 15 feet) the contact.

Before the test can be applied it is necessary to be confident that each 15-foot-long outcrop constitutes only one or part of one domain, i.e. that each sample of 10 measurements can be considered to be a random sample from a single Fisher distribution. The precision parameters of two adjacent Mount Head and Fernie domains for which Fisher distributions have been established are 247 and 207, respectively. Because both samples from the road cut have precision parameters of over 200 (Table 3:1), it is unlikely that either sample comes from more than one domain. This reasoning is far from rigorous, but over 30 readings are needed in a sample before its fit to a Fisher distribution can be tested statistically (Watson and Irving, 1957, p. 293). It was not possible to collect samples this large from close to the unconformity, so the above rough test had to be applied. Computer

programs for the rigorous test are available.

The results of the test on the two samples from the Shunda Gap road cut (locality 1) are given in Table 3:1. It can be seen from the table that because the value for the coplanarity statistic is greater than the corresponding F value, the hypothesis that the samples are from the same population should be rejected at the conventional level of significance, i.e. the Mount Head and Fernie Formations at Shunda Gap are discordant. It should be pointed out however, that because the estimated precision parameters of the Mount Head and Fernie samples are markedly different, this test may be only approximate.

The estimated mean orientations of bedding in the two formations are given in Table 3:2. The probable orientation of the Mount Head at the time of deposition of the Fernie, obtained by rotating the Mount Head bedding about an axis parallel to the Fernie strike by an angle equal to the dip of the Fernie, is in the last column in Table 3:2. Ramsay (1961) and Cummins (1964) have discussed the conditions under which such rotations are permissible.

The discordant contact between the two formations at the road cut in Shunda Gap could conceivably be a fault rather than an angular unconformity. On Shunda Mountain, six miles northwest of this locality, a chert and dolomite pebble-conglomerate rests on an irregular Mount Head surface (Brady, 1958). In the road cut, two feet of friable, calcareous pebbly sandstone and five feet of soft, thinly bedded mudstone overlie thinly bedded, buff dolomites of the Mount Head Formation. The Jurassic succession then becomes increasingly calcareous with the appearance of thin, black limestones. Therefore the contact between the two formations in the road cut gives over appearance of being an unconformity and not a fault.

THE UNCONFORMITY ELSEWHERE IN THE NORDEGG AREA

Three other localities where the actual contact between Mount Head and Fernie beds is not exposed, but where 10 measurements of bedding could be taken on either side of the contact and within 20 feet of it, were also examined. Locality 2 is on the old road through Shunda Gap, 50 yards west of the railway bridge over the road. Locality 3 is under the railway bridge over Shunda Creek on the south side of the creek. Locality 4 is on the creek flowing out of the gap between Shunda and Coliseum Mountains, 150 yards south of where the trail up to the Shunda Mountain Lookout crosses the creek for the first time. The data for localities 2-4 is greater than the corresponding F value, here too the attitude of the Fernie is significantly different from that of the underlying Mount Head. The mean orientations of bedding, and the probable attitude of the Mount Head at the time of deposition of the Fernie, are shown for each locality in Table 2. The similarity of these data to those for locality 1 suggest that the contacts at localities 2-4 are also unconformities. The ratio of the estimated precision parameters at each locality is not far from unity, so the F-test is probably applicable in each case.

CONCLUSIONS

At four localities in the Nordegg area, Fernie strata appear to lie with angular discordance on Mount Head beds. The angle of discordance ranges from 3.2 to 4.2 degrees. At the time of deposition of the basal Fernie the average orientation of the Mount Head as determined by the vector mean of the four determinations was approximately strike - N 50°W, dip -3.8°SW. This conclusion agrees with that which can be drawn from considerations regarding the overall stratigraphy of the area (see e.g. Bokman, 1963, Fig. 5).

In this appendix the author puts forward a method of recognizing significant small angular discordances between surfaces. Bedding-plane orientation data from either side of the Mississippian-Jurassic unconformity near Nordegg, used to illustrate the method, point to the angular nature of this contact. The method might also be used to identify unconformities.

ADDITIONAL REFERENCES

Cummins, W.A., 1964, Current Directions from Folded Strata, Geol. Mag., Vol. 107, pp. 169-173.

Ramsay, J.G., 1961, The Effects of Folding on the Orientation of Sedimentation Structures, Jour. Geol., Vol. 69, pp. 84-99.

TABLE 3:1 - SAMPLES SIZES (N_1, N_2), R_1 and R_2 VALUES AND PRECISION PARAMETERS (K_1, K_2) FOR MOUNT HEAD AND FERNIE SAMPLES, R_1, R_2, R, THE COPLANARITY STATISTIC (C.S.), AND THE CORRESPONDING F VALUE.

	Mount Head			Fernie					
Locality	N_1	R_1	K_1	N_2	R_2	K_2	R	C.S	$F_{2,2(N-2)}$
1	10	9.9570	209	10	9.9967	2690	19.9432	4.08	3.26
2	10	9.9920	1130	10	9.9933	1344	19.9764	10.90	3.26
3	10	9.9821	504	10	9.9677	279	19.9323	6.27	3.26
4	12	11.9761	460	16	15.9293	212	27.8930	3.50	3.16

TABLE 3: 2 - VALUES FOR THE ESTIMATED MEAN ORIENTATIONS OF BEDDING IN THE MOUNT HEAD AND FERNIE FORMATIONS, AND FOR THE PROBABLE ORIENTATIONS OF BEDDING IN THE MOUNT HEAD AT THE TIME OF DEPOSITION OF THE FERNIE, AT FOUR LOCALITIES IN THE NORDEGG AREA. OVERTURNED DIPS ARE MARKED WITH AN ASTERISK.

Locality	Mount Head		Fernie		Mount Head in Jurassic time	
	strike	dip	strike	dip	strike	dip
1	132.0°	84.8°SW*	133.3°	81.3°SW*	85°	4.1°SW
2	122.5°	77.8°SW*	121.2°	74.6°SW*	134°	3.2°SW
3	123.9°	77.7°SW*	127.8°	74.8°SW*	120°	4.2°SW
4	126.4°	18.8°SW	118.1°	16.4°SW	148°	3.8°SW

APPENDIX 4

COMPUTER PROGRAMS

1) To find the axes of cylindrical folds and to test for their cylindrical nature.

Purpose

The purpose of these programs is to delineate portions of a fold which are cylindrical, to calculate the fold axes of such portions and to place cones of confidence around these axes.

Method

The statistical basis of the method is derived in Watson (1960) and Creer (1962). Suppose N_i determinations of the bedding are made in the i^{th} of p domains and yield a mean normal with direction cosines (l_i, m_i, n_i) and length R_i. The null hypothesis is that all the p mean vectors lie in a plane. For domains with equal precision parameters a test of coplanarity is given by:

$$\frac{\sum N_i}{\sum (N_i - R_i)} \cdot (\text{min. eigen value of V}) < \chi^2_{(p-2)}$$

$$V = \begin{vmatrix} \sum R_i l_i^2 & \sum R_i l_i m_i & \sum R_i l_i n_i \\ \sum R_i l_i m_i & \sum R_i m_i^2 & \sum R_i m_i n_i \\ \sum R_i l_i n_i & \sum R_i m_i n_i & \sum R_i n_i^2 \end{vmatrix}$$

The maximum likelihood estimator of the direction of the normal to the best fitting plane is the eigen vector corresponding to the least eigen value of the Matrix V.

The direction of the axes of the ellipse of confidence round the eigen vector are given by the other eigen vectors, the minor axis corresponding to the eigen vector associated with the smaller eigen value. The lengths of the semi-axes are:

$$\theta_1 = \sin^{-1}\left(\frac{\sum (N_i - R_i)}{\sum N_i} \cdot \frac{\chi^2_2}{(A_{max} - A_{min})} \right)^{\frac{1}{2}}$$

$$\Lambda = \left| \begin{array}{ccc} \sum & \sum & \sum \\ \sum & \sum & \sum \\ \sum & \sum & \sum \end{array} \right|$$

$$\theta_2 = \sin^{-1}\left(\frac{\sum(N_i - R_i)}{\sum N_i} \cdot \frac{\chi^2_2}{(A_{int.} - A_{min})} \right)^{\frac{1}{2}}$$

where A are the eigen values of V.

For domains with unequal K (the more general case), a test of coplanarity is given by:

$$\text{min. eigen value of W} < \chi^2_{p-2}$$

$$W = \begin{vmatrix} \sum Bl_i^2 & \sum Bl_i m_i & \sum Bl_i n_i \\ \sum Bl_i m_i & \sum Bm_i^2 & \sum Bm_i n_i \\ \sum Bl_i n_i & \sum Bn_i m_i & \sum Bn_i^2 \end{vmatrix}$$

$$\underline{B} = \frac{\sum B_i (N_i - 1)}{\sum (N_i - R_i)}$$

The directions of the normal to the best fitting plane is given by the eigen vector associated with the least eigen value. The axes of the ellipse of confidence around the eigen vector are given by the other eigen vectors, the minor axis corresponding to the eigen vector associated with the intermediate eigen value. The semi axes are given by:

$$\theta_1 = \sin^{-1}\left(\frac{\chi^2_2}{A_{max} - A_{min}} \right)^{\frac{1}{2}}$$

$$\theta_2 = \sin^{-1}\left(\frac{\chi^2_2}{A_{int.} - A_{min}} \right)^{\frac{1}{2}}$$

A are the eigen values of W.

Restrictions

The input data for this program must be in the following form:

$$\theta' = \tan^{-1}\left(\frac{\quad}{\quad}\right)$$

$$\beta' = \tan^{-1}\left(\frac{\quad}{\quad}\right)$$

$$E = \frac{\sum |W - B'|}{\sum B' |W - 1|}$$

$$\Lambda = \begin{vmatrix} \sum B'^2 & \sum \\ \sum & \sum \end{vmatrix}$$

$$\theta' = \tan^{-1}\left(\frac{\quad}{\quad}\right)$$

Card 1

The number of matrices to be processed is punched in columns 2,3,4.

Card 2

A three figure number identifying the i^{th} domain to the user is punched in 2,3,4. The number lies within the range 0-998.

Card 3

The program as written considers only the downward directed normals to bedding planes. When the dips within a domain vary from nearly vertical to overtuned this could lead to variations of 180° in the trend of the normals and erroneous values of R_i. Consequently a parameter card consisting of dextral (punched in 2, 3, 4) sinistral (in 6, 7, 8) azimuthal limits for each i must be read in. It is sufficient to assign the dextral limit some value between 180 and 360, and the sinistral limit some value between 0 and 180, making about 90° with the dextral limit, then to keep these values for all i. 342, 062 are examples of such limits.

Data cards

The strike of the bedding is punched into 2, 3, 4.

The dip of the bedding is punched into 6, 7.

A code is punched into 9.

The code has the value 0 when the dip is 90.

1 when the dip is to 270-360, 0-89.

2 when the dip is to 90-269.

The value of the strike lies between 0-180.

The value of the dip lies between 0-90. No provision is made for overturned rocks.

A strike of 999 following a data card signifies the card was the N^{th} of the N_i readings from a domain. It is followed by card 2 identifying the next station. This is followed by card 3.

FORTRAN SOURCE LIST

```
ISN       SOURCE STATEMENT

  0 $IBFTC MAIN    NOLIST,DECK
  1       DOUBLE PRECISION V(20,20),S(20,20),D(3),PI,RZ,AL,AM,AN,TR,CF,PL,
         1           ATRE,DLIM,SLIM,A,B,C,E,R,Y,Z,TRE,APLU,PLU,
         2           CHISQ,TN,T1,T2,THET1,THET2,AR,ATN,ARTN,T1T,T2T
  2       READ(5,21)MIX
  4  21   FORMAT(1X,I3,1X)
  5       NMTRX=0
  6  111  DO22J=1,3
  7       DO22I=1,3
 10  22   V(I,J)=0D0
 13       CHISQ=5.99000000000000
 14       PI=3.14159265358979
 15       RZ=1.D0/180.D0
 16       CF=PI*RZ
 17       ATN=0D0
 20       AR=0D0
 21       ISTC=0
 22       MMTRX=NMTRX+1
 23       WRITE(6,217)MMTRX
 24  217  FORMAT(//11H MATRIX NO.,I3)
 25  32   N=0
 26       READ(5,41)NSTN
 30  41   FORMAT(1X,I3)
 31       AL=0D0
 32       AM=0D0
 33       AN=0D0
 34       IF(NSTN.LT.0)GO TO 13
 37       ISTC=ISTC+1
 40       READ  (5      ,51     ) LLIM,NLIM
 43  51   FORMAT(1X,I3,1X,I3)
 44  33   N=N+1
 45       READ  (5      ,52     ) NSTR,NDIP,NDIR
 51  52   FORMAT(1X,I3,1X,I2,1X,I1)
 52       IF(NSTR.EQ.999)GO TO 11
 55       PL=90-NDIP
 56       IF(NDIR-1)3,2,3
 57  2    TR=NSTR+90
 60       GO TO 5
 61  3    TR=NSTR-90
 62       IF(TR)4,5,5
 63  4    TR=TR+360.D0
 64  5    DLIM=LLIM
 65       IF(TR-DLIM)6,10,10
 66  6    SLIM=NLIM
 67       IF(SLIM-DLIM)8,9,9
 70  8    IF(TR-90.)10,10,9
 71  9    TR=TR+180.D0
 72       PL=PL*CF
 73       TR=TR*CF
 74       E=-DSIN(TR)
 75       GO TO 101
 76  10   PL=PL*CF
 77       TR=TR*CF
 00       E=DSIN(TR)
 01  101  A=DCOS(PL)
```

To compile and solve the matrix, V

FORTRAN SOURCE LIST MAIN

```
SN        SOURCE STATEMENT

02        B=DSIN(PL)
03        C=DCOS(TR)
04        AL=AL+A*C
05        AM=AM+E*A
06        AN=AN+B
07        GO TO 33
10   11   N=N-1
11        TN=N
12        R=DSQRT(AL*AL+AM*AM+AN*AN)
13        AN=AN/R
14        AL=AL/R
15        AM=AM/R
16        ATN=ATN+TN
17        AR=AR+TN-R
20        V(1,2)=V(1,2)+R*AL*AM
21        V(1,1)=V(1,1)+R*AL*AL
22        V(2,3)=V(2,3)+R*AN*AM
23        V(1,3)=V(1,3)+R*AL*AN
24        V(2,2)=V(2,2)+R*AM*AM
25        V(3,3)=V(3,3)+R*AN*AN
26        WRITE(6,12)NSTN
27   12   FORMAT(/16H  STATION NUMBER,3X,I3)
30        WRITE(6,15)N
31   15   FORMAT(17H  NO. OF READINGS,2X,I3)
32        GO TO 32
33   13   V(2,1)=V(1,2)
34        V(3,1)=V(1,3)
35        V(3,2)=V(2,3)
36        ARTN=ATN/AR
37        WRITE(6,14)ISTC
40   14   FORMAT(/17H  NO. OF STATIONS,2X,I3)
41        CALL JACOBI(N,V,S,TOLERC,NORM)
42        DO31CL=1,2
43        CO31OK=1,2
44        IF(DABS(V(K,K)).LE.DABS(V(K+1,K+1)))GO TO 310
47        DO31OI=1,3
50        Z=S(K,I)
51        S(K,I)=S(K+1,I)
52        S(K+1,I)=Z
53        Y=V(K,K)
54        V(K,K)=V(K+1,K+1)
55        V(K+1,K+1)=Y
56   310  CONTINUE
62        DO66J=1,2
63        DO311M=1,3
64   311  C(M)=S(J,M)
66        IF(C(1))36,40,36
67   36   ATRE=D(2)/D(1)
70        TRE=DATAN(ATRE)/CF
71        GO TO 37
72   40   IF(C(2))43,42,42
73   43   TRE=90.DO
74        GO TO 420
75   42   TRE=270.DO
76   420  APLU=D(3)/DSQRT(1.DO-D(3)**2)
```

FORTRAN SOURCE LIST MAIN

```
SN        SOURCE STATEMENT

177       PLU=DATAN(APLU)
200       PLU=DABS(PLU/CF)
201       GO TO 65
202   37  APLU=D(3)/DSQRT(1.D0-D(3)**2)
203       PLU=DATAN(APLU)
204       PLU=DABS(PLU/CF)
205       IF(D(3))61,60,60
206   60  D(1)=-D(1)
207       D(2)=-D(2)
210   61  IF(D(2))63,62,62
211   62  IF(D(1))64,65,65
212   63  TRE=TRE+180.D0
213       GO TO 65
214   64  TRE=TRE+360.D0
215   65  WRITE(6,214)J,PLU
216   214 FORMAT(/12H  PLUNGE OF ,I1,8H EVECTOR,2X,F7.3)
217   66  WRITE(6,215)J,TRE
221   215 FORMAT(11H  TREND OF ,I1,8H EVECTOR,2X,F8.3)
222       STA=ARTN*V(1,1)
223       WRITE(6,210)STA
224   210 FORMAT(/11H  STATISTIC,10X,F10.4)
225       T1=DSQRT(CHISQ/((V(3,3)-V(1,1))*ARTN))
226       T2=DSQRT(CHISQ/((V(2,2)-V(1,1))*ARTN))
227       T1T=T1/DSQRT(1.D0-T1**2)
230       THET1=DATAN(T1T)/CF
231       T2T=T2/DSQRT(1.D0-T2**2)
232       THET2=DATAN(T2T)/CF
233       WRITE(6,212)THET1
234   212 FORMAT(22H  RADIUS OF CONFIDENCE,1X,F7.3)
235       WRITE(6,212)THET2
236   50  CONTINUE
237       NMTRX=NMTRX+1
240       IF(NMTRX.LT.MIX)GO TO 111
243       CALL EXIT
244       END
```

450008 IBLDR -- JOB VCTORS

JECT PROGRAM IS BEING ENTERED INTO STORAGE.

RIX NO. 1

ATION NUMBER 373
OF READINGS 10

ATION NUMBER 326
OF READINGS 10

ATION NUMBER 327
OF READINGS 10

OF STATIONS 3

Results for the stations in Fig. 3

G UNDERFLOW AT C20474

G UNDERFLOW AT C20515

NGE OF 1 EVECTOR 13.354
ND OF 1 EVECTOR 316.341

NGE OF 2 EVECTOR 22.076
ND OF 2 EVECTOR 231.866

TISTIC 0.3619
IUS OF CONFIDENCE 1.246
IUS OF CONFIDENCE 7.004

FORTRAN SOURCE LIST

```
ISN       SOURCE STATEMENT

  0 $IBFTC MAIN    NOLIST,NODECK
  1        DOUBLE PRECISION V(20,20),S(20,20),D(3),PI,RZ,AL,AM,AN,TR,CF,PL,
          1           ATRE,DLIM,SLIM,A,B,C,E,R,Y,Z,TRE,APLU,PLU,
          2           CHISQ,TN,T1,T2,THET1,THET2,AX,T1T,T2T
  2        READ(5,21)MIX
  4  21    FORMAT(1X,I3,1X)
  5        NMTRX=0
  6  111   DO22J=1,3
  7        DO22I=1,3
 10  22    V(I,J)=0D0
 13        ISTC=0
 14        MMTRX=NMTRX+1
 15        WRITE(6,217)MMTRX
 16  217   FORMAT(//11H MATRIX NO.,I3)
 17  32    N=0
 20        CHISQ=5.9900000000000
 21        PI=3.14159265358979
 22        RZ=1.D0/180.D0
 23        CF=PI*RZ
 24        READ(5,41)NSTN
 26  41    FORMAT(1X,I3)
 27        AL=0D0
 30        AM=0D0
 31        AN=0D0
 32        IF(NSTN.LT.0)GO TO 13
 35        ISTC=ISTC+1
 36        READ  (5      ,51     ) LLIM,NLIM
 41  51    FORMAT(1X,I3,1X,I3)
 42  33    N=N+1
 43        READ  (5      ,52     ) NSTR,NDIP,NDIR
 47  52    FORMAT(1X,I3,1X,I2,1X,I1)
 50        IF(NSTR.EQ.999)GO TO 11
 53        PL=90-NDIP
 54        IF(NDIR-1)3,2,3
 55  2     TR=NSTR+90
 56        GO TO 5
 57  3     TR=NSTR-90
 60        IF(TR)4,5,5
 61  4     TR=TR+360.D0
 62  5     DLIM=LLIM
 63        IF(TR-DLIM)6,10,10
 64  6     SLIM=NLIM
 65        IF(SLIM-DLIM)8,9,9
 66  8     IF(TR-90.D0)10,10,9
 67  9     TR=TR+180.D0
 70        PL=PL*CF
 71        TR=TR*CF
 72        E=-DSIN(TR)
 73        GO TO 101
 74  10    PL=PL*CF
 75        TR=TR*CF
 76        E=DSIN(TR)
 77  101   A=DCOS(PL)
100        B=DSIN(PL)
101        C=DCOS(TR)
```

To compile and solve the matrix

W

FORTRAN SOURCE LIST MAIN

```
ISN       SOURCE STATEMENT

102       AL=AL+A*C
103       AM=AM+E*A
104       AN=AN+B
105       GO TO 33
106   11  N=N-1
107       TN=N
110       R=DSQRT(AL*AL+AM*AM+AN*AN)
111       AN=AN/R
112       AL=AL/R
113       AM=AM/R
114       AX=R*(TN-1.D0)/(TN-R)
115       V(3,3)=V(3,3)+AX*AN*AN
116       V(2,3)=V(2,3)+AX*AN*AM
117       V(2,2)=V(2,2)+AX*AM*AM
120       V(1,3)=V(1,3)+AX*AL*AN
121       V(1,2)=V(1,2)+AX*AM*AL
122       V(1,1)=V(1,1)+AX*AL*AL
123       WRITE(6,12)NSTN
124   12  FORMAT(/16H  STATION NUMBER,3X,I3)
125       WRITE(6,15)N
126       GO TO 32
127   15  FORMAT(17H  NO. OF READINGS,2X,I3)
130   13  V(2,1)=V(1,2)
131       V(3,1)=V(1,3)
132       V(3,2)=V(2,3)
133       WRITE(6,14)ISTC
134   14  FORMAT(/17H  NO. OF STATIONS,2X,I3)
135       CALL JACOBI(N,V,S,TOLERC,NORM)
136       DO310L=1,2
137       DO310K=1,2
140       IF(DABS(V(K,K)).LE.DABS(V(K+1,K+1)))GO TO 310
143       DO310I=1,3
144       Z=S(K,I)
145       S(K,I)=S(K+1,I)
146       S(K+1,I)=Z
147       Y=V(K,K)
150       V(K,K)=V(K+1,K+1)
151       V(K+1,K+1)=Y
152   310 CONTINUE
156       DO66J=1,2
157       DO311M=1,3
160   311 D(M)=S(J,M)
162       IF(D(1))36,40,36
163   36  ATRE=D(2)/D(1)
164       TRE=DATAN(ATRE)/CF
165       GO TO 37
166   40  IF(D(2))43,42,42
167   43  TRE=90.D0
170       GO TO 420
171   42  TRE=270.D0
172   420 APLU=D(3)/DSQRT(1.D0-D(3)**2)
173       PLU=DATAN(APLU)
174       PLU=DABS(PLU/CF)
175       GO TO 65
176   37  APLU=D(3)/DSQRT(1.D0-D(3)**2)
```

8 FORTRAN SOURCE LIST MAIN

```
ISN        SOURCE STATEMENT

177        PLU=DATAN(APLU)
200        PLU=DABS(PLU/CF)
201        IF(D(3))61,60,60
202   60   D(1)=-D(1)
203        D(2)=-D(2)
204   61   IF(D(2))63,62,62
205   62   IF(D(1))64,65,65
206   63   TRE=TRE+180.D0
207        GO TO 65
210   64   TRE=TRE+360.D0
211   65   WRITE(6,214)J,PLU
212   214  FORMAT(/12H  PLUNGE OF ,I1,8H EVECTOR,2X,F7.3)
213   66   WRITE(6,215)J,TRE
215   215  FORMAT(11H  TREND OF ,I1,8H EVECTOR,2X,F8.3)
216        WRITE(6,210)V(1,1)
217   210  FORMAT(/19H  LEAST LATENT ROOT,2X,F11.5)
220        T1=DSQRT(CHISQ/(V(3,3)-V(1,1)))
221        T2=DSQRT(CHISQ/(V(2,2)-V(1,1)))
222        T1T=T1/DSQRT(1.D0-T1**2)
223        THET1=DATAN(T1T)/CF
224        T2T=T2/DSQRT(1.D0-T2**2)
225        THET2=DATAN(T2T)/CF
226        WRITE(6,212)THET1
227   212  FORMAT(22H  RADIUS OF CONFIDENCE,1X,F7.3)
230        WRITE(6,212)THET2
231   50   CONTINUE
232        NMTRX=NMTRX+1
233        IF(NMTRX.LT.MIX)GO TO 111
236        CALL EXIT
237        END
```

FORTRAN SOURCE LIST

```
ISN       SOURCE STATEMENT

  0 $IBFTC JACOBI  DECK
  1       SUBROUTINE JACOBI(N,MATRIX,VECTOR,TOLERC,NORM)
  2       DOUBLE PRECISION SINE,COSINE,TS1,TS2,LAMDA,MU,OMEGA,TOLERC,
         1                 MATRIX(20,20),VECTOR(20,20),TS3
  3       N=3
  4       NORM=2
  5       TOLERC=0.000000000000000
  6       INTEGER I,J,P,Q,N,NM1,PP1,DONE,NORM
  7       IF(TOLERC.EQ.0.000000000000) TOLERC=0.000000000001
 12       NM1=N-1
 13       DO 1 I=1,N
 14       DO 1 J=1,N
 15       VECTOR(I,J)=0.000000000000000
 16  1    IF(I.EQ.J) VECTOR(I,I)=1.000000000000000
 23  2    DONE=0
 24       DO 5 P=1,NM1
 25       PP1=P+1
 26       DO 5 Q=PP1,N
 27       IF(DABS(MATRIX(P,Q)).LE.TOLERC)  GO TO 5
 32       DONE=1
 33       LAMDA=-MATRIX(P,Q)
 34       MU=.500000000000000*(MATRIX(P,P)-MATRIX(Q,Q))
 35       OMEGA=LAMDA/DSQRT(LAMDA*LAMDA+MU*MU)
 36       IF(MU.LT.0.000000000000000) OMEGA=-OMEGA
 41       SINE=OMEGA/DSQRT(2.000000000000000+2.000000000000000*
         1          DSQRT(1.000000000000000-OMEGA*OMEGA))
 42       COSINE=DSQRT(1.000000000000000-SINE*SINE)
 43       DO 4 I=1,N
 44       IF(I.EQ.P.OR.I.EQ.Q) GO TO 3
 47       TS1=COSINE*MATRIX(P,I)-SINE*MATRIX(Q,I)
 50       TS2=SINE*MATRIX(P,I)+COSINE*MATRIX(Q,I)
 51       MATRIX(P,I)=TS1
 52       MATRIX(Q,I)=TS2
 53       MATRIX(I,P)=TS1
 54       MATRIX(I,Q)=TS2
 55  3    TS1=VECTOR(I,P)*COSINE-VECTOR(I,Q)*SINE
 56       TS2=VECTOR(I,P)*SINE+VECTOR(I,Q)*COSINE
 57       VECTOR(I,P)=TS1
 60  4    VECTOR(I,Q)=TS2
 62       TS1=MATRIX(P,P)*COSINE*COSINE-2.000000000000000*MATRIX(P,Q)*
         1       COSINE*SINE + MATRIX(Q,Q)*SINE*SINE
 63       TS2=MATRIX(P,P)*SINE*SINE + 2.000000000000000*MATRIX(P,Q)*
         1      COSINE*SINE + MATRIX(Q,Q)*COSINE*COSINE
 64       TS3=(MATRIX(P,P)-MATRIX(Q,Q))*SINE*COSINE + MATRIX(P,Q)*
         1       (COSINE*COSINE-SINE*SINE)
 65       MATRIX(P,P)=TS1
 66       MATRIX(Q,Q)=TS2
 67       MATRIX(P,Q)=TS3
 70       MATRIX(Q,P)=TS3
 71  5    CONTINUE
 74       IF(DONE.NE.0) GO TO 2
 77       IF(NORM.NE.1) GO TO 8
102       DO 7 J=1,N
103       TS1=VECTOR(1,J)
104       DO 6 I=2,N
```

FORTRAN SOURCE LIST JACOBI

```
ISN        SOURCE STATEMENT

105   6    IF(DABS(TS1).LT.DABS(VECTOR(I,J)))TS1 = VECTOR(I,J)
111        DO 7 I=1,N
112   7    VECTOR(I,J) =VECTOR(I,J)/TS1
115        RETURN
116   8    DO 11 J=1,N
117        TS1 = 0.000000000000000
120        DO 9 I=1,N
121   9    TS1 =TS1 + VECTOR(I,J)*VECTOR(I,J)
123        TS1 = 1.0000000000000000/DSQRT(TS1)
124        DO 10 I=1,N
125   10   VECTOR(I,J) = VECTOR(I,J)*TS1
127   11   CONTINUE
131        RETURN
132        END
```

450008 IBLDR -- JOB VCTORS

ECT PROGRAM IS BEING ENTERED INTO STORAGE.

IX NO. 1

TION NUMBER 373
OF READINGS 10

Data from Fig. 3

TION NUMBER 326
OF READINGS 10

TION NUMBER 327
OF READINGS 10

OF STATIONS 3

UNDERFLOW AT 020467

GE OF 1 EVECTOR 12.650
D OF 1 EVECTOR 316.524

GE OF 2 EVECTOR 21.550
D OF 2 EVECTOR 231.609

T LATENT ROOT 0.37171
US OF CONFIDENCE 1.286
US OF CONFIDENCE 7.846

A negative station number signifies the p+1th station begins the calculation of the matrix.

Use of the program

The user should prepare a deck with the following:

(1) The standard control cards for the IBSYS monitor--at the University of Alberta these consist of a $IBSYS card, a $JOB card, a $TIME card --- five minutes is ample time to compute ten matrices, the number of lines of output will depend on the number of matrices (2 minutes is sufficient if a relocatable binary deck is used).

(2) A source deck or the corresponding relocatable binary deck.

(3) A $ENTRY card.

(4) The input data as written up under restrictions.

Check Out

The program has been used to divide a large anticline into cylindrical portions. About 20 such portions were determined. A rough check (to within 10°) on these results was made graphically. These checks tallied. The internal consistency of the results can also be checked roughly. This proved satisfactory. There is no way at the moment of making more accurate checks on these results.

The sub routine (JACOBI) to compute the eigen values of the matrices was written by G. Jackson of the Department of Computing Science in Fortran IV (double precision). (A program since published in the SHARE library SDA 3202 01, Real Symmetric Matrix Eigen System Solver, supersedes Jackson's program). A print out of JACOBI is included with the program to solve W.

2) To calculate the axes of folds assumed to be cylindrical.

Purpose

This program is a particular case not covered by the earlier programs--N_i is 1 in all cases.

FORTRAN SOURCE LIST

```
S\        SOURCE STATEMENT

  0 FIRFTC MAIN     NOLIST,NODECK
  1       DOUBLE PRECISION V(20,20),S(20,20),D(3),PI,RZ,AL,AM,AN,TR,CF,PL,
         1          ATRE,DLIM,SLIM,A,B,C,E,R,Y,Z,TRE,APLU,PLU,TOLERC
          NMTRX=0
  3       READ(5,21)NIX
  5  21   FORMAT(1X,I3,1X)
  6  111  DO22J=1,3
  7       DO22I=1,3
 10  22   V(I,J)=0D0
 13       PI=3.14159265358979
 14       RZ=1.D0/180.D0
 15       CF=PI*RZ
 16  32   N=0
 17       READ(5,41)NSTN
 21  41   FORMAT(1X,I3)
 22       AL=0D0
 23       AM=0D0
 24       AN=0D0
 25       READ  (5      ,51     ) LLIM,NLIM
 30  51   FORMAT(1X,I3,1X,I3)
 31  33   N=N+1
 32       READ  (5      ,52     ) NSTR,NDIP,NDIR
 36  52   FORMAT(1X,I3,1X,I2,1X,I1)
 37       IF(NSTR.EQ.999)GO TO 11
 42       PL=90-NDIP
 43       IF(NDIR-1)3,2,3
 44  2    TR=NSTR+90
 45       GO TO 5
 46  3    TR=NSTR-90
 47       IF(TR)4,5,5
 50  4    TR=TR+360.D0
 51  5    DLIM=LLIM
 52       IF(TR-DLIM)6,10,10
 53  6    SLIM=NLIM
 54       IF(SLIM-DLIM)8,9,9
 55  8    IF(TR-90.D0)10,10,9
 56  9    TR=TR+180.D0
 57       PL=PL*CF
 60       TR=TR*CF
 61       E=-DSIN(TR)
 62       GO TO 101
 63  10   PL=PL*CF
 64       TR=TR*CF
 65       E=DSIN(TR)
 66  101  A=DCOS(PL)
 67       B=DSIN(PL)
 70       C=DCOS(TR)
 71       V(1,1)=V(1,1)+A*A*C*C
 72       V(1,2)=V(1,2)+A*A*C*E
 73       V(2,2)=V(2,2)+A*A*E*E
 74       V(1,3)=V(1,3)+A*C*B
 75       V(2,3)=V(2,3)+A*E*B
 76       V(3,3)=V(3,3)+B*B
          GO TO 33
    11    N=N-1
          \
```

To compile & resolve the matrix, U

FORTRAN SOURCE LIST MAIN

```
IST       SOURCE STATEMENT

101       WRITE(6,12)NSTN
102    12 FORMAT(//15H STATION NUMBER,9X,I3)
103       WRITE(6,15)N
104    15 FORMAT(18H  NO. OF READINGS,6X,I3)
105    13 V(2,1)=V(1,2)
106       V(3,1)=V(1,3)
107       V(3,2)=V(2,3)
110       CALL JACOBI(N,V,S,TOLERC,NORM)
111       DO31CL=1,2
112       DO31CK=1,2
113       IF(DABS(V(K,K)).LE.DABS(V(K+1,K+1)))GO TO 310
116       Y=V(K,K)
117       V(K,K)=V(K+1,K+1)
120       DO31CI=1,3
121       V(K+1,K+1)=Y
122       Z=S(K,I)
123       S(K,I)=S(K+1,I)
124       S(K+1,I)=Z
125   310 CONTINUE
131       DO311M=1,3
132   311 D(M)=S(1,M)
134       IF(D(1))36,40,36
135    36 ATRE=D(2)/D(1)
136       TRE=DATAN(ATRE)/CF
137       GO TO 37
140    40 IF(D(2))43,42,42
141    43 TRE=90.DO
142       GO TO 420
143    42 TRE=270.DO
144   420 APLU=D(3)/DSQRT(1.DO-D(3)**2)
145       PLU=DATAN(APLU)
146       PLU=DABS(PLU/CF)
147       GO TO 65
150    37 APLU=D(3)/DSQRT(1.DO-D(3)**2)
151       PLU=DATAN(APLU)
152       PLU=DABS(PLU/CF)
153       IF(D(3))61,60,60
154    60 D(1)=-D(1)
155       D(2)=-D(2)
156    61 IF(D(2))63,62,62
157    62 IF(D(1))64,65,65
160    63 TRE=180.DO+TRE
161       GO TO 65
162    64 TRE=360.DO+TRE
163    65 WRITE(6,214)PLU
164   214 FORMAT(21H  PLUNGE OF FOLD AXIS,2X,F7.3)
165       WRITE(6,215)TRE
166   215 FORMAT(20H  TREND OF FOLD AXIS,2X,F8.3)
167       WRITE(6,210)V(1,1)
170   210 FORMAT(19H  LEAST LATENT ROOT,2X,F9.3)
171       NMTRX=NMTRX+1
172       IF(NMTRX.LT.MIX)GO TO 111
175    50 CONTINUE
7         CALL EXIT
7,        END
```

45CCC8 IBLDR -- JOB

OBJECT PROGRAM IS BEING ENTERED INTO STORAGE.

ATION NUMBER	1
NO. OF READINGS,	30
NO UNDERFLOW AT	02C037
PLUNGE OF FOLD AXIS	13.357
TREND OF FOLD AXIS	318.140
LEAST LATENT ROOT	0.098

Data from Fig. 3

Method

Watson (1960) leads to the conclusion that the fold axis of the readings (l_i, m_i, n_i) is the eigen vector associated with the least eigen value of the matrix U,

$$U = \begin{vmatrix} \sum l_i^2 & \sum l_i m_i & \sum l_i n_i \\ \sum l_i m_i & \sum m_i^2 & \sum m_i n_i \\ \sum l_i n_i & \sum m_i n_i & \sum n_i^2 \end{vmatrix}$$

Watson (1965) suggested that the least eigen value might be the basis of a test of coplanarity,

$$K \quad \text{(least eigen value of U)} \quad < \chi^2_{N-2}$$

when N is the total number of readings.

Restrictions

The input data must be in the form suggested in Program 1 with the proviso that "station" now be interpreted as the population of N readings whose axis is to be determined.

Negative station numbers need not be used.

Use of the program

As in program 1.

3) Calculation of the Coplanarity Statistic

Purpose

The purpose of this program is to calculate a coplanarity statistic to test the null hypothesis that a number of samples of planar structures or lineations come from a single population.

FORTRAN SOURCE LIST

```
ISN        SOURCE STATEMENT

  0 $IBFTC MFPL    NOLIST,DECK
  1        PI=3.1415926
  2        R180=1./180.
  3        CF=PI*R180
  4        NRT=0
  5        READ(5,53)NR
  7   53   FORMAT(1X,I3,1X)
 10   13   NRT=NRT+1
 11        TSTN=0
 12        TRV=0
 13        NT=0
 14        TSG=0
 15        TSB=0
 16        TSA=0
 17   68   READ(5,53)NSTN
 21   50   FORMAT(1X,I3)
 22        IF(NSTN.LT.0) GO TO 69
 25        WRITE(6,60)NSTN
 26   60   FORMAT(/8H STATIONI4)
 27        TSTN=TSTN+1.
 30        READ(5,51)LLIM,NLIM
 33   51   FORMAT(1X,I3,1X,I3)
 34        SA=0.0
 35        SB=0.0
 36        SG=0.0
 37        NCDS=0
 40   1    READ(5,52)NSTR,NDIP,NDIR
 44   52   FORMAT(1X,I3,1X,I2,1X,I1)
 45        IF(NSTR.LT.0) GO TO 14
 50        NCDS=NCDS+1
 51        PL=90-NDIP
 52        IF(NDIR-1)3,2,3
 53   2    TR=NSTR+90
 54        GO TO 5
 55   3    TR=NSTR-90
 56        IF(TR)4,5,5
 57   4    TR=TR+360.
 60   5    DLIM=LLIM
 61        IF(TR-DLIM)6,10,10
 62   6    SLIM=NLIM
 63        IF(SLIM-DLIM)8,9,9
 64   8    IF(TR-90.)10,10,9
 65   9    TR=TR+180.
 66        PL=PL*CF
 67        TR=TR*CF
 70        A=COS(TR)*COS(PL)
 71        B=SIN(TR)*COS(PL)
 72        G=-SIN(PL)
 73        GO TO 11
 74   10   PL=PL*CF
 75        TR=TR*CF
 76        A=COS(TR)*COS(PL)
 77        B=SIN(TR)*COS(PL)
           G=SIN(PL)
    11    SA=SA+A
```

To calculate the coplanarity statistic, C.S.

FORTRAN SOURCE LIST MFPL

```
      SOURCE STATEMENT

      SB=SB+B
   12 SG=SG+G
      GO TO 1
   14 R=SQRT((SA*SA)+(SB*SB)+(SG*SG))
      WRITE(6,65)NCDS
   65 FORMAT(/13H MEASUREMENTSI4)
      WRITE(6,59)R
   59 FORMAT(14H VECTOR LENGTH,3X,F9.4)
      TSA=TSA+SA
      TSB=TSB+SB
      TSG=TSG+SG
      NT=NT+NCDS
      TRV=TRV+R
      GO TO 68
   69 RV=SQRT((TSA*TSA)+(TSB*TSB)+(TSG*TSG))
      WRITE(6,61)RV
   61 FORMAT(//17H RESULTANT VECTOR,F9.4)
      FNT=NT
      F=(FNT-TSTN)*(TRV-RV)/((TSTN-1.)*(FNT-TRV))
      WRITE(6,62)F
   62 FORMAT(/10H STATISTIC,7X,F9.4)
      IF(NRT.LT.NR)GO TO 13
      CALL EXIT
      END
```

450005 IBLDR -- JOB MFPL

JECT PROGRAM IS BEING ENTERED INTO STORAGE.

TION 373

SUREMENTS 10
TOR LENGTH 9.9828

TION 326

Data from Fig. 3.

SUREMENTS 10
TOR LENGTH 9.9728

TION 327

SUREMENTS 10
TOR LENGTH 9.9758

LTANT VECTOR 29.4640

TISTIC 91.8766

ere is a significant
vergence from coplanarity)

Method

The lineations or normals to the planar structures are assumed to be distributed about the estimated means of their sample according to the probability density function P (θ),

$$P(\theta) = B\, e^{K\cos\theta} \quad \text{(Fisher, 1953)}$$

Watson (1956) has shown that the statistic

$$\frac{\sum N_i - P}{(P-1)} \cdot \frac{\sum R_i - R}{\sum N_i - \sum R_i}$$

referred to F-ratio tables with 2(p-1) and 2(N_i-p) degrees of freedom is a test of the above hypothesis. The i^{th} sample contains N_i readings whose vector sum has a length R_i. R is the length of the vector sum of the resultants of the readings and p is the number of samples.

The program outputs values of R_i, N_i and the coplanarity statistic.

Restrictions

The input data for this program must be in the following form:

Card 1

The number of separate tests of coplanarity to be made in this run is punched in 2, 3, 4.

Card 2

A 3 digit number identifying the sample to the programmer is punched in 2, 3, 4.

Card 3 and the data cards are as described in the programs for calculating the generatrix of folds.

The last reading within a sample is followed by a data card with a negative trend punched in it (in the format of Card 3).

The last reading within the group of samples whose coplanarity is being tested is followed by a negative trend and a negative identifying code (in the format of Card 2).

Use of the program

The user of the program should prepare a deck with the following:

(1) The standard control cards for the $IBSYS monitor--at the University of Alberta these consist of an $IBSYS card, a $JOB card and a $TIME card--thirty seconds is sufficient for the usual size test.

(2) A source deck of the corresponding relocatable binary deck.

(3) A $ENTRY card.

(4) The input data as written up under restrictions.

Check out

The values of R and R_i were checked by Muecke's mean S plane program (Muecke, 1965). A calculation of the statistic from the R values by hand corresponded with the figures produced by the program.

4a) Preparation of Pole Density Diagrams

The program given below is a translation into Fortran IV and slight modification (by V. Yanda and D. Cruden) of the program written in Fortran II by V. Yanda and G. Muecke (Muecke, 1965, pp. 18-30). The program is discussed exhaustively there and only modifications will be discussed here.

Parameter Cards

Card 1

A 1 digit number is punched in column 3. This determines the size of the cross section of the counting cone (1% - 9% of the area of the hemisphere) which surrounds the grid points.

Card 2

A 3 digit number which identifies the station to the programmer is punched in 2, 3, 4.

If the data is in the form of the plunges and trends of lineations, 1, is punched in column 6.

A negative station number indicates the end of a run of several stations.

Card 3 - data cards

Data cards are in Muecke's original format except that a negative strike now indicates the end of a set of data from a particular station. It should be followed by a card of type 2.

Use of the program

The user should prepare a deck with the following:

(1) The standard controle cards for the $IBSYS monitor--at the University of Alberta these consist of an $IBSYS card, a $JOB card, a $TIME card--two minutes is sufficient to process 300 readings in a typical station if a relocatable binary deck is used, each station requires 120 lines of output.

(2) A source deck or relocatable binar deck.

(3) A $ENTRY card.

(4) The point density counter given by Muecke (1965, Appendix 1).

(5) The input data with the appropriate parameter cards.

b) This program for the preparation of pole density diagrams has been modified in a way described in Appendix 5.

Parameter cards

Card 1

The direction cosines of the angular distances from a grid at which the weight of

To prepare pole density diagrams

```
 5
 DENSK,   GO
 DEOUNE   NOLIST.NODECK
 DIMENSION COSA(333).COSB(333).COSG(333).ND(333)
 DIMENSION A(2000).B(2000).G(2000)
 DO 2 I=1.333
 READ(5.51)COSA(I).COSB(I).COSG(I).J
 IF(I.NE.J) GO TO 23
 CONTINUE
 READ(5.52)KPCA
 IF(KPCA.EQ.0) GO TO 24
 DA=KPCA
 PI=3.1415926
 P180=1./180.
 CF=PI*P180
 TEST=2.*.01*PI*DA
 TEST=COS(TEST)
 DO 4 I=1.333
 ND(I)=0
 NCDS=0
 NZ=0
 IX=1
 READ(5.50)NSTN.NZ
 IF(NSTN.LT.0)CALL EXIT
 NZ=NZ+1
 GO TO (5.10).NZ
 READ  (5      ,53     ) NSTR,NDIP,NDIR
 IF(NSTR.LT.0)GO TO 12
 NCDS=NCDS+1
 PL =90-NDIP
 IF(NDIR.NE.1) GO TO 8
 TR=NSTR+90
 GO TO 11
 TR=NSTR-90
 GO TO 11
 READ (5,535) NTR,NPL
 IF(NTR.LT.0)GO TO 12
 NCDS=NCDS+1
 TR=NTR
 PL =NPL
 PL =PL *CF
 TR=TR*CF
 I=NCDS
 A(I)=COS (TR)*COS (PL)
 B(I)=SIN (TR)*COS (PL )
 G(I)=SIN (PL )
 GO TO (5.10),NZ
 CONTINUE
 ENCDS=NCDS
 PNCDS=100./ENCDS
 PMAX=0.
 DO 124 I=1,NCDS
 IF(PMAX.GE.G(I)) GO TO 124
 PMAX=G(I)
 CONTINUE
 PMAX=PMAX+TEST
 DO 15 I=1.333
 CSG=COSG(I)
 DENS=0.
```

```
      SA=COSA(I)
      SB=COSB(I)
      DO 14  J=1,NCDS
      GEE=G(J)
      IF(ABS(GEE-CSG).GT.TEST) GO TO 14
      IF(TEST.GT.ABS(CSA*A(J)+CSB*B(J)+CSG*GEE))GO TO 14
      DENS=DENS+1.
   14 CONTINUE
      ND(I)=DENS
      WRITE=1
      WRITE (6      ,58      ) ND(1)
      WRITE (6      ,66      ) ND(318),ND(319),ND(320),ND(321)
      WRITE (6      ,68      ) NSTN
      WRITE (6      ,59      ) (ND(I),I=2,10)
      WRITE (6      ,57      )
      WRITE (6      ,57      )
      WRITE (6      ,60      ) (ND(I),I=11,23)
      WRITE (6      ,57      )
      WRITE (6      ,57      )
      WRITE (6      ,61      ) (ND(I),I=24,38)
      WRITE (6      ,57      )
      WRITE (6      ,57      )
      WRITE (6      ,62      ) (ND(I),I=39,55)
      WRITE (6      ,57      )
      WRITE (6      ,57      )
      WRITE (6      ,62      ) (ND(I),I=56,72)
      WRITE (6      ,57      )
      WRITE (6      ,57      )
      WRITE (6      ,63      ) (ND(I),I=73,91)
      WRITE (6      ,57      )
      WRITE (6      ,57      )
      WRITE (6      ,63      ) (ND(I),I=92,110)
      WRITE (6      ,57      )
      WRITE (6      ,57      )
      WRITE (6      ,63      ) (ND(I),I=111,129)
      WRITE (6      ,67      ) ND(322),ND(323)
      WRITE (6      ,57      )
      WRITE (6      ,63      ) (ND(I),I=130,148)
      WRITE (6      ,67      ) ND(324),ND(325)
      WRITE (6      ,57      )
      WRITE (6      ,64      ) (ND(I),I=149,169)
      WRITE (6      ,57      )
      WRITE (6      ,67      ) ND(326),ND(327)
      WRITE (6      ,63      ) (ND(I),I=170,188)
      WRITE (6      ,57      )
      WRITE (6      ,67      ) ND(328),ND(329)
      WRITE (6      ,63      ) (ND(I),I=189,207)
      WRITE (6      ,57      )
      WRITE (6      ,57      )
      WRITE (6      ,63      ) (ND(I),I=208,226)
      WRITE (6      ,57      )
      WRITE (6      ,57      )
      WRITE (6      ,63      ) (ND(I),I=227,245)
      WRITE (6      ,57      )
      WRITE (6      ,57      )
      WRITE (6      ,62      ) (ND(I),I=246,262)
      WRITE (6      ,57      )
      WRITE (6      ,57      )
      WRITE (6      ,62      ) (ND(I),I=263,279)
```

```
WRITE (6      ,57      )
WRITE (6      ,61      ) (ND(I),I=200,204)
WRITE (6      ,57      )
WRITE (6      ,57      )
WRITE (6      ,60      ) (ND(I),I=205,307)
GO TO (17,18),KLIK
WRITE (6      ,54      )
GO TO 19
WRITE (6      ,60      )
WRITE (6      ,70      ) KPCA
WRITE (6      ,60      ) (ND(I),I=308,316)
WRITE (6      ,57      )
WRITE (6      ,66      ) ND(330),ND(331),ND(332),ND(333)
WRITE (6      ,65      ) ND(317)
GO TO (2 ,22),KLIK
DO 21 I=1,333
XND=ND(I)
ND(I)=XND*RNCDS+.5
KLIK=2
GO TO 16
GO TO 3
WRITE(6,71)
 CALL EXIT
WRITE(6,72)
CALL EXIT
FORMAT(1X,I3,1X,I1)
FORMAT(7X,3E11.8,12X,I3)
FORMAT(I3)
FORMAT(1X,I3,1X,I2,1X,I1,1X,I5)
FORMAT(1X,I3,1X,I2,3X,I5)
FORMAT(21H      NUMBER OF POINTS)
FORMAT(1X)
FORMAT(21HDENSITY DISTRIBUTION,29X,I5)
FORMAT(20X,9I5)
FORMAT(20X,13I5)
FORMAT(15X,15I5)
FORMAT(11X,17I5)
FORMAT(5X,19I5)
FORMAT(21I5)
FORMAT(5X,I5)
FORMAT(20X,I5,I6,I10,I6)
FORMAT(I6,92X,I5)
FORMAT(12H STATION NO.,I4)
FORMAT(21H PERCENTAGE OF POINTS)
FORMAT(4H PER,I3,13H PERCENT AREA)
FORMAT(23H ERROR= CONSTANTS OUT OF SEQUENCE)
FORMAT(42H ERROR= PERCENTAGE OF AREA CONSTANT MISSING OR ZERO.)
END
```

Data from stations in Fig. 3

42	1	10	60	326
42	1	10	60	326
4	1	10	60	326
41	1	10	60	326
30	1	10	60	326
30	1	10	60	326
30	1	10	60	326
30	1	10	60	326
37	1	10	60	326
4	1	10	60	326
2	1	1	6	373
24	1	1	6	373
22	1	1	6	373
25	1	1	6	373
22	1	1	6	373
24	1	1	6	373
24	1	1	6	373
2	1	1	6	373
27	1	1	6	373
22	1	1	6	373
16	1	10	60	327
2	1	10	60	327
10	1	10	60	327
17	1	10	60	327
17	1			
15	1			
10	1	10	60	327
15	1	10	60	327
18	1	10	60	327
15	1	10	60	327

TY DISTRIBUTION

UN NO. 1

							90													
									0											
							0	0		0	0									
					0	0	0	0	0	0	0	0	0							
			0	0	0	0	0	0	0	0	0	0	0	0	0					
		0	0	0	0	0	0	0	0	0	0	0	0	0	0	0				
	0	0	0	0	0	0	0	0	0	0	0	0	0	0	0	0	0			
	0	0	0	0	0	0	0	0	0	0	0	0	0	0	0	0	0			
0	0	0	0	0	0	0	0	0	0	0	0	0	0	0	0	0	0	0		
0	0	0	0	0	0	0	0	0	0	0	0	0	0	0	0	0	0	0		
0	0	0	0	0	0	0	0	0	0	0	0	0	0	0	0	0	0	0	0	0
0	0	0	0	0	0	0	0	0	0	0	0	0	0	0	0	0	0	0	0	0
0	0	0	0	0	0	0	0	0	0	0	0	0	0	0	0	0	0	0	0	0
																			0	
0	0	0	0	0	0	0	2	6	2	0	0	0	0	0	0	0	0	0		
																			0	
0	0	0	0	0	0	0	11	18	8	0	0	0	0	0	0	0	0	0		
0	0	0	0	0	4	6	6	10	4	0	0	0	0	0	0	0	0	0		
0	0	0	0	0	3	9	5	0	0	0	0	0	0	0	0	0	0	0		
	0	0	0	0	0	1	2	0	0	0	0	0	0	0	0	0	0			
	0	0	0	0	0	0	0	0	0	0	0	0	0	0	0	0	0			
		0	0	0	0	0	0	0	0	0	0	0	0	0	0	0				
			0	0	0	0	0	0	0	0	0	0	0	0	0					
					0	0	0	0	0	0	0	0	0							
							0	0		0	0									
									0											

MBER OF POINTS
PEPCENT AREA

D

Y DISTRIBUTION

A NO. 1

									0										
							0	0		0	0								
					0	0	0	0	0	0	0	0	0						
			0	0	0	0	0	0	0	0	0	0	0	0	0				
		0	0	0	0	0	0	0	0	0	0	0	0	0	0	0			
	0	0	0	0	0	0	0	0	0	0	0	0	0	0	0	0	0		
	0	0	0	0	0	0	0	0	0	0	0	0	0	0	0	0	0		
0	0	0	0	0	0	0	0	0	0	0	0	0	0	0	0	0	0	0	
0	0	0	0	0	0	0	0	0	0	0	0	0	0	0	0	0	0	0	
0	0	0	0	0	0	0	0	0	0	0	0	0	0	0	0	0	0	0	
																			0
0	0	0	0	0	0	0	0	0	0	0	0	0	0	0	0	0	0	0	
																			0
0	0	0	0	0	0	0	0	0	0	0	0	0	0	0	0	0	0	0	0
																			0
0	0	0	0	0	0	0	7	20	7	0	0	0	0	0	0	0	0	0	
																			0
0	0	0	0	0	0	0	37	60	27	0	0	0	0	0	0	0	0	0	
0	0	0	0	0	13	20	20	33	13	0	0	0	0	0	0	0	0	0	
0	0	0	0	0	10	30	17	0	0	0	0	0	0	0	0	0	0	0	
	0	0	0	0	0	3	7	0	0	0	0	0	0	0	0	0	0		
	0	0	0	0	0	0	0	0	0	0	0	0	0	0	0	0	0		
		0	0	0	0	0	0	0	0	0	0	0	0	0	0	0			
			0	0	0	0	0	0	0	0	0	0	0	0	0				
					0	0	0	0	0	0	0	0	0						
							0	0		0	0								
									0										

TAGE OF POINTS
PERCENT AREA

DATA ENCOUNTERED ON SYSTEM INPUT FILE.

FORTRAN SOURCE LIST

```
ISN       SOURCE STATEMENT

  0 $IBFTC DCOUNT  NODECK,NOLIST
  1        DIMENSION COSA(333),COSB(333),COSG(333),ND(333)
  2        DIMENSION A(2000),B(2000),G(2000)
  3        DO 2 I=1,333
  4        READ(5,51)COSA(I),COSB(I),COSG(I),J
  6        IF(I.NE.J) GO TO 23
 11    2    CONTINUE
 13        PI=3.1415926
 14        R180=1./180.
 15        CF=PI*R180
 16    3   DO 4 I=1,333
 17    4   ND(I)=0
 21        NCDS=0
 22        NZ=0
 23        TND=0
 24        IX=1
 25        READ(5,300)QTA,QTB,QTC,QTD
 26        READ(5,301)THA,THB,THC,THD,K,DCF
 30   301  FORMAT(1X,4F5.0,2X,I4,F5.2)
 31   300  FORMAT(1X,4F11.8)
 32        READ(5,50)NSTN,NZ
 35        IF(NSTN.LT.0)CALL EXIT
 40        NZ=NZ+1
 41        GO TO (5,10),NZ
 42    5   READ  (5     ,53    ) NSTR,NDIP,NDIR
 46        IF(NSTR.LT.0)GO TO 12
 51        NCDS=NCDS+1
 52        PL=90-NDIP
 53        IF(NDIR.NE.1) GO TO 8
 56        TR=NSTR+90
 57        GO TO 11
 60    8   TR=NSTR-90
 61        GO TO 11
 62   10   READ (5,535) NTR,NPL
 65        IF(NTR.LT.0)GO TO 12
 70        NCDS=NCDS+1
 71        TR=NTR
 72        PL=NPL
 73   11   PL=PL*CF
 74        TR=TR*CF
 75        I=NCDS
 76        A(I)=COS (TR)*COS (PL)
 77        B(I)=SIN (TR)*COS (PL)
 00        G(I)=SIN (PL)
 01        GO TO (5,10),NZ
 02   12   CONTINUE
 03        FNCDS=NCDS
 04        RNCDS=100./FNCDS
 05        PMAX=0.
 06        DO 124 I=1,NCDS
 07        IF(PMAX.GE.G(I)) GO TO 124
 12        PMAX=G(I)
 13   124  CONTINUE
 15        PMAX=PMAX+QTA
           DO 15 I=1,333
```

To prepare modified pole density diagrams

FORTRAN SOURCE LIST DCOUNT

```
SN        SOURCE STATEMENT

17        CSG=COSG(I)
20        DENS=0.
21        IF(PMAX.LE.CSG) GO TO 15
24        CSA=COSA(I)
25        CSB=COSB(I)
26        DO 14 J=1,NCDS
27        GEE=G(J)
30        IF(ABS(GEE-CSG).GT.QTA)GO TO 14
33        REX=ABS(CSA*A(J)+CSB*B(J)+CSG*GEE)
34        IF(QTA.GT.REX)GO TO 14
37        DENS=DENS+THA
40        IF(QTB.GT.REX)GO TO 14
43        DENS=DENS+THB
44        IF(QTC.GT.REX)GO TO 14
47        DENS=DENS+THC
50        IF(QTD.GT.REX)GO TO 14
53        DENS=DENS+THD
54   14   CONTINUE
56   15   ND(I)=DENS
60        KLIK=1
61        DO 25 I=1,333
62        VND=ND(I)
63   25   TND=TND+VND
65        IF(TND.LT.20.*FNCDS)GO TO 302
70        TND=FNCDS*20.
71   302  CONTINUE
72   20   DO 21 I=1,333
73        XND=ND(I)
74   21   ND(I)=XND*100./TND+.5
76   16   WRITE (6      ,58     ) ND(1)
77        WRITE (6      ,66     ) ND(318),ND(319),ND(320),ND(321)
00        WRITE (6      ,68     ) NSTN
01        WRITE (6      ,59     ) (ND(I),I=2,10)
06        WRITE (6      ,57     )
07        WRITE (6      ,57     )
10        WRITE (6      ,60     ) (ND(I),I=11,23)
15        WRITE (6      ,57     )
16        WRITE (6      ,57     )
17        WRITE (6      ,61     ) (ND(I),I=24,38)
24        WRITE (6      ,57     )
25        WRITE (6      ,57     )
26        WRITE (6      ,62     ) (ND(I),I=39,55)
33        WRITE (6      ,57     )
34        WRITE (6      ,57     )
35        WRITE (6      ,62     ) (ND(I),I=56,72)
42        WRITE (6      ,57     )
43        WRITE (6      ,57     )
44        WRITE (6      ,63     ) (ND(I),I=73,91)
51        WRITE (6      ,57     )
52        WRITE (6      ,57     )
53        WRITE (6      ,63     ) (ND(I),I=92,110)
60        WRITE (6      ,57     )
61        WRITE (6      ,57     )
          WRITE (6      ,63     ) (ND(I),I=111,129)
          WRITE (6      ,67     ) ND(322),ND(323)
```

FORTRAN SOURCE LIST DCOUNT

```
SN        SOURCE STATEMENT

70        WRITE (6      ,57     )
71        WRITE (6      ,63     ) (ND(I),I=130,148)
76        WRITE (6      ,67     ) ND(324),ND(325)
.7        WRITE (6      ,57     )
00        WRITE (6      ,64     ) (ND(I),I=149,169)
05        WRITE (6      ,57     )
06        WRITE (6      ,67     ) ND(326),ND(327)
07        WRITE (6      ,63     ) (ND(I),I=170,188)
14        WRITE (6      ,57     )
15        WRITE (6      ,67     ) ND(328),ND(329)
16        WRITE (6      ,63     ) (ND(I),I=189,207)
23        WRITE (6      ,57     )
24        WRITE (6      ,57     )
25        WRITE (6      ,63     ) (ND(I),I=208,226)
32        WRITE (6      ,57     )
33        WRITE (6      ,57     )
34        WRITE (6      ,63     ) (ND(I),I=227,245)
41        WRITE (6      ,57     )
42        WRITE (6      ,57     )
43        WRITE (6      ,62     ) (ND(I),I=246,262)
50        WRITE (6      ,57     )
51        WRITE (6      ,57     )
52        WRITE (6      ,62     ) (ND(I),I=263,279)
57        WRITE (6      ,57     )
60        WRITE (6      ,57     )
61        WRITE (6      ,61     ) (ND(I),I=280,294)
66        WRITE (6      ,57     )
67        WRITE (6      ,57     )
70        WRITE (6      ,60     ) (ND(I),I=295,307)
75        WRITE(6,54)NCDS
76        WRITE(6,69)K
77        WRITE (6      ,59     ) (ND(I),I=308,316)
04        WRITE (6      ,57     )
05        WRITE (6      ,66     ) ND(330),ND(331),ND(332),ND(333)
06        WRITE (6      ,65     ) ND(317)
07        GO TO (303,22),KLIK
10  303   DO304I=1,333
11        XND=ND(I)
12  304   ND(I)=XND*FNCDS*DCF/200.+.5
14        KLIK=2
15        GO TO 16
16  22    GO TO 3
17  23    WRITE(6,71)
20         CALL EXIT
21  24    WRITE(6,72)
22        CALL EXIT
23  50    FORMAT(1X,I3,1X,I1)
24  51    FORMAT(7X,3F11.8,12X,I3)
25  52    FORMAT(I3)
26  53    FORMAT(1X,I3,1X,I2,1X,I1,1X,I5)
27  535   FORMAT(1X,I3,1X,I2,3X,I5)
30  57    FORMAT(1X)
31  58    FORMAT(21H1DENSITY DISTRIBUTION,29X,I5)
    59    FORMAT(30X,9I5)
    60    FORMAT(20X,13I5)
```

FORTRAN SOURCE LIST DCOUNT

```
ISN        SOURCE STATEMENT

434    61  FORMAT(15X,15I5)
435    62  FORMAT(10X,17I5)
436    63  FORMAT(5X,19I5)
437    64  FORMAT(21I5)
440    69  FORMAT(4H  K=,I4)
441    54  FORMAT(2X,I4,9H READINGS)
442    65  FORMAT(50X,I5)
443    66  FORMAT(39X,I5,I6,I10,I6)
444    67  FORMAT(I6,93X,I5)
445    68  FORMAT(12H STATION NO.,I4)
446    70  FORMAT(4H PER,I3,13H PERCENT AREA)
447    71  FORMAT(33H ERROR= CONSTANTS OUT OF SEQUENCE)
450    72  FORMAT(52H ERROR= PERCENTAGE OF AREA CONSTANT MISSING OR ZERO.)
451        END
```

ITY DISTRIBUTION

TION NO. 1

										0											
								0	0		0	0									
						0	0	0	0	0	0	0	0	0							
				0	0	0	0	0	0	0	0	0	0	0	0	0	0				
			0	0	0	0	0	0	0	0	0	0	0	0	0	0	0	0			
		0	0	0	0	0	0	0	0	0	0	0	0	0	0	0	0	0	0		
		0	0	0	0	0	0	0	0	0	0	0	0	0	0	0	0	0	0		
	0	0	0	0	0	0	0	0	0	0	0	0	0	0	0	0	0	0	0	0	
	0	0	0	0	0	0	0	0	0	0	0	0	0	0	0	0	0	0	0	0	
	0	0	0	0	0	0	0	0	0	0	0	0	0	0	0	0	0	0	0	0	
0																					0
	0	0	0	0	0	0	0	0	0	0	0	0	0	0	0	0	0	0	0	0	
0																					0
0	0	0	0	0	0	0	0	0	0	0	0	0	0	0	0	0	0	0	0	0	0
0																					0
	0	0	0	0	0	0	0	0	2	0	0	0	0	0	0	0	0	0	0	0	
0																					0
	0	0	0	0	0	0	0	8	33	10	0	0	0	0	0	0	0	0	0	0	
	0	0	0	0	0	2	7	5	9	1	0	0	0	0	0	0	0	0	0	0	
	0	0	0	0	0	0	21	3	0	0	0	0	0	0	0	0	0	0	0	0	
		0	0	0	0	0	0	0	0	0	0	0	0	0	0	0	0	0	0		
		0	0	0	0	0	0	0	0	0	0	0	0	0	0	0	0	0	0		
			0	0	0	0	0	0	0	0	0	0	0	0	0	0	0	0			
				0	0	0	0	0	0	0	0	0	0	0	0	0	0				
						0	0	0	0	0	0	0	0	0							
								0	0		0	0									
										0											

Values D_x

30 READINGS

= 500

Data from Fig. 3

TY DISTRIBUTION

CN NO. 1

Values. $\frac{2D_x}{qc^2}$

READINGS
00

ta from Fig. 3

F-DATA ENCOUNTERED ON SYSTEM INPUT FILE.

a reading at that grid point changes value are punched on this card. They start at the largest angle and specify its direction cosines to eight figures. Values are taken from Table 5:1.

Card 2

The increments of each weighting are punched in 5, 10, 15 and 20. The value of the precision parameter assumed in these calculations is punched in 23 - 26 (no decimal figures). $\frac{1}{\sum D_i}$ for this value of the precision parameter is punched in 27 30 (to 2 decimal figures).

Cards 3 and 4 are as cards 2 and 3 of the unmodified program.

The use of the program is the same as the unmodified program.

Checkout

The program was checked out by comparison with the unmodified program.

5) Determination of Mean S planes

This program was originally written by Muecke in Fortran II and a full acount of it is contained in Muecke (1965, pp. 31-40). The program was translated directly into Fortran IV by V. Yanda and D. Cruden. As it stands, the program is rather inelegant though quite functional.

Method

Fisher (1953, p. 296) showed that the best estimate (λ, μ, γ) of the true mean direction is the vector sum of the individual directions $(\lambda_i, \mu_i, \gamma_i)$. That is

$$\lambda = \frac{\sum \lambda_i}{R}, \quad \mu = \frac{\sum \mu_i}{R}, \quad \gamma = \frac{\sum \gamma_i}{R}$$

where

$$R^2 = \left(\sum \lambda_i\right)^2 + \left(\sum \mu_i\right)^2 + \left(\sum \gamma_i\right)^2$$

The aximuth and the inclination of the resultant vector are determined using the relationships,

$$\tan D = \frac{\sum \mu_i}{\sum \lambda_i} \qquad \sin I = \frac{\sum \gamma_i}{R}$$

where D is the declination and I the inclination of the resultant vector.

The accuracy of the calculated mean direction (λ, μ, γ) can be estimated by the angle between this mean and the true mean. Fisher (1953, p. 303) showed that, at a probability level of (1-R), the true mean direction of the population lies within a circular cone about the resultant vector of semi-vertical angle ,

$$\cos \alpha = 1 - \frac{N-R}{R}\left(\left(\frac{1}{P}\right)^{\frac{1}{N-1}} - 1\right)$$

where N is the total number of vectors included in the analysis and the precision parameter, K, is greater than 3. If K is greater than 3,

$$\hat{K} = \frac{N-1}{N-R}$$

Use of the program

The user should prepare a deck with the following:

(1) The standard control cards of the IBSYS monitor--at the University of Alberta these consist of a IBSYS card, a JOB card, a TIME card--two minutes is ample time for ten samples of ten readings on the IBM7040 (if a relocatable binary deck is used), lines of output are shown in a sample of the output.

(2) A source deck or corresponding relocatable binary deck.

(3) A $ENTRY card.

(4) Muecke's parameter cards 1 and 2 before each 5.

(5) A data set.

Check out

The program rewritten in Fortran IV was checked using Muecke's test data. The results were identical.

```
VS
            450202 MEAN FRACTURE PLANE (MODIFIED)
            3,300
OR          GO,NODECK
TC MEPL
      DIMENSION A(500),B(500),G(500)
      PI=3.1415926
      R180=1./180.
      CF=PI*R180
      READ (5      ,50     ) NSTN,NDEN,NCDS,NP
      IF(NSTN.LT.0) GO TO 69
      P=NP
      READ (5      ,51     ) LLIM,NLIM
      SA=0.0
      SB=0.0
      SG=0.0
      DO 12 I=1,NCDS
      READ (5      ,52     ) NSTR,NDIP,NDIR
      PL=90-NDIP
      IF(NDIR-1)3,2,3
      TR=NSTR+90
      GO TO 5
      TR=NSTR-90
      IF(TR)4,5,5
      TR=TR+360.
      DLIM=LLIM
      IF(TR-DLIM)6,10,10
      SLIM=NLIM
      IF(SLIM-DLIM)8,9,9
      IF(TR-90.)10,10,9
      TR=TR+180.
      PL=PL*CF
      TR=TR*CF
      A(I)=COS (TR)*COS (PL)
      B(I)=SIN (TR)*COS (PL)
      G(I)=-SIN (PL)
      GO TO 11
      PL=PL*CF
      TR=TR*CF
      A(I)=COS (TR)*COS (PL)
      B(I)=SIN (TR)*COS (PL)
      G(I)=SIN (PL)
      SA=SA+A(I)
      SB=SB+B(I)
      SG=SG+G(I)
      R=SQRT ((SA*SA)+(SB*SB)+(SG*SG))
      SININ=SG/R
      TADE=SB/SA
      REIN=ATAN (SININ/SQRT (1.-SININ*SININ))
      REIN=REIN/CF
      RFIN=ABS (RFIN)
      PEDE=ATAN (TADE)
      REDE=REDE/CF
      IF(SG)21,122,122
      SA=-(SA)
      SB=-(SB)
      IF(SA)15,13,13
      IF(SB)16,17,17
      REDE=180.+REDE
      GO TO 17
```

Determination of Mean S Planes

```
REDE=360.+REDE
CDS=NCDS
XK=(CDS-1.)/(CDS-R)
WRITE (6      ,60     ) NSTN,NDEN
WRITE (6      ,65     ) NCDS
WRITE (6      ,63     ) REDE
WRITE (6      ,62     ) REIN
WRITE (6      ,61     ) XK
PERC=(100.-P)
P=P*.01
Q=1./(CDS-1.)
RR=(CDS-R)/R
PP=((1./P)**Q)-1.
RR=RR*PP
COSAL=1.-RR
FUN=ABS ((1.-COSAL*COSAL)/(COSAL))
FUN=SQRT (FUN)
AL=ATAN (FUN)
AL=AL/CF
DELTA=SQRT (2.*(CDS-R)/CDS)
ETA=DELTA/SQRT (CDS)
DELTA=DELTA/CF
ETA=ETA/CF
WRITE (6      ,64     ) PERC,AL
WRITE (6      ,66     ) DELTA
WRITE (6      ,67     ) ETA
GO TO 68
CALL EXIT
FORMAT(1X,I3,1X,I2,1X,I3,1X,I1)
FORMAT(1X,I3,1X,I3)
FORMAT(//8H STATION14,14H MEAN FRACTUREI3)
FORMAT(20H PRECISION PARAMETER,12X,F10.3)
FORMAT(22H RESULTANT INCLINATION,10X,F8.3)
FORMAT(22H RESULTANT DECLINATION,10X,F8.3)
FORMAT(1X,F4.0,1X,28H PER CENT CONFIDENCE RADIUS F8.3)
FORMAT(//13H MEASUREMENTSI23)
FORMAT(14H RMS DEVIATION,18X,F8.3)
FORMAT(19H STANDARD DEVIATION,13X,F8.3)
CALL EXIT
END
```

MFPL

450005 IBLDR -- JOB MFPL

JECT PROGRAM IS BEING ENTERED INTO STORAGE.

TION 373 MEAN FRACTURE 2

SUREMENTS	10
LTANT DECLINATION	207.932
LTANT INCLINATION	66.947
ISION PARAMETER	521.763
PER CENT CONFIDENCE RADIUS	2.116
DEVIATION	3.365
CARD DEVIATION	1.064

TION 326 MEAN FRACTURE 2

Results for stations in Fig. 3.

UREMENTS	10
LTANT DECLINATION	218.248
LTANT INCLINATION	50.365
ISION PARAMETER	330.720
PER CENT CONFIDENCE RADIUS	2.659
DEVIATION	4.227
CARD DEVIATION	1.337

TION 327 MEAN FRACTURE 2

UREMENTS	10
LTANT DECLINATION	201.941
LTANT INCLINATION	73.379
ISION PARAMETER	371.885
PER CENT CONFIDENCE RADIUS	2.507
DEVIATION	3.986
CARD DEVIATION	1.261

OF-DATA ENCOUNTERED ON SYSTEM INPUT FILE.

APPENDIX 5

THE CONTOURING OF PI DIAGRAMS

The relative concentrations of readings in different parts of a pi diagram are often best displayed by contours. These concentrations have been used, Friedmann, (1964, pp. 468-469), to make statistical inferences about the population of which the readings are a sample. This use makes it clear that contouring attempts to estimate the probabilities of finding readings within different small areas on the sphere. It is implied that one is five times more likely to find a point within the 5% contour than within the same area within the 1% contour.

The distribution of probability is customarily investigated by Monte Carlo methods - throwing grids on circular counters across the equal area projection on which the readings have been plotted and counting the number of points within each cell. The number of readings within the cell is then an estimate of the probability of finding a reading within a small area at the centre of the cell. These probability values can be contoured (usually as percentages of the total numbers of points plotted) and, it is argued, the distribution of probability displayed.

One source of inaccuracy in this method has been pointed out by Strand (1944). Although the points are plotted on an equal-area net, there is a progressive distortion of these areas on the net from the centre outwards. Fully accurate contouring requires continual changes in the shape of the counter (Flinn, 1958). One way this tedious procedure could be avoided has been suggested independently by Noble and Eberly (1964) and Muecke (1965). They used computer techniques to count out the points on the original sphere. A grid of 333 points is specified in Muecke's program (by their direction cosines) and when a reading (also given by its direction cosines) falls within a cone with n% cross sectional area (n = 1 - 9 at the programmer's choice) around a grid point, the counter at that grid point

is given an increment. The values of the counters are then plotted out on an equal-area net.

Because the computer technique elimates plotting errors, only errors in field observations remain. It has previously been shown that the distribution of the probability of finding the true pole to a bedding plane might reasonably be assumed to have a Fisher distribution about the best estimate of the pole. In other words, the probability of the true pole lying at angle greater than θ with the best estimate of the pole, falls off with increasing θ according to the Fisher probability density function, $P(\theta)$.

The probability of a pole with a Fisher distribution is continuous over the hemisphere of projection. Further poles plotted will increase the probability of a pole at any locality. This will be the sum of the probabilities of individual poles at the locality (assuming the poles are disconnected events). For instance the probability of finding at least one pole within δA in Fig. 4 is the sum of the probabilities of finding A there and B there.

Treating probability as a continuous function should lead to some reconsideration of techniques of contouring it. For as it makes little sense to contour a topographic map by using stations determined by averaging elevations over an area, so it is illogical to contour probability by averaging it over areas as large as 1% of the hemisphere.

Consider the probability P of a pole in a small area δA lying between θ_1 and θ_2 from P.

$$P' = \int^{S} f \, \delta A$$

where P is the probability density function. The integration is over the surface element, δA.

If A is very small the probability has a constant value over that area.

Watson and Irving (1957) show that if K, the precision parameter, is large, the probability, X^1, of the true mean of a reading lying between θ_1, θ_2 of the estimated mean is given by

$$X^1 = e^{-K(1-\cos\theta_1)} - e^{-K(1-\cos\theta_2)}$$

The probability P^1 that it lies in the area δA is given by

$$P^1 = \frac{\delta A \cdot X^1}{c^2\pi(\theta_2^2 - \theta_1^2)}$$

if θ_1, θ_2 are small and the hemisphere has unit radius, and $c = 1^\circ$ in radians.

Let us now define the density of the probability, D, as the probability per unit area

$$D^1 = \frac{X^1}{c^2\pi(\theta_2^2 - \theta_1^2)}$$

where D^1 is the density of probability in the small area between θ_1, and θ_2. A table (Table 5:1) of values of D^1 for different values of K has been computed. This table also includes a rough weighting of the probability of finding the reading in a small area at differing angles from its estimated position. The table allows the adaptation of Yanda and Muecke's program (Muecke, 1965) to increment the grid of counting locations by the approximate density of probaility of the reading in the small area δA around the counter. The resulting diagram can be directly contoured to appreciate the distribution of probability.

Whereas the relative densities of probability are sufficient to show the distribution of probability on the diagram, it is often required to predict the number of points from a larger sample of the same population which would fall within a given area. This is the object of constructing contours of percentages of points per percentage area. In fact, we seek a number N such that N x R (where R is the percentage of the diagram within the N contour line) is the number of points

enclosed within the contour line. The total density of probability, S, associated with 1 point is given by

$$S = \int_0^{\theta} D \, d\theta$$

where θ is the angular distance at which the density becomes negligible.

This integral can be approximated by

$$S = \sum_{i=0}^{i=\theta} D_i$$

where i takes integer values

$\sum D_i$ is calculated in the table for various values of K.

Suppose the counters are so placed that only q% of the density of probability is recorded. Then the value of the density at each counter must be increased by $\frac{100}{q}$. Throughout the table a factor πC^2 has been dropped for computational convenience so that if D_x is the value of a particular counter

$2 D_x R / qC^2$ = the number of readings falling within the R% of the diagram which the D_x contour encloses. Yanda and Mueck's program has therefore been redesigned to plot out a second diagram giving values of $2D_x/qC^2$ for each counter.

The procedure outlined has some analogy with that suggested by Mellis and advocated by Flinn and Friedmann. They suggest drawing a circle 1% of the area of the hemisphere around each plotted pole and contouring areas of 1, 2, n intersecting circles. This procedure has a sound basis but is unable to distinguish between the extreme cases illustrated below, (Fig. 4). The extra sensitivity of the computer method lies in its ability to distinguish between cases like this, its elimination of plotting errors, and its sensitivity to varying K values of the input. Fig. 5 shows this schematically.

TABLE 5:1 VARIATION OF DENSITY OF PROBABILITY WITH ANGULAR DISTANCE FROM THE ESTIMATED MEAN OF THE SAMPLE

$\theta_1-\theta_2$	K=50 X	K=50 D	K=50 Weight $\frac{(20Di)}{\sum Di}$	K=100 X	K=100 D	K=100 Weight $\frac{(20Di)}{\sum Di}$	K=200 X	K=200 D	K=200 Weight $\frac{(20Di)}{\sum Di}$	K=500 X	K=500 D	K=500 Weight $\frac{(20Di)}{\sum Di}$
0 - 1	0.008	0.0080		0.015	0.015	3	0.030	0.030	4	0.09	0.090	7
1 - 2	0.023	0.0077		0.044	0.015		0.080	0.026		0.15	0.050	4
2 - 3	0.035	0.0070		0.069	0.014		0.125	0.025	3	0.24	0.048	
3 - 4	0.409	0.0070		0.089	0.013		0.150	0.021		0.20	0.028	
4 - 5	0.058	0.0062	2	0.100	0.011	2	0.150	0.015		0.15	0.017	2
5 - 6	0.067	0.0061		0.105	0.010		0.140	0.013	2	0.09	0.008	
6 - 7	0.071	0.0055		0.105	0.008		0.110	0.008		0.04	0.003	1
7 - 8	0.074	0.0050		0.100	0.007	1	0.080	0.008	1			
8 - 9	0.072	0.0042		0.090	0.006		0.060	0.004				
9 -10	0.075	0.0040		0.070	0.003		0.040	0.002				
10-11	0.069	0.0033		0.060	0.003		0.020					
11-12	0.069	0.0030		0.040	0.002							
12-13	0.06	0.002	1	0.030	0.001							
13-14	0.05	0.002										
14-15	0.04	0.002										
$\sum Di$		0.0656			0.111			0.162			0.252	

Fig. 1

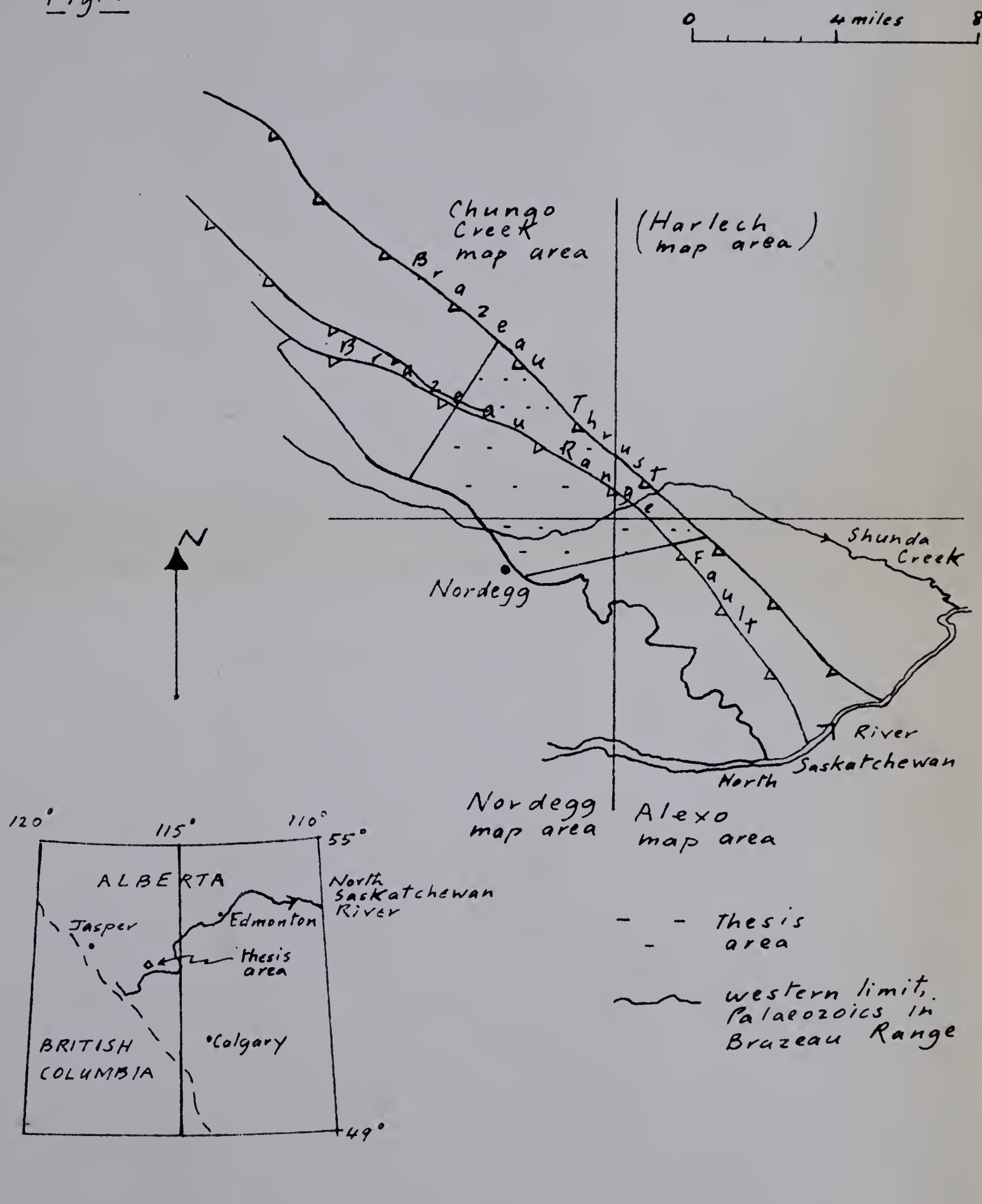
0
4 miles
8
Chungo Creek map area
(Harlech map area)
Brazeau Thrust
Brazeau Range
Shunda Creek
Nordegg
Fault
River
Saskatchewan
North
Nordegg map area
Alexo map area
N
120°
115°
110°
55°
ALBERTA
North Saskatchewan River
Jasper
Edmonton
Thesis area
BRITISH COLUMBIA
Calgary
49°
Thesis area
western limit, Palaeozoics in Brazeau Range

Fig. 2

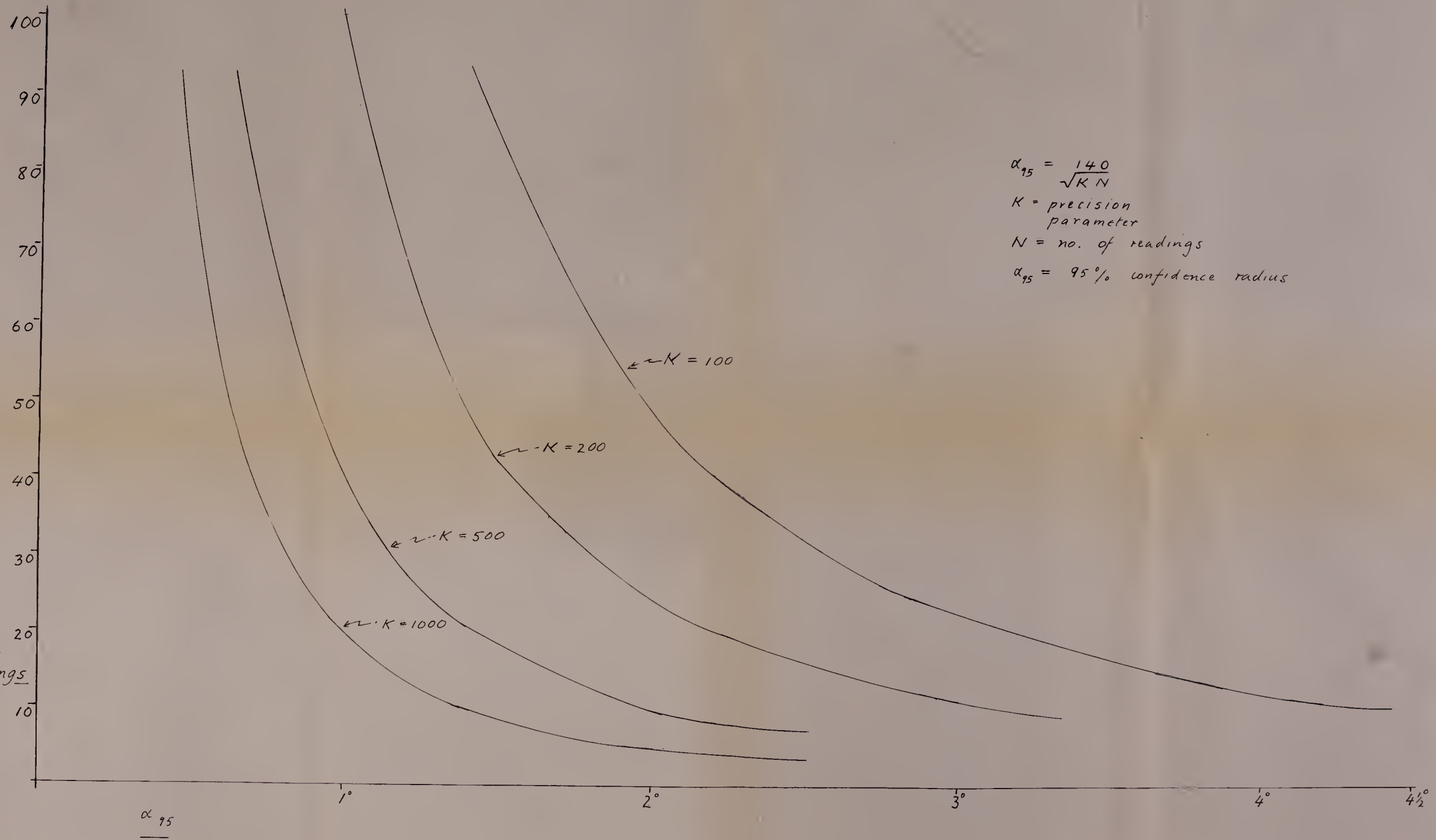

$\alpha_{95} = \frac{140}{\sqrt{K N}}$

K = precision parameter

N = no. of readings

α_{95} = 95% confidence radius

Fig. 3

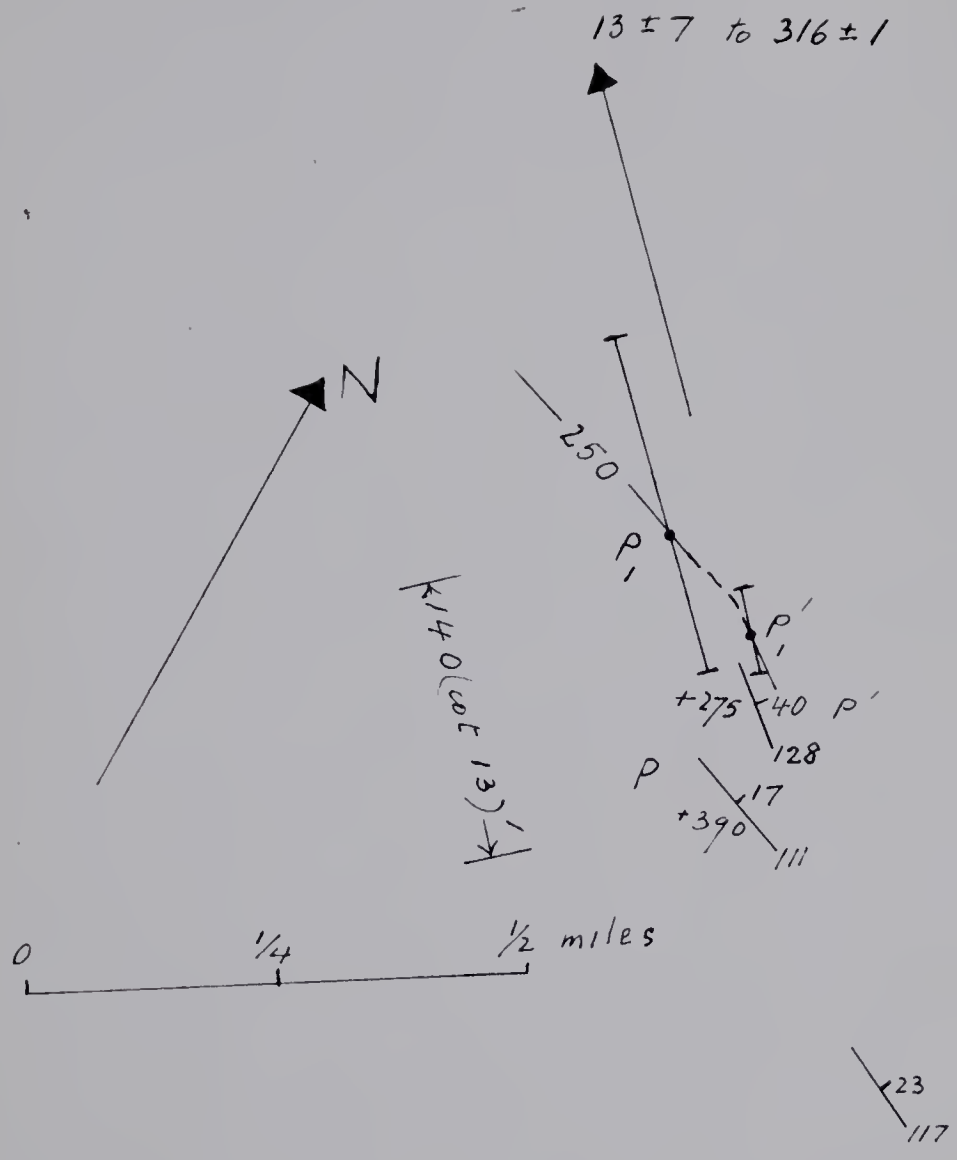
13 ± 7 to 316 ± 1
N
250
P1
P1'
+275
40
P'
128
P
17
+390
111
k140(cot 13)'
0
1/4
1/2 miles
23
117

Fig. 4

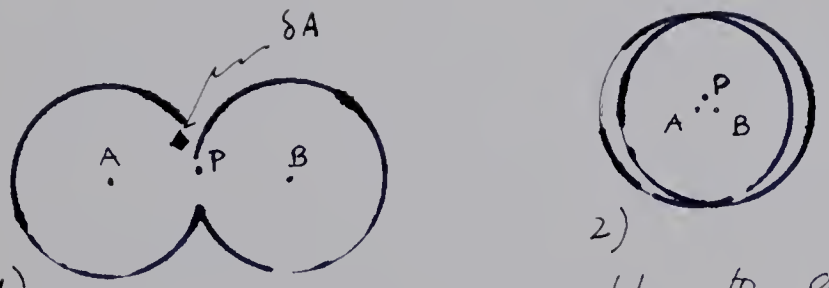

1) 2)

Mellis' method is unable to distinguish situation ① from ②, though the probability of A and B at P is obviously different Circles are 1% surface area of the hemisphere of projection.

Fig. 5

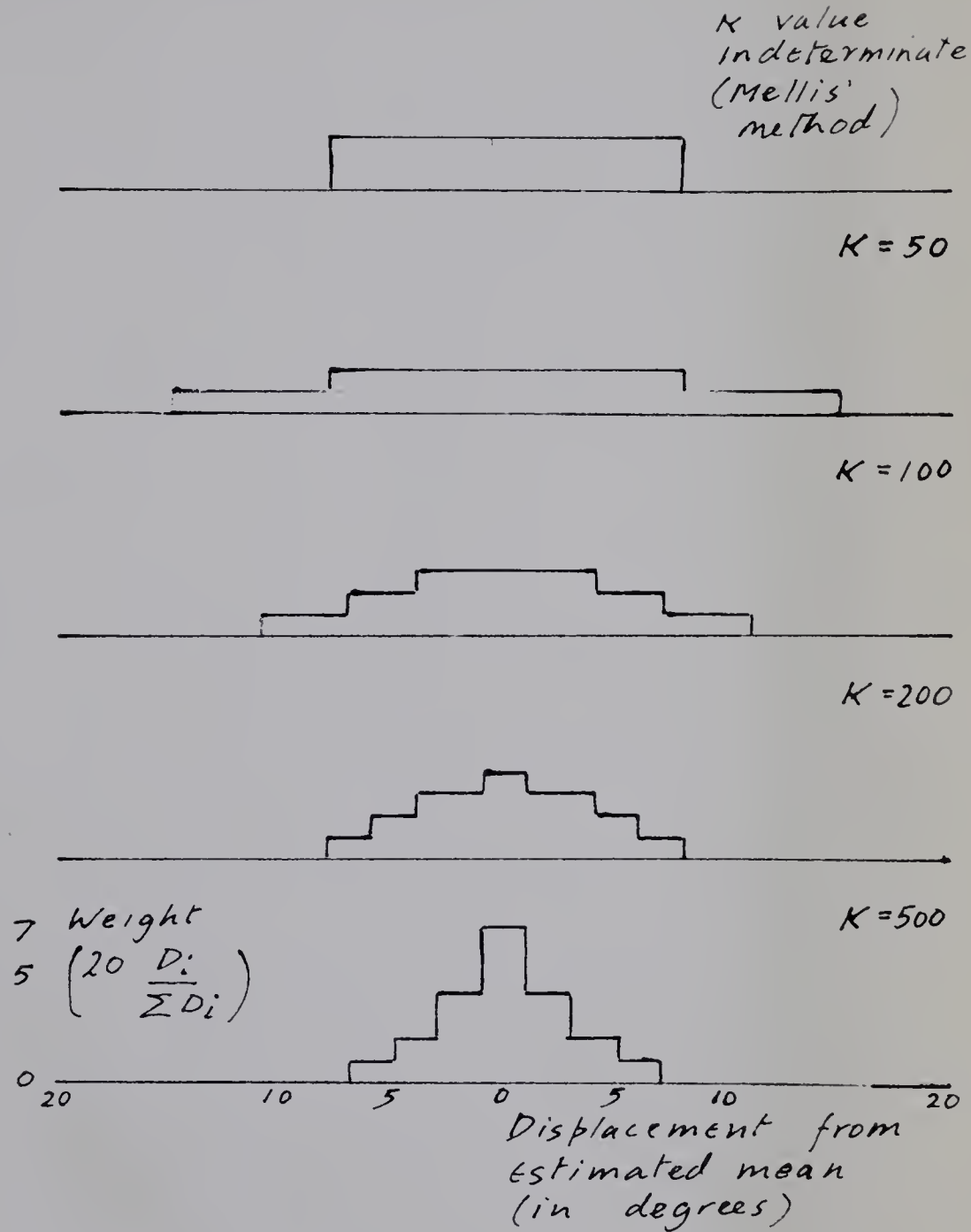
κ value indeterminate (Mellis' method)
K = 50
K = 100
K = 200
K = 500
7
5
0
Weight
$\left(20 \frac{D_i}{\Sigma D_i}\right)$
20
10
5
0
5
10
20
Displacement from estimated mean (in degrees)

Fig. 6

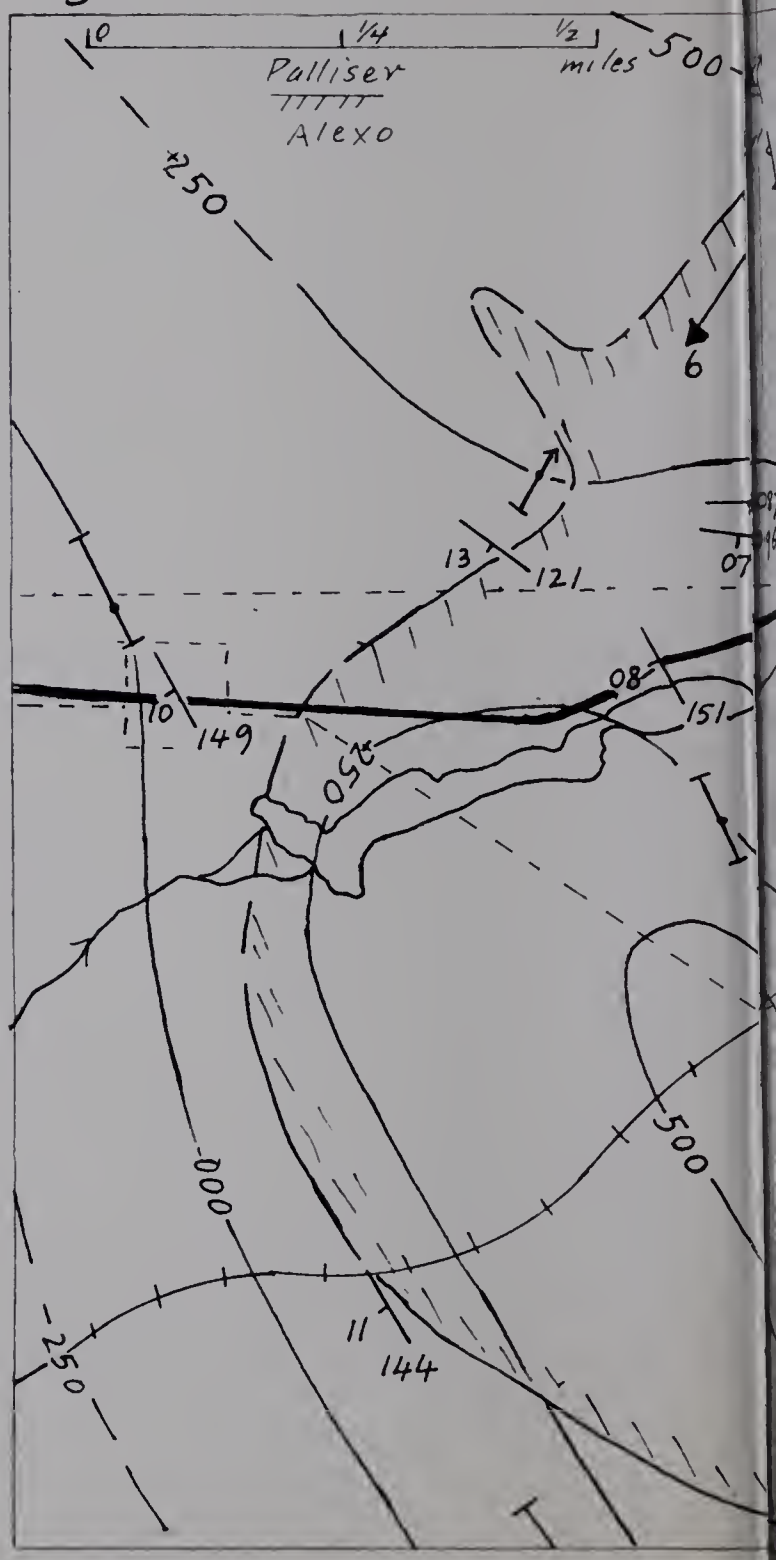
0
1/4
1/2
miles
Palliser
Alexo
500
250
6
13
121
07
08
10
149
151
050
500
000
250
11
144

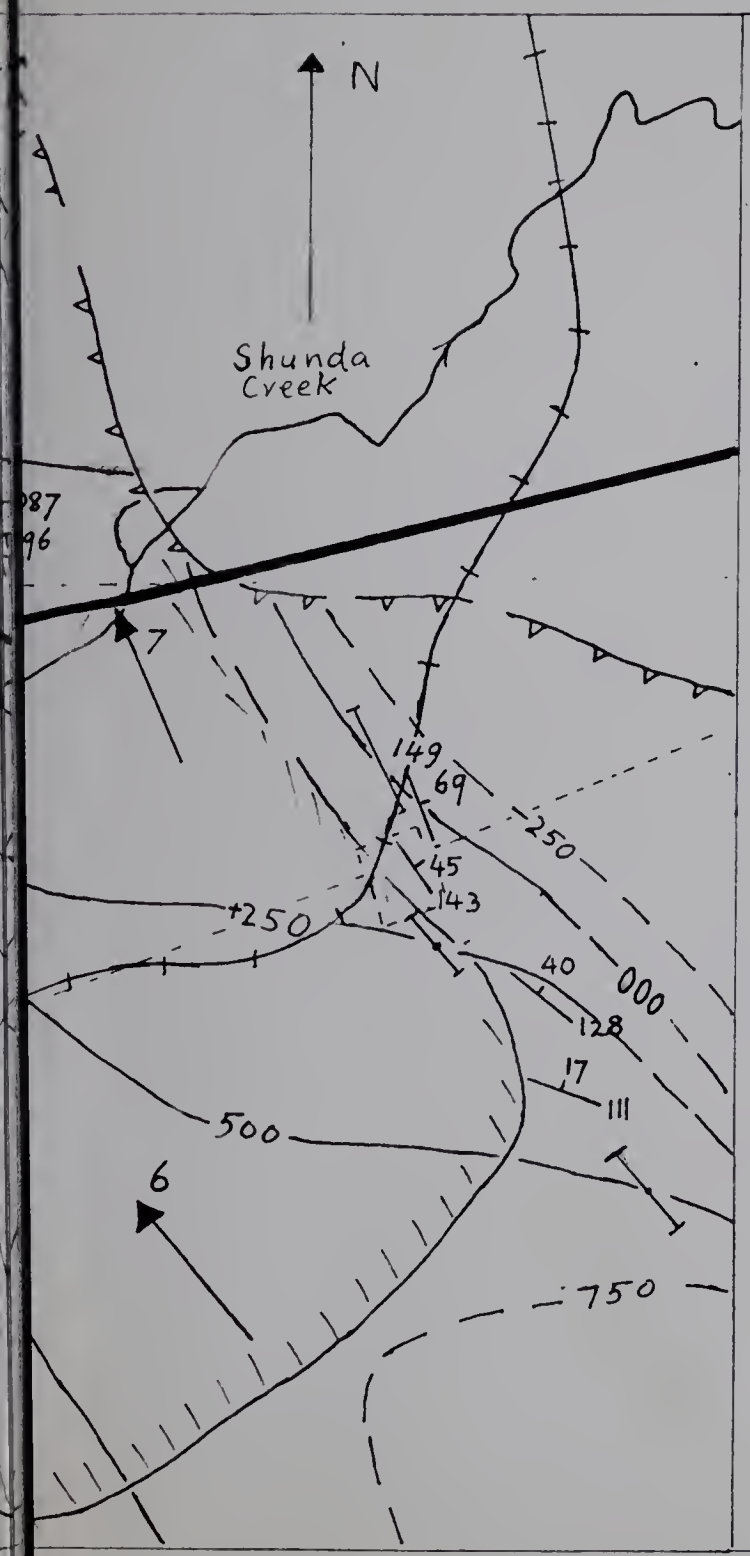

Legend (for structure contour maps)

Calculated plunge of domain — 6

Domain boundary ------

Limits on extrapolated position of contour line

(No limit in direction of arrow)

Most probable position of contour line (calculated) is dotted

Structure contour (000' = 4280' O.D) — 000

Fig. 7. Palliser top

Fig. 8
Banff top.

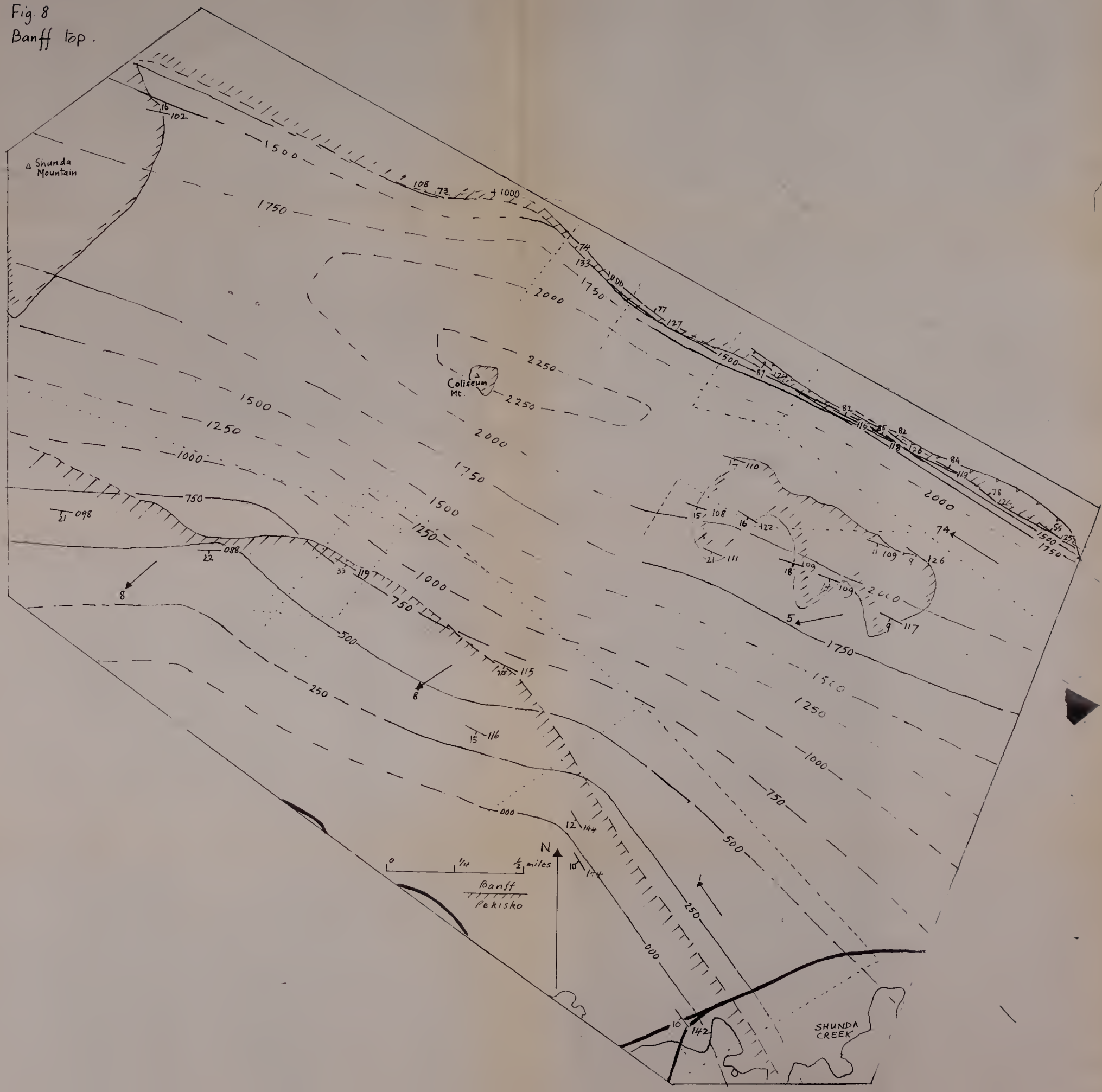

Fig. 9

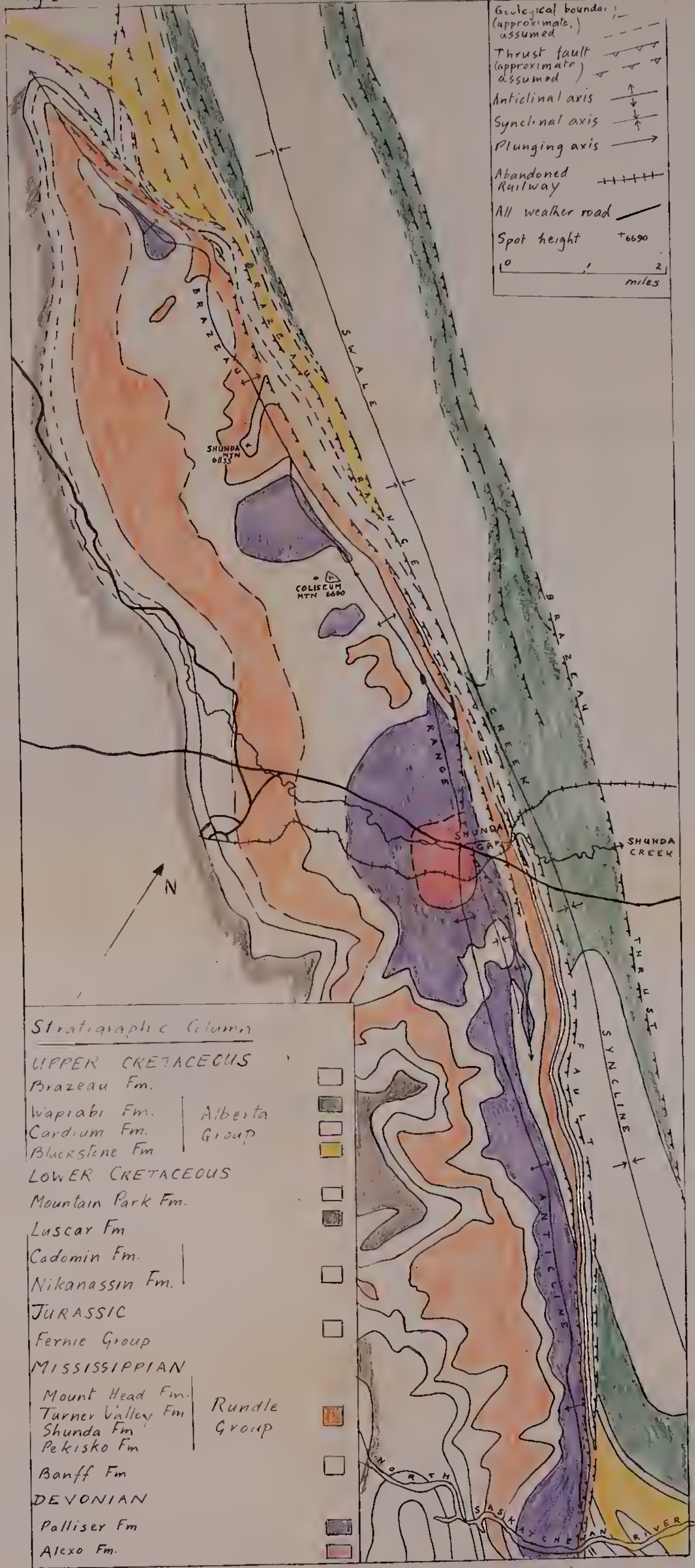
Geological boundary (approximate, assumed)
Thrust fault (approximate, assumed)
Anticlinal axis
Synclinal axis
Plunging axis
Abandoned Railway
All weather road
Spot height
+6690
0
1
2
miles
BRAZEAU
SWALE
RANGE
CREEK
BRAZEAU
THRUST
SYNCLINE
FAULT
ANTICLINE
SHUNDA MTN 6835
COLISEUM MTN 6690
SHUNDA GAP
SHUNDA CREEK
N
NORTH SASKATCHEWAN RIVER
Stratigraphic Column
UPPER CRETACEOUS
Brazeau Fm.
Wapiabi Fm.
Cardium Fm.
Blackstone Fm
Alberta Group
LOWER CRETACEOUS
Mountain Park Fm.
Luscar Fm
Cadomin Fm.
Nikanassin Fm.
JURASSIC
Fernie Group
MISSISSIPPIAN
Mount Head Fm.
Turner Valley Fm
Shunda Fm
Pekisko Fm
Rundle Group
Banff Fm
DEVONIAN
Palliser Fm
Alexo Fm.

Fig. 10

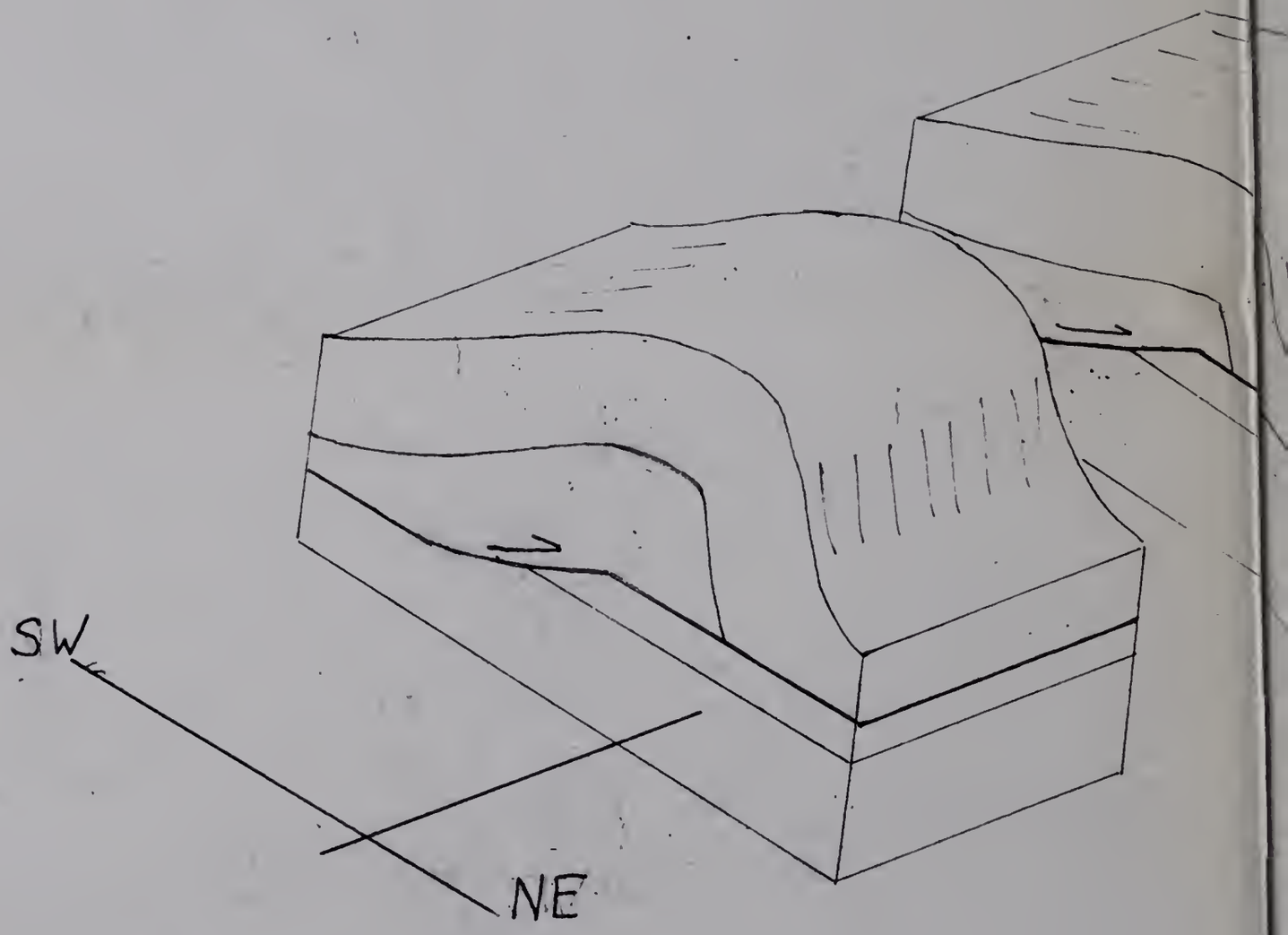

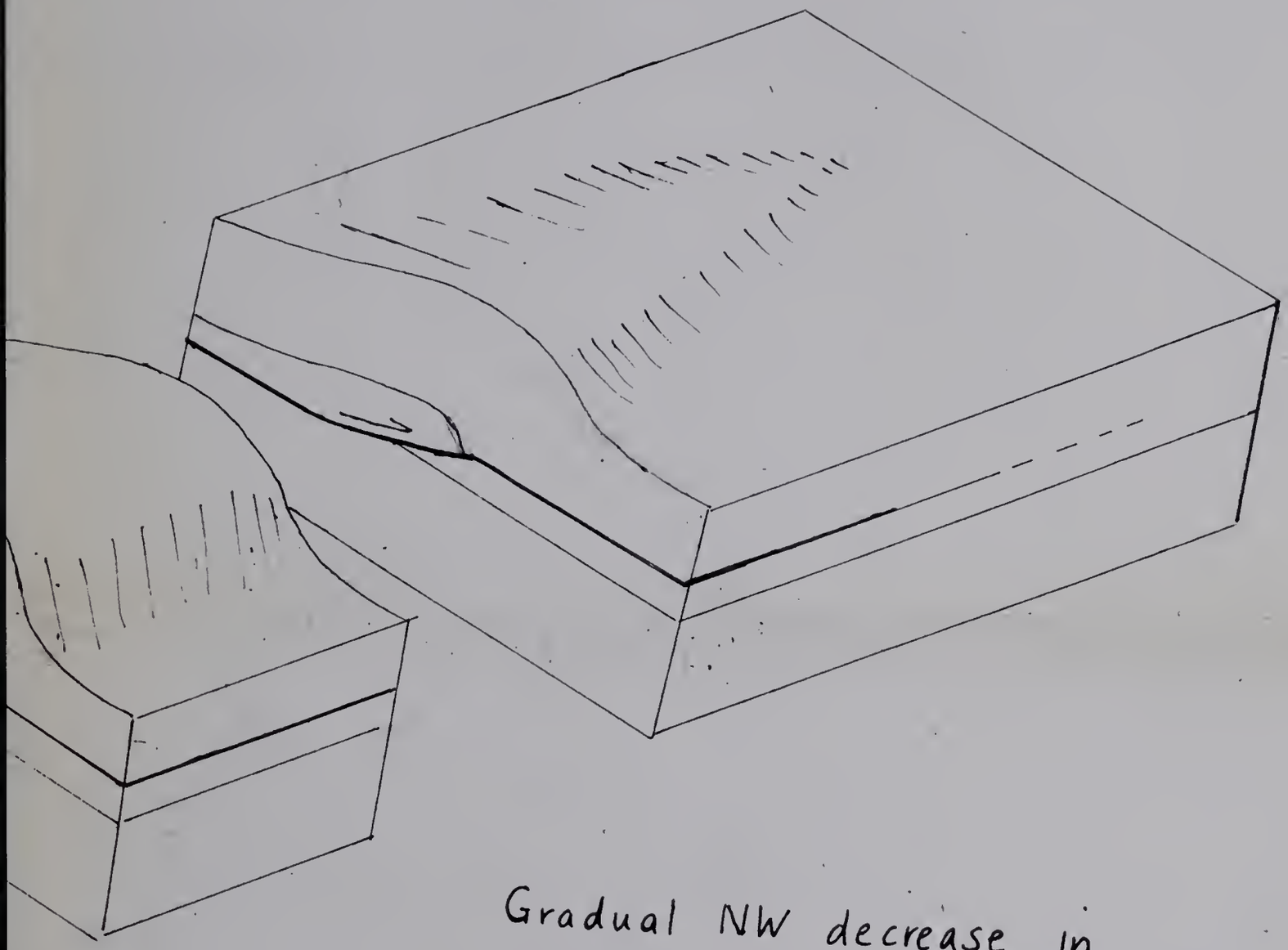

Gradual NW decrease in total transport causes the fold to die out. The axial trace is arcuate

Fig. 11

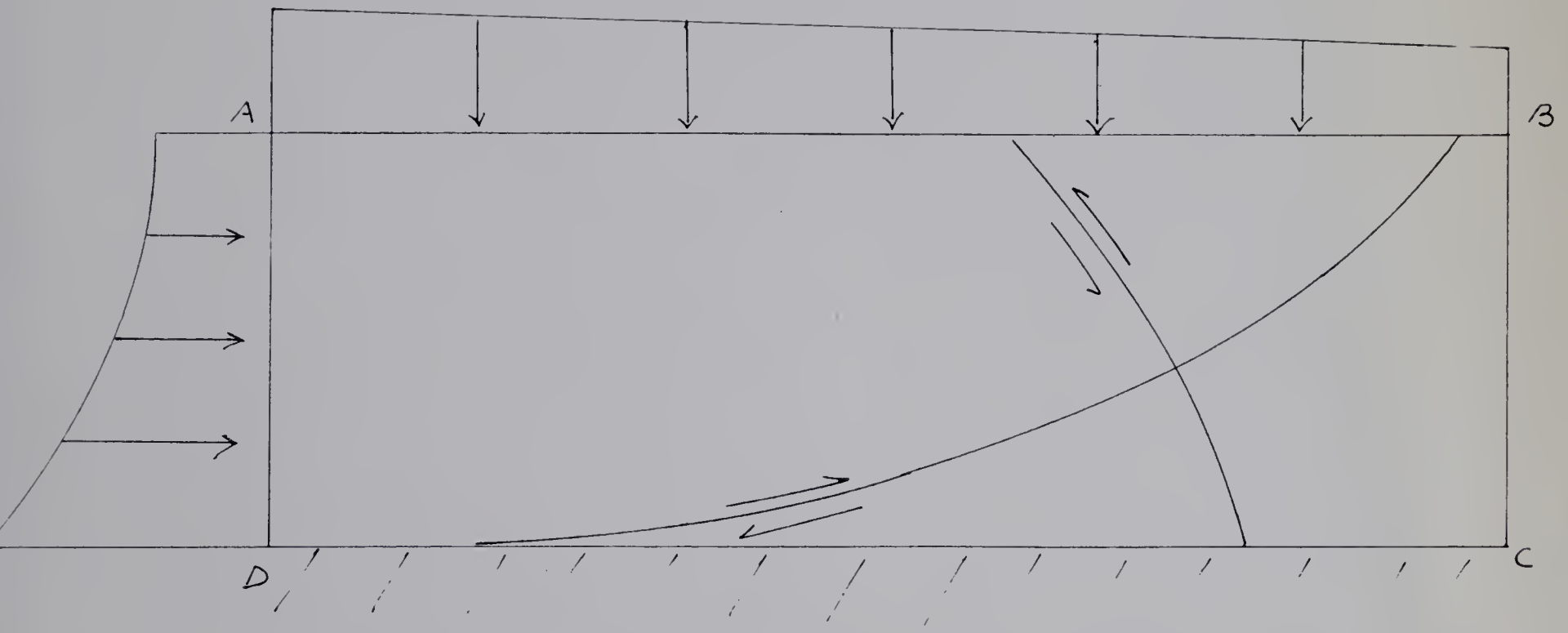

After Jaeger Fig. 53, boundary stresses on DC, BC omitted for clarity scale for stresses is arbitrary

DC is $y = -a$

BC is parallel to the x axis